# AUTOMATED RECOGNITION OF URBAN AREAS BASED ON LAND COVER COMPOSITION AND CONFIGURATION

OU YANG

Ph.D

The Hong Kong Polytechnic University

2016

Hong Kong Polytechnic University

Department of Land Surveying and Geo-Informatics

# Automated Recognition of Urban Areas Based on Land Cover Composition and Configuration

**OU Yang**

A thesis submitted in partial fulfilment of the requirements for

the degree of Doctor of Philosophy

March 2014

## CERTIFICATE OF ORIGINALITY

I hereby declare that this thesis is my own work and that, to the best of my knowledge and belief, it reproduces no material previously published or written, nor material that has been accepted for the award of any other degree or diploma, except where due acknowledgement has been made in the text.

OU Yang

# Abstract

Nowadays, urban areas keep growing as a result of rapid economic development, technological advances and population migration. Recognition of an urban area means the identification of the spatial extent of the urban area. It is important to recognize the urban areas of cities, because it provides a basis for classifying urban and rural populations, monitoring and analyzing urban growth, and making governmental decisions and policies. In recent years, increasing availability of remotely sensed data and processing techniques facilitate the development of new approaches to studying urban issues. Remote sensing based approaches have been widely developed for urban land cover / land use classification, urban object extraction and urban landscape analysis. Some efforts have been made to recognize urban areas from remote sensing images, but these methods consider urban area as a thematic class and identify urban areas through a per-pixel classification. These methods do not recognize an urban area as a geographical entity. This research aims to develop an algorithm to recognize urban areas using remote sensing data and techniques. It reviews currently definitions of urban areas to identify common urban characteristics and urban-rural differences from them. Based on the urban-rural differences, relevant information and processes are selected to compose the algorithm.

Four urban characteristics are identified through a review of current urban definitions. They are a) urban areas contain large and dense built-up areas; b) urban areas contain heterogeneous elements; c) urban areas are dominant by non-agricultural activities; and d) urban areas are distinguishable from their surrounding rural areas. Eight remote sensing image features are related to the urban characteristics, they are, the four proportions of vegetation, impervious surface, soil and water / shade, and the four textural features including angular second moment, inverse difference moment, contrast and entropy. They correspond to two types of information. Four proportional features correspond to land cover composition, and four textural features correspond to land cover configuration. The experiment results show that the combination of the eight features is valid for characterizing different kinds of areas and effective for distinguishing between urban and rural areas. The multi-resolution image segmentation algorithm is suitable for dividing a city region into homogeneous sub-regions that accord with the physical landscape. In the experiment of the algorithm with Landsat TM data, all the seven spectral bands show a decrease in the average grey-level range along a continuous region splitting process performed for all administrative regions of the study area. The average grey-level ranges in six of the seven bands are further reduced by removing the administrative boundary constraint. An urban area is successfully recognized through an iterative clustering and merging process, performed on the homogeneous regions output from the image segmentation process with the eight proportional and textural features. An experiment shows that the iterative clustering and identification is able to identify an area that can be definitely labelled as urban. Another experiment shows that the iterative merging process is able to identify the urban and rural areas of a city region with the maximum distance between them in the feature space. The resulting urban area is evaluated by a fact consistency checking. By overlapping the resulting urban area with some referenced data, it is verified that all the facts identified about the study area are satisfied by the recognition result.

# Acknowledgements

I would like to express my sincere gratitude to my supervisors, Prof. Zhilin Li and Prof. Lilian Pun. I made many mistakes before finding my way. Without their professional advice and patient guidance, I could not have completed this thesis. I am also indebted to Prof. Wu Chen for his support and encouragement.

I am thankful to the Hong Kong Polytechnic University and the Global Land Cover Facility of the University of Maryland for offering the remotely sensed data, to the GADM database of Global Administrative Areas for providing the administrative boundary data, and to the U.S. Census Bureau for providing the data of urban areas used in this thesis.

I would also like to express my special thanks to my family, for long distance love and support. I appreciate everyone who taught me, encouraged me and helped me during these years in Hong Kong.

# Table of Contents

# List of Figures

# List of Tables

# List of Abbreviations

| | |
|---|---|
| **ETM** | Enhanced Thematic Mapper |
| **GIS** | Geographical Information System |
| **GLCM** | Gray-Level Co-occurrence Matrix |
| **MNDWI** | Modified Normalized Difference Water Index |
| **MNF** | Minimum Noise Fraction |
| **MODIS** | Moderate Resolution Imaging Spectroradiometer |
| **MSAVI** | Modified Soil Adjusted Vegetation Index |
| **NDBaI** | Normalized Difference Barren Index |
| **NDBI** | Normalized Difference Built-up Index |
| **NDSI** | Normalized Difference Snow Index |
| **NDVI** | Normalized Difference Vegetation Index |
| **NDWI** | Normalized Difference Water Index |
| **PCA** | Principal Component Analysis |
| **PPI** | Pixel Purity Index |
| **RMS** | Root Mean Square |
| **SAR** | Synthetic Aperture Radar |
| **SAVI** | Soil Adjusted Vegetation Index |
| **SPOT** | a satellite name (French: *Satellite Pour l'Observation de la Terre*) |
| **TM** | Thematic Mapper |
| **V-I-S** | Vegetation-Impervious surface-Soil |

# Chapter 1 Introduction

An urban area is a concentration of human beings and activities. Nowadays, urban areas keep growing as a result of rapid economic development, technological advances, and population migration (Brockerhoff, 2000). Urban areas are spreading into their surrounding landscapes, sucking food, energy, water and resources from the natural environment (Netzband and Jurgens, 2008). The process of turning rural places into urban areas is called urbanization, which can be reflected by the growth of urban population. The world urban population increased from less than 30% by 1950 to over 50% by 2011. It is predicted that it is going to increase by 72% from 3.6 billion in 2011 to 6.3 billion in 2050 (United Nations, 2012). As urban problems are closely related to human life, a range of disciplines related to urban areas have been established, including Urban Geography, Urban Sociology, Urban Economics, Urban Ecology, Urban Anthropology, Urban Morphology and Urban Planning. In recent years, increasing availability of remotely sensed data and processing techniques facilitate the development of new tools and approaches for urban studies.

## 1.1 Importance of Urban Area Recognition

Recognition of urban areas is a primary step in analyzing natural and human phenomena and processes, such as transformation of landscapes and change in population structure. Results are important for making governmental decisions or policies. For example, the United States Census Bureau began defining and identifying urban and rural areas in 1880. It states in its documentations of *Urban and Rural Classification* that “the Census Bureau delineates urban and rural areas for statistical purposes; that is, to tabulate and present data for the urban and rural population, housing, and territory within the United States, Puerto Rico, and the Island Areas" and that "the urban and rural classification provides an important baseline for analyzing changes in the distribution and characteristics of urban and rural populations…also supports the Office of Management and Budget's delineation of metropolitan and micropolitan statistical areas". Specifically, the following use of urban area data are mentioned (US Census Bureau, 2015).

a) The National Center for Education Statistics uses the urban and rural definitions in its locale codes classification.
b) The US Department of Agriculture uses the urban-rural classification as the basis for various urban and rural classifications used to analyze and report on demographic and economic patterns in rural areas.
c) Federal Highways Administration uses the urbanized areas to qualify Metropolitan Planning Organizations.
d) Other government agencies use the urban and rural definitions to determine program eligibility and funding formulas for making the grants.
e) Data users and researchers analyze the urban and rural areas and data tabulated for those areas for urban and rural population and housing.
f) Analysts use urban area data to study patterns of urbanization, suburban growth and development, and urban/rural land area change.

The recognition of urban areas is an important process. Many findings or decisions made by governmental, commercial and research organizations are based on it.

## 1.2 Automated Urban Area Recognition: State-of-the-Art

An urban area is a concentration of human beings and activities. Recognition of an urban area means the identification of the spatial extent of the urban area. This section describes how an urban area is represented in a data form that supports the applications and analyses mentioned in Section 1.1, and existing methods for producing the urban area data.

### 1.2.1 Representations of Urban Areas

An urban area is a geographical entity, with spatial information, thus it is represented as spatial data of the object model, comprise a number of literal attributes, e.g. its name and size, and a spatial attribute, i.e. a geometry representing its spatial extent. This kind of spatial data is stored in vector data formats, for use in Geographic Information Systems (GIS). For example, Figure 1.1 shows a part of the urban area data produced by the U.S. Census Bureau. To clarify the locations of the urban areas, a Google Map layer is laid beneath the data layer. The urban areas are displayed in light red, in order to make a clear contrast with the base map.

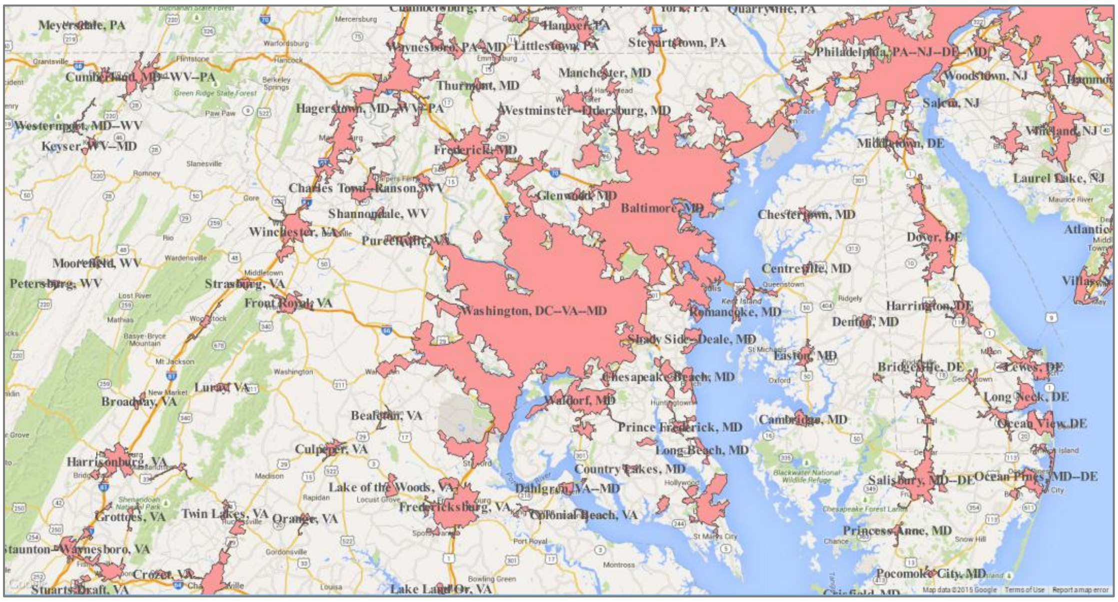


Figure 1.1 Representation of Urban Areas as Polygons

Geometrically, each urban area is represented as a polygon. A clear boundary is drawn for the urban area. Figure 1.2 indicates the urban boundary of Washington DC-VA-MD. It can be seen from this urban area that the U.S. Census Bureau considers some parts of three districts, i.e. Washington DC, VA and MD, as a single urban area. Also, it can be seen that the urban area contains some holes, which means that single-connectedness is not required in U.S. Census Bureau’s realization of an urban area.


Figure 1.2 The Urban Boundary of Washington DC-VA-MD

Besides vector data, urban areas can also be found represented as binary images. Each image pixel is of one of the two possible values, i.e. urban (foreground) or non-urban (background). Figure 1.3 shows a raster image of urban areas in Beijing, produced using the urban area extraction method of Zha et al. (2003). The black line delineates the administrative boundary of Beijing. The image background is white and urban pixels are displayed in red. This kind of representation results from image classification methods, in which urban area is not conceptualized as a geographical entity but a thematic class. The classification process determines whether the area covered by the pixel is urban or not.

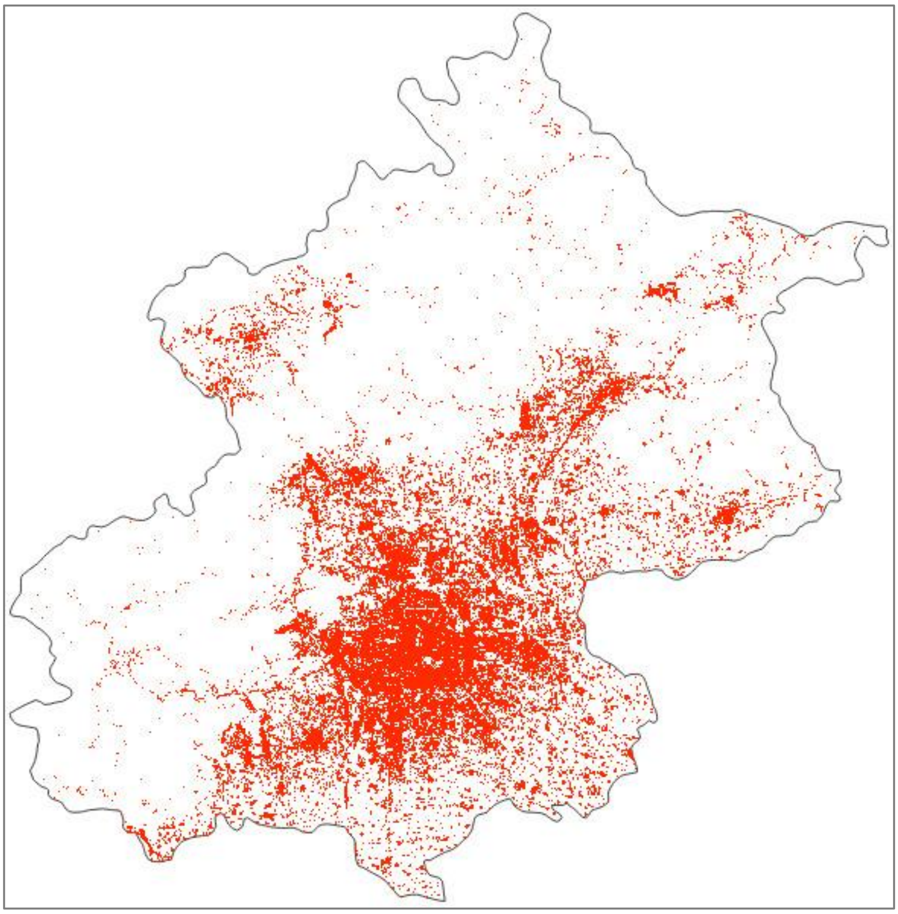

Figure 1.3 Binary Image Representation of Urban Areas

### 1.2.2 Recognition of Urban Areas

Recognition of an urban area means the identification of the spatial extent of the urban area. In other words, an urban-rural boundary can be drawn to delineate an urban area as a geographical entity, as shown in Figure 1.2. Traditionally, it is done by censuses and surveys. Census and survey data provide most of the knowledge of the social environment of places. However, it is recognized that there is a spatial mismatch in census data, as people are enumerated at their places of residence, who typically work in a different location during the daytime. Moreover, the cost of generating and maintaining census and survey data is enormous. Furthermore, the urban and rural areas classification using census and survey data is not efficient. In recent years, increasing availability of remotely sensed data and processing techniques facilitate the development of new approaches to studying urban issues. Some methods have been developed to recognize urban areas using remote sensing images and techniques. Due to the raster nature of image data, these methods are classification approaches. The per-pixel classification process determines whether the area covered by the pixel is urban or not, but no boundary is drawn to delineate an urban area. The urban area is not conceptualized as a geographical entity but a thematic class. Hence, these classification based methods do not really identify a geographical entity, but produce a raster representation of the environment, as shown in Figure 1.3. An approach to recognize urban areas as geographical entities using remote sensing images and techniques is still needed to be developed.

## 1.3 Aim and Objectives

This research aims to develop an algorithm for urban area recognition by extracting urban areas as geographical entities with distinct boundaries. In order to achieve this aim, the following objectives need to be fulfilled:

a) To identify urban features from images for rural-urban separation;

b) To develop an algorithm for automating the identification of the boundary of an urban area.

## 1.4 Thesis Outline

Apart from this introductory chapter, the rest of this thesis is organized as follows.

Chapter 2 reviews current definitions of urban area, including census definitions used by different countries and urban scholars' definitions adopted in urban studies. Common characteristics of an urban area are identified from those definitions. It then reviews some remote sensing techniques that are widely used in urban studies. Both traditional and remote sensing based methods for urban area recognition and their problems are discussed.

Chapter 3 describes a new strategy for recognizing urban areas using remote sensing images and techniques. Firstly, the urban-rural differences are formulated by summarizing the urban characteristics identified in Chapter 2. Secondly, based on the urban-rural differences, relevant information and processes are identified to develop an algorithm for urban area recognition. The proposed algorithm comprises four steps, i.e. zoning, clustering, identification and merging. Finally, the study area used throughout the research is described in detail.

Chapter 4 identifies eight remote sensing image features that are related to the urban characteristics. The eight features correspond to two types of information. Four proportional features correspond to land cover composition, and four textural features correspond to land cover configuration. Experiments are conducted to evaluate if the eight features are effective to characterize urban and rural areas. The eight features are extracted from Landsat TM data for the sixteen administrative regions of the study area. K-means clustering algorithm is applied to classify the regions into two, three and four groups respectively. By comparing the clustering results with the reference divisions, the eight features show a pattern that is consistent with the referenced data.

Chapter 5 discusses the zoning method for the approach. The multi-resolution segmentation algorithm is used to divide a city region into homogeneous sub-regions that accord with the physical landscape. An experiment is conducted to compare the homogeneous division with the administrative division. A continuous region splitting process is developed to observe the change of the average grey-level ranges in all image bands. The administrative boundary constraint is further removed to see if the resulting regions become more homogeneous.

Chapter 6 proposes an iterative clustering and merging algorithm for urban area recognition, which is applied on the output regions of the zoning step, with the eight proportional and textural features. A clustering analysis is made for observing the change of output clusters along a series of clustering operations. A merging analysis is then made for observing the change of the distance between urban and rural areas in the feature space along a series of merging steps. The result shows that the proposed algorithm recognizes the urban area successfully. The recognized urban area is evaluated by overlapping it with referenced data to check if it satisfies the facts about the study area.

Finally, Chapter 7 concludes the thesis. A summary and the main conclusions of the research are presented. Limitations are explained and future work is proposed.

# Chapter 2 Remote Sensing Based Urban Area Recognition: A Review

This chapter firstly reviews current definitions of urban area, including census definitions used by different countries, and urban scholars' definitions adopted in urban studies. It then reviews remote sensing techniques that are widely used in urban studies, including urban land cover / land use classification, urban object extraction and urban landscape analysis. Both traditional and remote sensing based methods for urban area recognition and their problems are discussed.

## 2.1 Definitions of an Urban Area

The *Oxford English Dictionary* defines 'urban' as 'relating to, situated or occurring in, or characteristic of, a town or city, esp. as opposed to the countryside' (Oxford University Press, 1989). The word 'urban' is in itself adjectival and needs to be allied with another word, such as population or area. The strongest contemporary research focus is less concerned with defining urban as a quality than with defining urban areas as entities, i.e. cities in the literature (Herbert and Thomas, 1990). Most people recognize a city easily when they see one, but no one finds a way to define it easily. It is undoubtful that no single definition can apply to all cities or even to the same city at different times. For census purpose, many countries or regions have developed their own quantitative criteria to classify cities or urban areas. For analytical purpose in urban studies, qualitative definitions are of greater interest, which identify the unique nature of human activities and way of life that make a place a distinct urban character. This section reviews urban definitions by these two types, and identifies the common urban characteristics implied in these definitions.

### 2.1.1 Census Definitions (Quantitative Definitions)

For census purpose, quantitative definitions are of interest as they affect the estimate of urban population. The criteria for defining an urban area vary from one country or region to the other. Of the 228 countries tracked by the United Nations, 36% use strictly administrative division, 25% use population size and 11% have no definitive criteria (Beall and Fox, 2009). A list of urban definitions of 124 countries can be found in the latest available United Nations Demographic Yearbook (UNDESA, 2013). From those national definitions used for demographic estimates and projections, some common criteria are identified and summarized in Table 2.1. The current census definitions of urban area are based on one or more criteria.

Table 2.1 Common Criteria in Census Definitions of Urban Area

(Example definitions are taken from (UNDESA, 2013))

| **Criterion** | **Example** |
|---|---|
| population size | Iceland: Localities of 200 or more inhabitants. |
| population density | Canada: Places of 1,000 or more inhabitants, having a population density of 400 or more per square kilometer. |
| building density | France: Communes containing an agglomeration of more than 2,000 inhabitants living in contiguous houses or with not more than 200 meters between houses, also communes of which the major portion of the population is part of a multi-communal agglomeration of this nature. |
| dominant type of economic activity | Netherlands: Urban: Municipalities with a population of 2,000 and more inhabitants. Semi-urban: Municipalities with a population of less than 2,000 but with not more than 20 per cent of their economically active male population engaged in agriculture, and specific residential |

| | |
|---|---|
| | municipalities of commuters. |
| conformity to legal or administrative status | Egypt: Governorates of Cairo, Alexandria, Port Said, Ismailia, Suez, frontier governorates and capitals of other governorates, as well as district capitals (Markaz). |
| urban characteristics | Panama: Localities 1,500 or more inhabitants with such urban characteristics as streets, water supply systems, sewerage systems and electric light. |

The use of single criterion of population size is the most popular, which is adopted by more than 50 countries. This is because it is technically simple and the information base of statistics is readily available. Over 30 countries use only administrative divisions. Many countries adopt more than one criterion. For example, India uses a combination of four criteria to define an urban area. It can be seen that the definitions differ significantly, though some criteria are common. Large differences can also be found in each single criterion type. For example, Denmark and Sweden use a population size criterion of a minimum of 200 inhabitants, while Japan uses 50,000.

The United Nations accepts each country's definition for calculating urban population estimates and projections based on the assumption that governments know best what features distinguish urban from rural places in their own countries (Brockerhoff, 2000). Nevertheless, it pointed out that there are shortcomings in using those census definitions. Not only do the definitions differ from one country to the other, but they may also no longer reflect the original intention for distinguishing urban from rural. The urban areas that are defined based on administrative divisions become fixed and resistant to change. Comparisons of time-series data of those areas are not useful.

In china, the National Bureau of Statistics of the People's Republic of China defines an urban area based on administrative division and some census criteria. That is to say, urban areas are classified from administrative districts, and urban boundaries are in accordance with administrative boundaries. Such a kind of urban definition gives rise to two problems. Firstly, the urban boundaries are fixed, and the urban areas do not necessarily accord with the physical extents of the urban landscape. Secondly, the urban areas change according to administrative and governmental policies, rather than to the urbanization process that transforms the physical environment. During 1980s, the government took a number of administrative actions to turn countries into cities, resulting in a dramatic increase of the number of cities and towns. The proportion of urban population increased from 20.6% in the third national census in 1982 to 51.7% in 1989, of which 63.5% are agricultural population. Up to then, the urban and rural concepts made no sense at all. Due to such a fact, some international organizations, e.g. United Nations and World Bank, did not accept the population statistics of China after 1982. Thereafter, the fourth national census in 1990 amended the criteria for the urban-rural division to fix the problem. The proportion of urban population fell back to 26.23% (Xu et al., 1997). Figure 3.1 shows the administrative division of Beijing, China. Correspondingly, Table 2.2 shows the population data of those administrative districts of Beijing, which were collected by the fifth and the sixth national censuses in 2000 and 2010 respectively (National Bureau of Statistics PRC, 2001; 2012). According to the population density criterion of a minimum of 1,500 people per square kilometers in the *Regulation on the Division of Urban and Rural Areas in Statistics* published by the National Bureau of Statistics in 1999, the urban area of Beijing is indicated in Figure 2.1. The urban area includes six administrative districts (districts 1 to 6 in Figure 2.1).

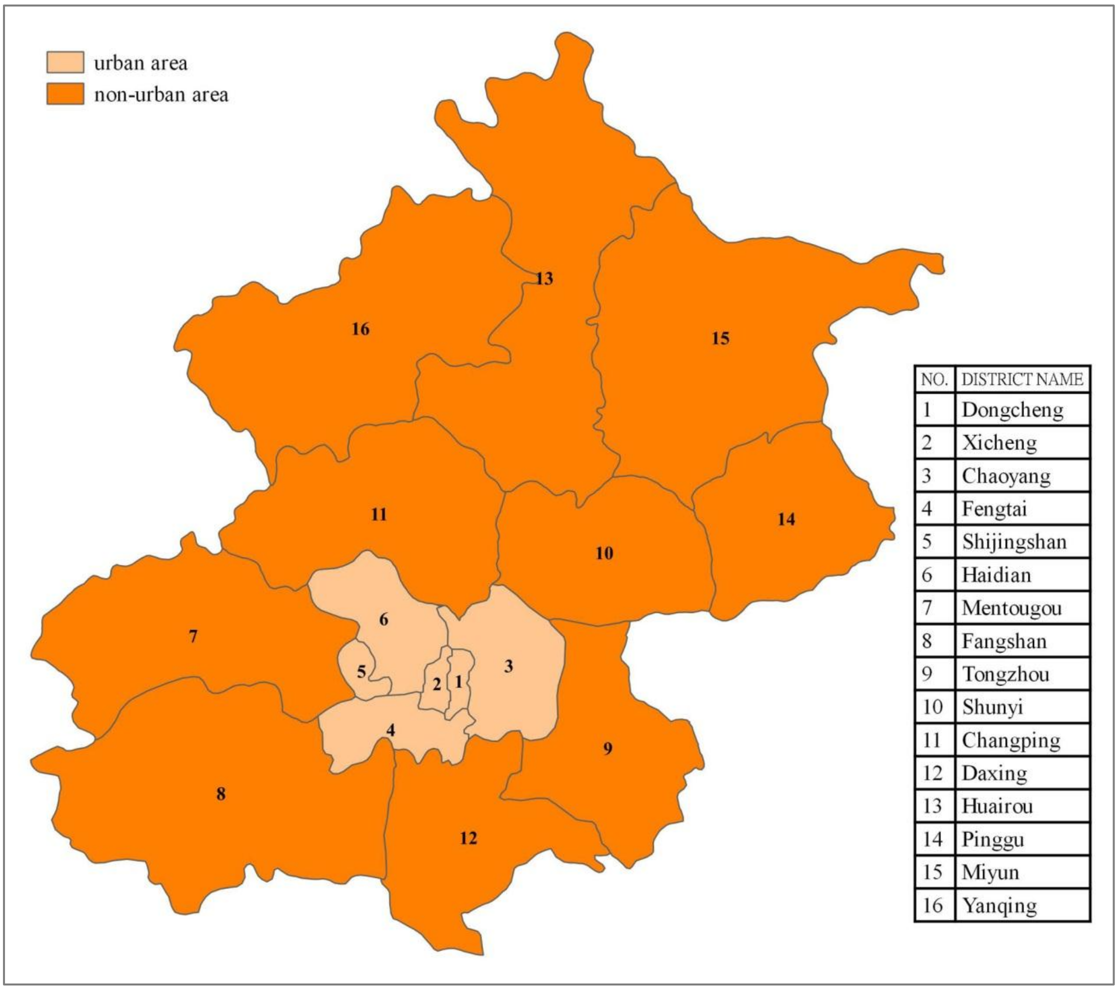


Figure 2.1 Administrative Regions of Beijing, China

Table 2.2 Population Distribution of Beijing in 2000 and 2010 (National Bureau of Statistics PRC, 2001; 2012)

| **District Name** | **Area ($km^2$)** | **Population in 2000 (people)** | **Population Density in 2000 (people/$km^2$)** | **Population in 2010 (people)** | **Population Density in 2010 (people/$km^2$)** |
|---|---|---|---|---|---|
| Dongcheng | 42.0 | 882,000 | 21,000 | 919,000 | 21,881 |
| Xicheng | 51.0 | 1,233,000 | 24,176 | 1,243,000 | 24,373 |
| Chaoyang | 470.8 | 2,290,000 | 4,864 | 3,545,000 | 7,530 |
| Fengtai | 304.2 | 1,369,000 | 4,500 | 2,112,000 | 6,943 |
| Shijingshan | 89.8 | 489,000 | 5,445 | 616,000 | 6,860 |
| Haidian | 426.0 | 2,240,000 | 5,258 | 3,281,000 | 7,702 |
| Mentougou | 1,331.3 | 267,000 | 201 | 290,000 | 218 |
| Fangshan | 1,866.7 | 814,000 | 436 | 945,000 | 506 |

| | | | | | |
|---|---|---|---|---|---|
| Tongzhou | 870.0 | 674,000 | 775 | 1,184,000 | 1,361 |
| Shunyi | 980.0 | 637,000 | 650 | 877,000 | 895 |
| Changping | 1,430.0 | 615,000 | 430 | 1,661,000 | 1,162 |
| Daxing | 1,012.0 | 672,000 | 664 | 1,365,000 | 1,349 |
| Huairou | 2,557.3 | 397,000 | 155 | 373,000 | 146 |
| Pinggu | 1,075.0 | 296,000 | 275 | 416,000 | 387 |
| Miyun | 2,335.6 | 420,000 | 180 | 468,000 | 200 |
| Yanqing | 1,980.0 | 275,000 | 139 | 317,000 | 160 |

From Table 2.2, the total population of Beijing in 2010 was 19,612 thousands. Compared to 13,570 thousands in 2000, it increased by 44.5%. The population of the six districts that comprise the urban area increased by 34.7%, from 6,263 thousands to 8,435 thousands. However, if using the criteria of population density, the urban area was unchanged, which did not reflect the evident urban growth over ten years as reflected by the increase of population. In fact, the National Bureau of Statistics recognized the problems resulted from the use of the population density criterion. In the amended *Regulation on the Division of Urban and Rural Areas in Statistics* that has been effective since 2008, it abolished the use of the population density criterion, and defined the basis of the division of urban and rural areas as built facilities, which were further defined as public facilities, residential facilities and other facilities that were built up or under construction (National Bureau of Statistics PRC, 2006; Qiu, 2012). It is reflected in this definition that the physical environment, instead of people, characterizes a place. Urban areas are geographical entities that are determined by its physical landscape rather than by administrative designation. Such a kind of view is of more interest by urban scholars. The urban scholars' definitions are reviewed in the next section.

### 2.1.2 Urban Scholars' Definitions (Qualitative Definitions)

Different from the census definitions, which are simply and technically used for estimates of urban populations, scholars in urban studies are more interested in those qualitative definitions that reflect the relationship between man and environment. Scholars from a number of disciplines are interested in urban phenomena, including geographers, sociologists, historians and philosophers. They made an effort to define an urban area, i.e. a city in the literature, some of which are widely accepted and used in urban studies. Table 2.3 lists several famous urban scholars' definitions that are widely cited in Urban Geography and Sociology books (e.g. Johnson, 1972; Berger, 1978; Herbert and Thomas, 1990; Paddison, 2001; Kaplan et al., 2004; Lorinc, 2008; Beall and Fox, 2009; Knox and McCarthy, 2012; Harding and Blokland, 2014).

Table 2.3 Urban Scholars' Definitions of Urban Area

| **Author** | **Definition** |
|---|---|
| Maunier (1910) | A city is a complex community of which the geographic localization is especially limited in relation to the city's size, of which the amount of territory is relatively small with reference to the number of human beings |
| Mumford (1937) | The essential physical meanings of a city existence are the fixed site, the durable shelter, the permanent facilities for assembly, interchange, and storage; the essential social meanings are the social division of labor, which serves not merely the economic life but the cultural processes. The city in its complete sense, then, is a geographical plexus, an economic organization, an institutional process, a theater of social action, and an aesthetic symbol of collective unity. |
| Wirth (1938) | A city is a relatively large, dense, and permanent settlement of socially heterogeneous individuals |

| | |
|---|---|
| Childe (1950) | A city is defined with 10 general metrics:<br>Size and density of the population should be above normal.<br>Differentiation of the population. Not all residents grow their own food, leading to specialists.<br>Payment of taxes to a deity or king.<br>Monumental public buildings.<br>Those not producing their own food are supported by the king.<br>Systems of recording and practical science.<br>A system of writing.<br>Development of symbolic art.<br>Trade and import of raw materials.<br>Specialist craftsmen from outside the kin-group. |
| Sjoberg (1965) | A city is a community of substantial size and population density that shelters a variety of non-agricultural specialists, including a literate elite. |
| Wheatley (1969) | particular set of functionally integrated institutions which were first devised some five thousand years ago to mediate the transformation of relatively egalitarian, ascriptive, kin-oriented groups into socially stratified, politically organized, territorial based societies, and which have since progressively extended both the scope and autonomy of their institutional spheres so that today they mold the actions and aspirations of vastly the larger proportion of mankind |

It can be seen from those definitions that urban scholars pay more attentions than census definitions to the social, economic, political and cultural aspects that make urban places different from rural ones. Among those scholars, Louis Wirth was a well-known sociologist of the Chicago School. His article *Urbanism as a Way of Life* is a classic in the study of urbanism (Wirth, 1938). His definition of a city (see Table 2.3) has been regarded as one of the most basic and enduring definitions by urban geographers (Beall and Fox, 2009). He argued that these conditions, i.e. size, density, and heterogeneity, create a distinctly urban way of life and an identifiable urban personality.

Lewis Mumford, who is known as one of the greatest urban scholars of the twentieth century, defined a city in terms of its physical and social aspects (see Table 2.3). His definition highlights the spatial dynamics of a built environment that serves as a 'theater' of human interactions as well as a reflection of social relations. Similar to Wirth's view, Mumford also paid an attention to the fundamental influences of size and density in his article *What is a City* (Mumford, 1937). Although many urban scholars have sought to define or redefine a city, the definitions offered by Wirth and Mumford are cited as fundamental and universal ones by contemporary scholars, as they are defining characteristics of urban agglomerations over time and everywhere (Beall and Fox, 2009).

### 2.1.3 Common Urban Characteristics

From the current definitions of urban area, two facts can be drawn. Firstly, there is no universal, determinate and stable definition of an urban area. Census statisticians recognize that no international standard definition appears to be possible. Likewise, urban scholars argue that current various approaches to urban definition have not given rise to any consensus view, and will inevitably be inconclusive, because an urban area is a complicated phenomenon, and the meaning of urban varies considerably over both space and time. Secondly, however, some characteristics are common. No matter when and where, for census or urban studies, urban is used to distinguish people or places from rural counterparts. This section identifies those characteristics that are commonly used for or implied in various definitions of urban area, which are discussed in the following sub-sections.

#### 2.1.3.1 Large Size and Density of Built-up Areas

Obviously, size and density are important and widely used criteria in urban definitions. Such measures can be applied to describe either people or places. In census definitions, they are mostly applied to population. In urban scholars' definitions, some apply them to population, e.g. Childe's, while the others apply them to settlement, e.g. Wirth's. Size and density of population and those of settlement are related. Large and dense population requires large and dense built-up space to accommodate it. Recent research pointed out that the use of population to define an urban area resulted in a bias in the classification of a place, as people are enumerated at their place of residence, while urban residents typically work in a different location from where they live (Weeks, 2008). This view is also reflected by the latest census definition of urban area of China, which abolished the use of the population density criterion, and classifies urban and rural areas based on built facilities instead, as reviewed in Section 2.1.1. Even if the size and density are used to describe population or built-up space in different definitions, a common view shared by those definitions is that they are large in urban areas. All census definitions that use the criterion of population size or density apply a minimum threshold of it, but a maximum threshold never exists. Also, urban studies share the same view in all time. However, how large they should be for defining urban is impossible to conclude. Census definitions adopt various and varying minimum thresholds. Urban scholars' definitions are more indeterminate in qualifying size and density, such as 'relatively large' in Wirth's definition, 'above normal' in Childe's, 'substantial' in Sjoberg's (see Table 2.3). From the above discussion, the first common urban characteristic implied in those definitions is that urban and rural areas are distinguishable by the size and density of built-up areas where human beings and activities concentrate. An urban area is identifiable at a certain point along the size and density continuum.

#### 2.1.3.2 Composition and Configuration of Heterogeneous Elements

Wirth (1938) argued that no definition based on size alone would be adequate. Definitions based on population density give rise to the same objections, as people come to a place to work during the day and leave at night, reducing both the size and density of population below that observed elsewhere. Wirth included a third condition for defining and identifying an urban area, i.e. heterogeneity. This condition implies that an urban area must be composed of different elements. This can be found in urban scholars' definitions, such as 'a community' in Sjoberg's definition, 'a complex community' in Maunier's, 'a geographical plexus' in Mumford's, 'systems' in Childe's, 'particular set of functionally integrated institutions' in Wheatley's. An urban area as a complex system results in a composition of heterogeneous elements in its physical environment, as human activities decide the construction, organization and use of space. The second common urban characteristic is that an urban area is a composition and configuration of heterogeneous elements. In contrast, a rural area appears more homogeneous.

#### 2.1.3.3 Dominance of Non-Agricultural Activities

Another distinct common view easily found in the current definitions of urban area is that 'urban' implies 'non-agricultural'. From those census definitions that employ the criterion of dominant type of economic activity, it can be seen that no specific kinds of activities are explicitly required for an urban area, but agricultural activity is excluded, e.g. Netherland, India and Israel. This can also be seen in the definitions of urban scholars, e.g. Childe's 'not all residents grow their own food, leading to specialists' and Sjoberg's 'a variety of non-agricultural specialists'. Urban geographers have provided the explanation of the requirement of dominance of non-agricultural activities for defining an urban area. This urban characteristic is related to urban origins. There are a number of theories of urban origins, one of which is agricultural surplus (Childe, 1950; Woolley, 1963; Johnston, 1980). Earlier farmers produced enough food to feed themselves and their family. They became better to produce more food than needed for them. Such an agricultural surplus allowed for a social surplus. It freed up resources so that not every person had to farm, who was then able to pursue non-agricultural work, which resulted in an early division of labor between farmers and non-agricultural specialists, and in later stratified social structures and institutions that created the urban way of life. An early argument on the urban origin in terms of the need of non-agricultural specialists was identified in Plato's *The Republic* (Herbert and Thomas, 1990). This became a common view shared along the history of urban studies. Urban scholars considered non-agricultural 'specialist' and 'elite' as essential when they attempted to define an urban area. From the above discussion, the third common urban characteristic is identified, that is, an urban area is a place dominant by non-agricultural activities.

#### 2.1.3.4 Distinction from Surrounding Area

A recent trend of the definitional arguments is based on the concept of urbanism, which was developed by Wirth (1938). Urbanism is defined as "the way of life unique to habitation in a city". Urban scholars acknowledge that the unique nature of the social, political, economic and cultural life of cities, i.e. urbanism, makes urban a distinct character. An urban area is a district in which the urban way of life is clearly present. Also, from the first three common urban characteristics discussed above, it can be seen that though urban scholars failed to quantify the features they selected to define an urban area, it is a consensus view that urban is distinguishable and identifiable quality. Therefore, the fourth common urban characteristic implied in urban definitions is that an urban area is an area that is clearly distinguishable from its surrounding area.

In conclusion, an urban area can be defined by integrating the four urban characteristics as an area that is composed of large and dense built-up areas, of heterogeneous elements, where non-agricultural activities take place, and is clearly distinguishable from its surrounding area. These characteristics can be measured and analyzed using remote sensing techniques.

## 2.2 Remote Sensing for Urban Studies

Remotely sensed data are increasingly available in a digital form. Powerful image processing methods are developed to extract information of various objects and phenomena on the earth surface in a computer-aided or fully automated manner. Remote sensing techniques have been widely used in urban studies for classifying urban land cover and land use, extracting urban objects and analyzing urban landscape. This section reviews the remote sensing techniques that are widely used in urban studies.

### 2.2.1 The Vegetation-Impervious Surface-Soil (V-I-S) Model

The Vegetation-Impervious Surface-Soil (V-I-S) model was developed as a theoretical foundation for characterizing urban environment universally and for comparing urban morphology within or between cities (Ridd, 1995). It has been suggested that the great variety of urban land cover can be grouped into three general categories (Figure 2.2): green vegetation, impervious surface (e.g. roads and building roofs), and soil, since they exhibit highly contrasting influences on the two most important factors in an ecosystem: energy and moisture flux. Variations in each category can be further recognized by identifying sub-categories of vegetation, impervious surfaces, and soil. Each place is viewed as a linear composition of the three land cover types. An area composed entirely of vegetation would be a dense forest, grassland or field of crops, whereas an area containing a large proportion of bare soil would be characteristic of desert wilderness, both of which mostly exist in natural or rural environment. A high percentage of surfaces impervious to water usually indicate an area of building blocks, driveways or parking lots, which is highly relevant to artificial or urbanized environment.

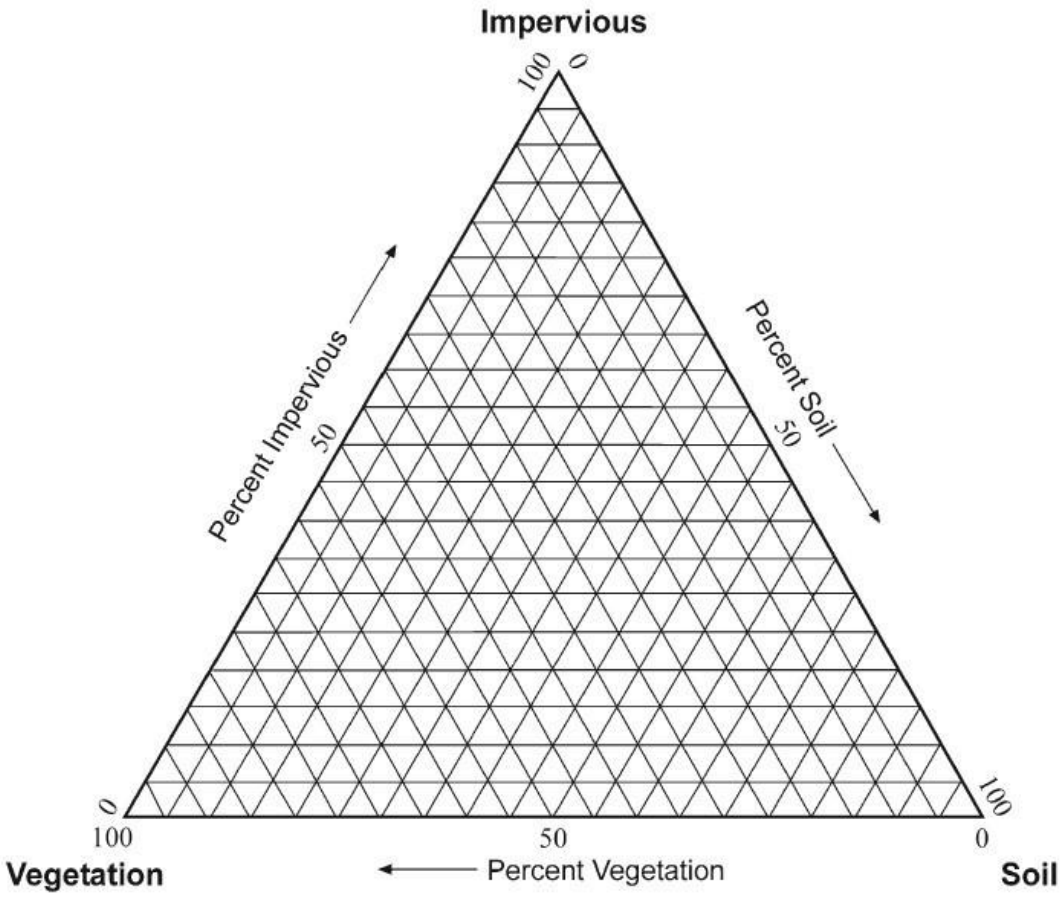


Figure 2.2 The V-I-S Model of Land Cover Composition (Ridd, 1995)

The composition of the three cover types differs between urban and rural environment, as well as among various kinds of urban environment. The change in composition reveals the change in environment, which can be used to describe the process of urbanization. The V-I-S model is capable of capturing such environmental differences and changes, as illustrated in the following figures.

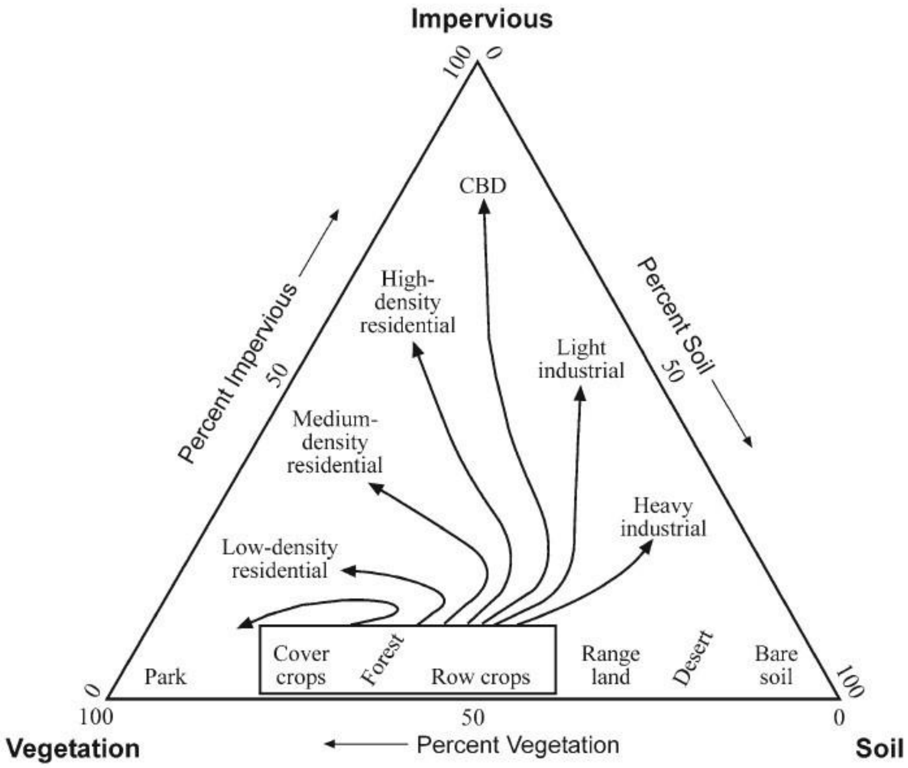


(a) V-I-S transitions from green landscapes to urban features

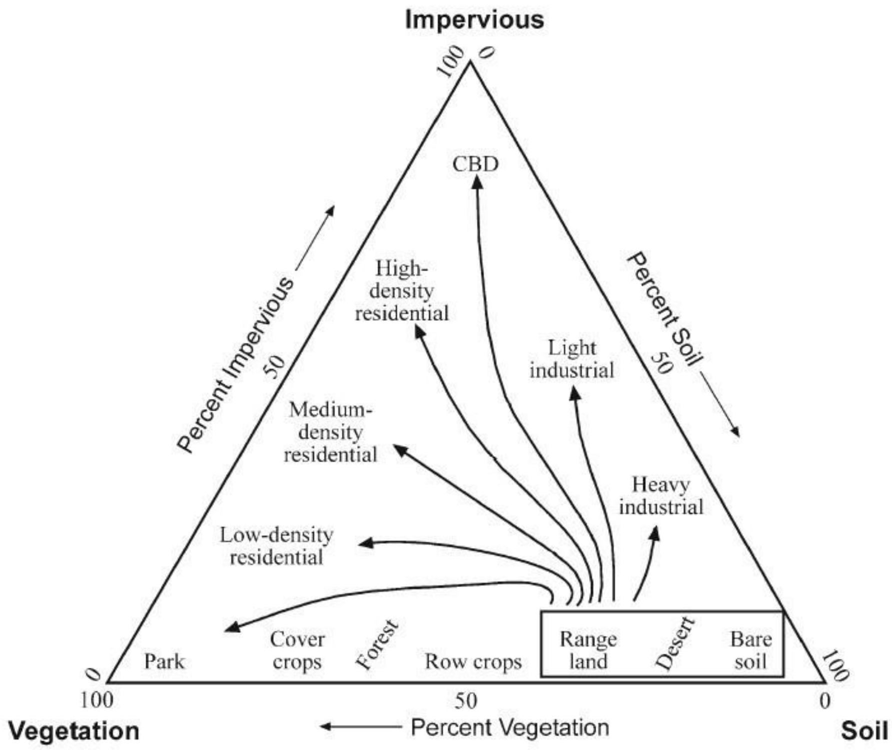


(b) V-I-S transitions from dry landscapes to urban features

Figure 2.3 Environmental Changes and Differences in V-I-S Composition (Ridd, 1995)

The V-I-S model can be applied on various scales of observation. V-I-S composition can be calculated within a pixel, a group of pixels covering a certain range or an entire urban region.

The fourth component, i.e. water or shade, was suggested for improving the model in settings outside the United States (Ward et al., 2000). When combined with impervious surfaces in urban areas, it becomes a measure of building height based on the shadows cast by buildings. When combined with vegetation, it provides a measure of the amount of water in soil and the shade cast by tall vegetation. In combination with bare soil, it is largely a measure of shadows cast by trees, although there can be some components of shade from large buildings in heavy industrial areas (Weeks et al., 2005). Shades are hardly to be separated from water bodies, since the two kinds have similar spectral signatures that record low reflectance of energy.

To sum up, the V-I-S model suggests that the four components (i.e. vegetation, impervious surfaces, soil, and water/shade), are a basic division of land cover, and each of them can be further divided into sub-classes. Although there are more than three basic classes in the model, and usually many sub-classes in different classification schemes extending the model, it is still referred to as the V-I-S model. The V-I-S model is widely used in urban remote sensing research as a classification scheme for deriving compositional information (e.g. Chen, 1996; Ward et al., 2000; Madhaven et al., 2001; Hung, 2003; Kaya et al., 2004; Weeks et al., 2005; Gluch et al., 2006; Qiao et al., 2009; Tang et al., 2012; Deng and Wu, 2013; Zhang et al., 2014).

### 2.2.2 Remote Sensing Image Features for Urban Studies

#### 2.2.2.1 Spectral Features

Spectral indices are a kind of widely used numerical indictors of various land cover types. Normalized difference spectral indices are a group of spectral indices whose values are normalized to a range from -1 to 1. They were created for discrimination of specific land cover types from others. Usually, when creating an index, a spectral band in which a target cover type shows strong reflectance and is distinct from others and a spectral band showing distinguishably weak reflectance are identified, and then the difference or ratio value of these two bands is calculated to enhance the spectral characteristic of the cover type. Spectral indices can be calculated in different ways. Normalized difference spectral indices are the most common way in which they are created, which are in a form as follows:

$$\frac{band_{strong} - band_{weak}}{band_{strong} + band_{weak}}$$

This kind of index ranges from -1 ($band_{weak}$ far exceeds $band_{strong}$, with measured spectra violating cover spectra) to 1 (measured spectra equal cover spectra). Pixels with an index over 0 are thought to be containing an amount of land cover, meaning that a higher index contains a larger amount. A number of normalized difference spectral indices have been developed for discriminating specific land cover types from remotely sensed imagery. The Normalized Difference Vegetation Index (NDVI) is the earliest one for measuring vegetation, which has been widely used in forest and agricultural assessment (Rouse et al., 1973).

$$NDVI = \frac{NIR - Red}{NIR + Red} \qquad (2.1)$$

where NIR and Red represent near-infrared and red bands respectively.

A Soil-Adjusted Vegetation Index (SAVI) was developed to minimize soil brightness influences on canopy spectra by incorporating a soil adjustment factor into the NDVI (Huete, 1988).

$$SAVI = \frac{NIR - Red}{NIR + Red + L}(1 + L) \tag{2.2}$$

where $L$ is a soil adjustment factor. Also, Huete (1988) found that the use of a constant $L$ = 0.5 could reduce soil noise effectively through a wide range of vegetation amounts.

Following this improvement, Qi et al. (1994) developed a self-adjustable functional $L$ factor, which is able to automatically optimize its value without prior knowledge of vegetation amounts. A Modified Soil Adjusted Vegetation Index (MSAVI) is then induced.

$$MSAVI = \frac{2NIR + 1 - \sqrt{(2NIR + 1)^2 - 8(NIR - Red)}}{2} \tag{2.3}$$

Almost at the same time, two kinds of Normalized Difference Water Index (NDWI) were developed (i.e. $NDWI_{McFeeters}$ and $NDWI_{Gao}$)for detecting open water bodies (McFeeters, 1996) and estimating vegetation moisture (Gao, 1996). $NDWI_{McFeeters}$ was afterwards modified to remove built-up land noise, known as the Modified Normalized Difference Water Index (MNDWI) (Xu, 2006), so it is considered more suitable for extracting water information in urban environment.

$$NDWI_{McFeeters} = \frac{Green - NIR}{Green + NIR} \tag{2.4}$$

$$NDWI_{Gao} = \frac{NIR - MIR}{NIR + MIR} \tag{2.5}$$

$$MNDWI = \frac{Green - MIR}{Green + MIR} \tag{2.6}$$

where Green, NIR and MIR represent green, near-infrared and mid-infrared bands respectively.

The Normalized Difference Snow Index (NDSI) was devised to estimate and map snow cover (Salomonson and Appel, 2004), and uses Bands 4 and 6 of Moderate Resolution Imaging Spectroradiometer (MODIS) data to define and compute the NDSI, corresponding to green and mid-infrared spectral bands respectively. As a result, the NDSI has the same form as the MNDWI.

$$NDSI = \frac{Green - MIR}{Green + MIR} \tag{2.7}$$

where Green and MIR represent green and mid-infrared bands respectively.

The Normalized Difference Built-up Index (NDBI) was developed for mapping built-up areas (Zha et al., 2003), and was referred to as the Normalized Difference Soil Index (also called NDSI) in some other kinds of literature (Rogers and Kearney, 2004). The built-up areas identified by the NDBI reflect only the local understanding of built-up areas of the authors, according to the sample spectra used in their own research.

$$NDBI = \frac{MIR - NIR}{MIR + NIR} \tag{2.8}$$

where NIR and MIR represent near-infrared and mid-infrared bands respectively.

The Normalized Difference Bareness Index (NDBaI) was developed for distinguishing bare soil (Zhao and Chen, 2005).

$$NDBaI = \frac{MIR - TIR}{MIR + TIR} \tag{2.9}$$

where MIR and TIR represent mid-infrared and thermal-infrared bands respectively.

Spectral indices can be calculated for every pixel or for groups of pixels, i.e. image segments or objects, as object features. These spectral indices are widely used in urban remote sensing studies (e.g. Ward et al., 2000; De Kok et al., 2003; Zha et al., 2003; Yuan and Bauer, 2007; Xu, 2008; Zhou and Troy, 2008; Chen et al., 2009; Lu and Weng, 2009; Zhou and Troy, 2009; Zhou et al., 2009; He et al., 2010; Taubenbock et al., 2010; Mhangara et al, 2011; Zhang et al., 2014; Shanmukha Rao et al., 2015).

**2.2.2.2 Textural Features**

Texture is one of the most important characteristics used for interpretation of remote sensing images (Tempfli et al., 2009). Haralick et al. (1973) proposed a computational approach to examining and characterizing image texture. This approach is based on the gray-level co-occurrence matrices (GLCM), which were called gray-tone spatial-dependence matrices when they were initially presented by Haralick et al. (1973; 1979). A gray-level co-occurrence matrix is a matrix of adjacency frequencies. It is square with dimension $N_g$, which is expressed as

$$\boldsymbol{G} = \begin{bmatrix} p(1,1) & p(1,2) & \cdots & p(1,N_g) \\ p(2,1) & p(2,2) & \cdots & p(2,N_g) \\ \vdots & \vdots & \ddots & \vdots \\ p(N_g,1) & p(N_g,2) & \cdots & p(N_g,N_g) \end{bmatrix} \tag{2.10}$$

where $N_g$ is the number of grey levels in the image. Element $p(i, j)$ of the matrix is generated by counting the number of times a pixel with value $i$ is adjacent to a pixel with value $j$, and then dividing the entire matrix by the total number of such comparisons made. Each entry is therefore considered to be the probability that a pixel with value $i$ will be found adjacent to a pixel of value $j$. Since adjacency can be defined to occur in each of the four directions in a two-dimensional image, e.g. horizontal, vertical, left and right diagonals, four such matrices can be generated. After creating the gray-level co-occurrence matrices, some statistical features can be derived from them. Haralick (1973) derived fourteen features from the gray-level co-occurrence matrices with the intent of characterizing texture of images. Of Haralick's fourteen features, angular second moment $f_1$, inverse difference moment $f_2$, contrast $f_3$ and entropy $f_4$ were further evaluated by Gotlieb and Kreyszig (1990) and considered as optimal texture classifiers, which are expressed as follows.

$$f_1 = \sum_i \sum_j \{p(i,j)\}^2 \tag{2.11}$$

$$f_2 = \sum_i \sum_j \frac{p(i,j)}{1 + (i-j)^2} \tag{2.12}$$

$$f_3 = \sum_{n=0}^{N_g - 1} n^2 \left\{ \sum_{i=1}^{N_g} \sum_{j=1}^{N_g} p(i,j) \right\},\ |i-j| = n \tag{2.13}$$

$$f_4 = -\sum_i \sum_j p(i,j) \log p(i,j) \tag{2.14}$$

The $f_1$ and $f_2$ are measures of homogeneity. Their values are high if the image is locally homogeneous. The $f_3$ is a measure of contrast or the amount of local variations in the image. The $f_4$ is a measure of chaos, whose value is high if the elements of the gray-level co-occurrence matrix are distributed equally. These textural features are found implemented in remote sensing software and used in urban remote sensing studies (e.g. Trias-Sanz et al., 2004; Zhou et al., 2006; Taubenbock et al., 2010; Dong et al., 2011; Mhangara et al, 2011; Han et al., 2012; Mhangara and Odindi, 2013; Yue et al., 2013; Pradhan et al., 2014; Tang and Dai, 2014; Shanmukha Rao et al., 2015).

### 2.2.3 Linear Spectral Unmixing

In remotely sensed imagery, it is very unlikely that an entire pixel captures only the energy from one kind of material. Because of the spatial resolution of a sensor, disparate materials can jointly occupy an area that is covered by a single pixel, giving rise to spectral measurement that is a composite of the individual spectra. The values of most pixels result from a mixture of signals received from more than one distinct substance. Spectral unmixing is a process of decomposing a mixed pixel into a set of fractional abundances that indicate the proportion of each kind of material. It is widely used in urban remote sensing studies (e.g. Mathieu-Marni et al., 1996; Kressler et al., 2000; Roessner et al., 2001; Small, 2001; Phinn et al., 2002; Wu and Murray, 2003; Lu and Weng, 2004; Weeks et al., 2005; Lu et al., 2008; Wei et al., 2008; Zoran et al., 2008; Zhao et al., 2010).

The basic physical assumption underlying linear spectral unmixing is that each field within a ground pixel contributes an amount to a received signal at the sensor which is characteristic of the cover type in that field and proportional to the area covered (Adams et al., 1986; 1990; Quarmby et al., 1992). Under this assumption, the energy recorded in each image pixel is regarded as a linear composition of the one received from spectrally pure cover types, which is called endmembers. Accordingly, the linear spectral mixture model can be expressed as follows:

$$R_i = \sum_{j=1}^{n} f_j R_{ij} + \varepsilon_i \quad (i = 1 \text{ to number of bands}) \tag{2.15}$$

where $R_i$ is the spectral reflectance of band $i$ of a pixel; $n$ is the number of endmembers (i.e. the land cover types of interest in the analysis); $f_j$ is the proportion/fraction of endmember $j$ within a pixel; $R_{ij}$ is the spectral reflectance of endmember $j$ on band $i$; and $\varepsilon_i$ is the noise/error term in band $i$.

The simultaneous equations (Expression 2.15) are expressed in a matrix form as follows:

$$\boldsymbol{R} = \boldsymbol{S}\boldsymbol{f} + \boldsymbol{\varepsilon} \tag{2.16}$$

where $\boldsymbol{R}$ is the vector of pixel values in all bands; $\boldsymbol{S}$ is the matrix representing the spectra of all endmembers; $\boldsymbol{f}$ is the vector of the fractions of the endmembers, which is to be estimated; $\boldsymbol{\varepsilon}$ is the vector of additive noise in all bands, and satisfying the expectation $E(\boldsymbol{\varepsilon}) = 0$.

Linear spectral unmixing aims at decomposing each image pixel into spectrally pure and distinct endmembers, which can be achieved by solving simultaneous equations of the linear spectral mixture model for each $f_j$. In order to construct and solve the equations, the following conditions must be satisfied:

a) selected endmembers should be independent of each other;
b) selected spectral bands should not be correlated;
c) the number of endmembers should not exceed the number of spectral bands used.

For example, in Landsat TM/ETM+ data, except the band 6 (i.e. the thermal band) with an inconsistent spatial resolution to other multi-spectral bands, and the panchromatic band available since the use of ETM+ sensor on Landsat 7, there are 6 spectral bands in total can be used in unmixing procedures. According to Condition (c), no more than 6 endmembers can be distinguished by linear spectral unmixing with raw TM/ETM+ data. However, this number is further depleted by considering Condition (b). The spectral bands of raw TM/ETM+ data do not satisfy this condition, and thus need to be transformed to new non-correlated bands, thus leading to less usable bands for analysis.

The unmixing problem can be decomposed into three consecutive procedures. A number of research works have been done to develop techniques for resolving the problems, which are described in detail as follows.

#### 2.2.4.1 Decorrelation and Dimension Reduction

As a common condition of a linear composition in which components must be linearly independent so that each component cannot be linearly combined by other components and thus are eliminated, the linear spectral mixture model requires that the spectral bands selected for the model should not be correlated. However, remotely sensed data do not always satisfy this condition. For example, it is found that Landsat TM/ETM+ data are highly correlated between adjacent spectral wavebands (Barnsley, 1999). Therefore, the use of TM/ETM+ imagery in linear spectral unmixing does not produce reasonable results of land cover fractions. Decorrelation is needed to transform raw TM/ETM+ data for calculating the fractions of land cover types of interest. In remote sensing, two techniques are well developed and widely used for this purpose, namely Principle Component Analysis (PCA) and Minimum Noise Fraction (MNF).

Principle Component Analysis was developed by Pearson (1901) for transforming a number of possibly correlated variables into a number of uncorrelated variables called principal components. It is a rotation of the coordinate system of data space so the greatest variance by any projection of data comes to lie on the first coordinate (i.e. the first principal component) of the new coordinate system, and the second greatest variance on the second coordinate, and so on. After the transformation, the resultant spectral bands called principle components are uncorrelated. The first principle component contains most useful information, and less information is contained in higher dimensions of PCA space, and the last principle component contains most noise. By segregating noise, PCA is also used for data compression, which is not useful to this research and will not be further discussed.

Alternatively, Minimum Noise Fraction is a recent method developed on PCA, and serves the same purposes as PCA (Boardman and Kruse, 1994). As a two-step combination of PCA, it firstly decorrelates and rescales data noise based on an estimated noise covariance matrix, producing transformed data in which noise has unit variance and not band-to-band correlations, and then implements a standard PCA of noise-whitened data. Hence, MNF results have the same characteristics as those of PCA. Previous studies showed that MNF produced better results than PCA.

#### 2.2.4.2 Endmember Selection

In order to construct equations of the linear spectral mixture model, $R_{ij}$ in each equation (i.e. the spectral reflectance of endmember *j* on band *i*) must be determined by endmember selection (i.e. selecting pixels containing pure land cover types of interest as representative pixels of those types). Endmember selection is traditionally and still prevalently performed through human-computer interaction (i.e. manual selection). In manual endmember selection, scatter diagrams of two data bands are used. Previous research revealed that when pixel distribution in scatter diagrams appears triangular in general, pixels become purer when they are closer to triangle vertices. This has been widely accepted as the basis of endmember selection, and thus pure endmembers are usually selected near triangle vertices from scatter diagrams, and associated with land cover types of interest by selectors using their expert knowledge (Figure 2.4). Such manual selection is a subjective process, relying on the experience of the performer, and his/her prior knowledge about land cover types as well as the map area to be analyzed.

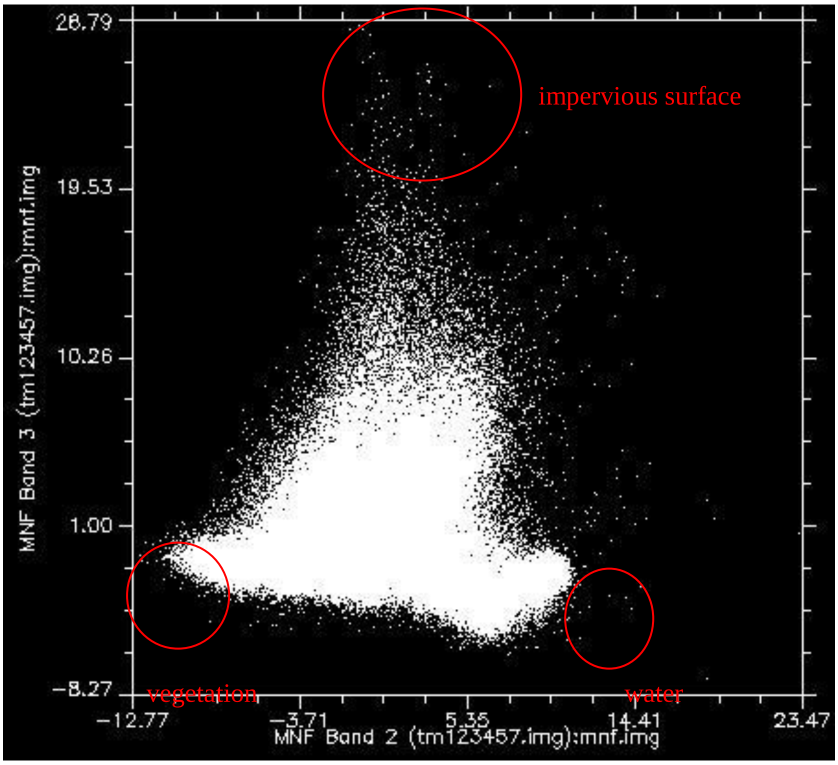


Figure 2.4 Manual Endmember Selection using Scatter Diagram

(Red circles highlight the parts of data distribution where potential endmembers are located.)

A method for automated identification of pure pixels called the Pixel Purity Index (PPI) is developed by Boardman *et al.* (1995). The PPI algorithm repeatedly projects pixels in data space onto random unit vectors, and extreme pixels in each projection are noted. The times each pixel is found to be extreme is related to pixel purity via a convex geometry argument (Boardman, 1993), and thus used as an index of pixel purity. PPI can be used to identify the purest pixels in the map area automatically and rapidly. However, those pixels are thought to be spectrally pure with respect to data space in which they are calculated, but not with respect to any known cover types. According to the theoretical basis and computation algorithm of PPI, “pure pixels” or endmembers it produced are a subset of convex hull vertices that encloses data.

The separability of the selected endmembers can be evaluated prior to the unmixing process, using the Jeffries-Matusita and Transformed Divergence separability measures (Richards and Jia, 2006). The Jeffries-Matusita distance is a function of separability that directly relates to the probability of how good the resultant estimation or classification will be (Wacker, 1971). The Jeffries-Matusita distance between a pair of classes *i* and *j* is defined as

$$J_{ij} = 2(1 - e^{-B}) \tag{2.17}$$

in which

$$B = \frac{1}{8}\left(m_i - m_j\right)^T \left\{\frac{\Sigma_i + \Sigma_{\mathrm{j}}}{2}\right\}^{-1} \left(m_i - m_j\right) + \frac{1}{2}\ln\left\{\frac{\left|(\Sigma_i + \Sigma_{\mathrm{j}})/2\right|}{|\Sigma_i|^{\frac{1}{2}}|\Sigma_j|^{\frac{1}{2}}}\right\} \tag{2.18}$$

where $\Sigma_{\mathrm{i}}$ and $\Sigma_{\mathrm{j}}$ are the covariance matrices of the spectral signatures of classes *i* and *j* respectively, $m_{\mathrm{i}}$ and $m_{\mathrm{j}}$ are the mean vectors of the spectral signatures of classes *i* and *j* respectively. The Expression 2.18 is referred to as the Bhattacharyya distance (Kailath, 1967). The transformed divergence of a pair of classes *i* and *j* is defined as

$$d_{ij}^T = 2(1 - e^{\frac{-d_{ij}}{8}}) \tag{2.19}$$

in which

$$d_{ij} = \frac{1}{2}T_r\{\left(\Sigma_i - \Sigma_j\right)\left(\Sigma_i{}^{-1} - \Sigma_j{}^{-1}\right)\} + \frac{1}{2}T_r\left\{\left(\Sigma_i{}^{-1} + \Sigma_j{}^{-1}\right)\left(m_i - m_j\right)\left(m_i - m_j\right)^T\right\} \tag{2.20}$$

where $T_r\{\}$ denotes the trace of a matrix, $\Sigma_i$, $\Sigma_j$, $m_i$ and $m_j$ are the same as in Expression 2.18 (Swain and Davis, 1978). Both the measures range from 0 to 2 and indicate how well the pairs of selected endmembers of two land cover classes are statistically separable. Values greater than 1.9 indicate good separability.

### 2.2.4.3 Inversion

The process of inversion estimates the fractional abundances of each mixed pixel from its spectrum and the endmember spectra. The class of inversion algorithms based on minimizing squared-error start from the simplest form of least squares inversion and increase in complexity as further assumptions and parametric structure are imposed on the problem. Variations of the least squares concept have been adopted to solve problems associated with linear mixture models (Keshava and Mustard, 2002). The least squares solution to the equation in Expression 2.16 is expressed as follows.

$$\hat{\boldsymbol{f}} = (\boldsymbol{S}^T\boldsymbol{S})^{-1}\boldsymbol{S}^T\boldsymbol{R} \tag{2.21}$$

The least squares solution in Expression 2.21 is unconstrained. The proportional abundance of each endmember in the linear mixture model must satisfy two physical constraints, namely, full additivity, which is an equality constraint (Expression 2.22), and non-negativity, which is an inequality constraint (Expression 2.23).

$$\sum_{=1}^{n} f_i = 1 \tag{2.22}$$

$$f_i \geq 0 \;\; (i = 1, \dots, n) \tag{2.23}$$

Least squares with equality constraints can be easily processed, which is described by Kay (1993). The least squares solution with full addicativiy of the equation in Expression 2.16 can be calculated as follows:

$$\hat{\boldsymbol{f}}_{constrained} = \hat{\boldsymbol{f}} - (\boldsymbol{S}^T\boldsymbol{S})\mathbf{1}[\mathbf{1}^T(\boldsymbol{S}^T\boldsymbol{S})^{-1}\mathbf{1}]^{-1}(\mathbf{1}^T\hat{\boldsymbol{f}} - \mathbf{1}) \qquad (2.24)$$

Least squares problems with inequality constraints are a constrained quadratic programming problem, which is more complicated than the one with equality constraints. Methods have been developed to address this problem (Haskell and Hanson, 1981; Portugal et al., 1994; Bro and Sidiropoulos, 1998). The algorithm for Problem NNLS (Nonnegative Least Squares) by Lawson and Hanson (1974) can be used to obtain a non-negatively constrained least squares solution to the equation in Expression 2.16.

#### 2.2.4.4 Evaluation

There are three ways to evaluate the results of spectral unmixing, also the goodness of fit of the linear mixture model constructed. The first method is visual evaluation. Visual evaluation relies on the expertise and experience of the analyst to determine whether the unmixed land cover fractions are consistent with other information existing about the study area. If the pattern of the unmixed fractions accords well with the additional information obtained from ground truth or other sources, then the model can be accepted. The second method is the calculation of the root mean square (RMS) error (Adams et al., 1989). The RMS error is calculated for every pixel individually, as the square root of the arithmetic mean of the squares of the error terms of all image bands. It is calculated as follows.

$$\varepsilon_{RMS} = \sqrt{\frac{\sum_{i=1}^{n} \varepsilon_i^2}{n}} \tag{2.25}$$

where $n$ is the number of bands, and $\varepsilon_i$ is the error term in band $i$. A small RMS error indicates that the linear mixture model constructed is mathematically good, while a high RMS error indicates that the model is not good enough for unmixing the image (Gong and Zhang, 1999; Hope, 1999; Kressler et al., 2000; Small, 2001; Foppa et al., 2002; Lu et al., 2008; Zhao et al., 2010). The third method is comparing the unmixing result with a traditional hard classification data as a reference. To do so, the unmixed land cover fractions are used to produce a hard classification for comparison, by assigning each pixel to the land cover type with the highest proportion in the pixel (Kressler et al., 2000; Weeks et al., 2005; Raymaekers et al., 2005).

### 2.2.4 Multi-Resolution Image Segmentation

Baatz and Schape (2000) developed a multi-resolution image segmentation method that is based on homogeneity definition in combination with local and global optimization techniques. The multi-resolution segmentation is a bottom up region merging technique. It starts with individual pixels, which form the smallest segments. In numerous subsequent steps, pairs of image segments are merged into larger ones. The merging decision is based on local homogeneity criteria, describing the similarity of adjacent image segments. Throughout the merging process, the underlying optimization procedure minimizes the weighted heterogeneity of resulting segments, which is defined by the size of a segment and a parameter of heterogeneity. In each step, the pair of adjacent segments that results in the smallest growth of the defined heterogeneity is merged. The process stops when the smallest growth exceeds the threshold defined by a scale parameter. The procedure simulates the simultaneous growth of segments over a scene in each step to achieve adjacent image segments of similar size and thus comparable scale.

The increase of heterogeneity is defined as

$$\Delta h = w_{spectral} \cdot \Delta h_{spectral} + w_{shape} \cdot \Delta h_{shape} \tag{2.26}$$

$$w_{spectral} \in [0,1],\ w_{shape} \in [0,1],\ w_{spectral} + w_{shape} = 1 \tag{2.27}$$

where $w_{spectral}$ and $w_{shape}$ are weight parameters; $\Delta h_{spectral}$ and $\Delta h_{shape}$ are changes of spectral heterogeneity and shape heterogeneity.

The spectral heterogeneity allows multi-variant segmentation by adding a weight to each image channel. The difference in spectral heterogeneity $\Delta h_{spectral}$ is defined as

$$\Delta h_{spectral} = \sum_{c} w_c [n_m \cdot \sigma_{c,m} - (n_1 \cdot \sigma_{c,1} + n_2 \cdot \sigma_{c,2})] \tag{2.28}$$

where $w_c$ is the weight of an image channel $c$; $n_m$, $n_1$ and $n_2$ are the number of pixels of the merged segment, and the two segments before the merge respectively; $\sigma_{c,m}$, $\sigma_{c,1}$ and $\sigma_{c,2}$ are the standard deviations of the pixel values in channel $c$ of the merged segment, and the two segments before the merge respectively.

The difference in shape heterogeneity $\Delta h_{shape}$ describes the improvement of the shape with regard to smoothness and compactness of a segment's shape. It is expressed as

$$\Delta h_{shape} = w_{smooth} \cdot \Delta h_{smooth} + w_{compt} \cdot \Delta h_{compt} \tag{2.29}$$

where $w_{smooth}$ and $w_{compt}$ are the weights of $\Delta h_{smooth}$ and $\Delta h_{compt}$ respectivley, which are defined as

$$\Delta h_{smooth} = n_m \cdot \frac{l_m}{b_m} - (n_1 \cdot \frac{l_1}{b_1} + n_2 \cdot \frac{l_2}{b_2}) \tag{2.30}$$

$$\Delta h_{compt} = n_m \cdot \frac{l_m}{\sqrt{n_m}} - (n_1 \cdot \frac{l_1}{\sqrt{n_1}} + n_2 \cdot \frac{l_2}{\sqrt{n_2}}) \tag{2.31}$$

where $l_m$, $l_1$ and $l_2$ are the perimeters of the merged segment, and the two segments before the merge respectively; $b_m$, $b_1$ and $b_2$ are the perimeters of the bounding box of the merged segment, and the two segments before the merge respectively; $n_m$, $n_1$ and $n_2$ are the same as used in the expression of $\Delta h_{shape}$.

The stop criterion for the optimization procedure is an input scale parameter. Prior to the merge of two segments, the resulting increase of heterogeneity $\Delta h$ is calculated. If the resulting increase exceeds threshold determined by the scale parameter, then the merge is not performed and the segmentation process stops (Baatz and Schape, 2000; Benz et al., 2004).

The multi-resolution image segmentation has been widely used in urban remote sensing studies, e.g. for urban land cover classification (Gitas et al. 2004; Brennan and Webster, 2006; Zhou and Wang, 2008; Zhou and Troy, 2009; Zhou et al., 2009; Hu and Weng, 2011), for urban object extraction (Hofmann, 2001a; Hofmann, 2001b;

Marangoz et al., 2002; Miliaresis and Kokkas, 2007, Chen et al., 2009; Ali Rizvi and Krishna Mohan, 2010; Yu et al., 2010; Mhangara et al, 2011), and for urban landscape analysis (De Kok et al., 2003; Zhou et al., 2006; Zhou and Troy, 2008; Zhou et al., 2008; Mhangara and Odindi, 2013).

## 2.3 Traditional Methods for Urban Area Recognition

Recognition of an urban area means the identification of the spatial extent of the urban area. Traditionally, it is done by censuses and surveys. Countries have different ways to carry out censuses and maintain survey data about the built environment. In the United States, the Census Bureau defines and identifies urban and rural areas to support decision making and analyses of government agencies and research organizations. The Census Bureau’s urban areas comprise a densely settled core of census tracts and/or census blocks that meet minimum population density requirements, along with adjacent territory containing non-residential urban land uses as well as territory with low population density included to link outlying densely settled territory with the densely settled core (U.S. Census Bureau, 2015). Census blocks provide the building blocks for measuring population density and delineating urban areas. A census is taken every ten years. The decennial census has been conducted since 1790. The first decennial census counted approximately four million people for the purpose of apportioning the U.S. House of Representatives. In the 2010 census, one million enumerators were sent to count more than three hundred million of the nation's inhabitants. On the other hand, the Census Bureau created a database for documenting geographical and cartographical information, including the boundaries of geographical entities. It is the U.S. Census Bureau's Master Address

File/Topologically Integrated Geographic Encoding and Referencing (MAF/TIGER) database. Initially, the Census Bureau used the U.S. Geological Survey (USGS) 1:100,000-scale Digital Line Graph (DLG), USGS 1:24,000-scale quadrangles, the Census Bureau's 1980 geographic base files (GBF/DIME Files), and a variety of miscellaneous maps for selected areas outside the contiguous 48 states to create the TIGER database (predecessor to the current MAF/TIGER database). The Census Bureau continually makes additions and corrections to its database, mainly through partner supplied data, the use of aerial imagery and fieldwork. The Census Bureau has numerous partner programs where federal, state, and local government partners' supply updates to boundaries, features and addresses (U.S. Census Bureau, 2014).

There are three problems in census and survey data for the recognition of urban areas. Firstly, Weeks (2008) pointed out that there is a spatial mismatch that has the potential to produce a bias in the classification of a place, as people are enumerated at their place of residence, and urban residents typically work in a different location from where they live. An example is a central business district (CBD), which has only a small residential population. Secondly, the cost of generating and maintaining census and survey data is enormous. The 2010 census of the U.S. involved one million enumerators. The update of the boundaries, features and addresses of geographical entities involves numerous partner programs and various partner supplied data. Lastly, the urban and rural areas classification using census and survey data is not efficient. The Census Bureau reviews and updates urbanized area and urban cluster boundaries every ten years, following the decennial census. Because population estimates and survey data are not available at the census block level between censuses, there is no nationally consistent set of population data at the level of geographic detail needed to delineate urban areas between censuses (U.S. Census Bureau, 2014).

## 2.4 Remote Sensing Based Urban Area Recognition

Increasing availability of remotely sensed data and processing techniques facilitates the development of new approaches to studying urban issues. The advantages of remote sensing data include their broad spatial coverage, capacity for routine and unobtrusive updating and ability to provide self-consistent measurements of critical physical properties that are difficult or expensive to obtain in situ (Miller and Small., 2003). Weeks (2008) pointed out that remote sensing data offer indirect ways to classify a place regardless of who resides in it. Section 2.2 reviews the remote sensing techniques that are widely used in urban studies, including urban land cover / land use (LCLU) classification, urban objects extraction and urban landscape analysis. Besides these urban studies, some attempts have been made to recognize urban areas using various kinds of remote sensing data, including areal images (Gamba et al., 2007; Sirmacek and Unsalan, 2009; Sirmacek and Unsalan, 2010; Kovacs and Sziranyi, 2013), multi-spectral data (Baraldi and Parmiggiani, 1990; Bessettes and Desachy, 1998; Yu et al., 1999; Lorette et al., 2000; Ward et al., 2000; Bianchin and Foramiti, 2001; Zha et al., 2003; Zhong and Wang, 2007; Qiao et al., 2009; Schneider et al., 2009; Schneider et al., 2010; Angiuli and Trianni, 2014; Stathakis and Faraslis, 2014; Hu et al., 2015; Shi et al., 2015; Wan et al., 2015), synthetic aperture radar (SAR) data (Dekker, 2003; Grey and Luckman, 2003; Moriyama et al., 2004; He et al., 2006; Yang et al., 2008; Corbane et al., 2009; Gamba et al., 2011; Kayabol and Zerubia, 2012; Aghababaee et al., 2013; Gamba and Lisini, 2013; Kajimoto and Susaki, 2013; Ban et al., 2015; Chen et al., 2015; Susaki and Mishimoto, 2015), night-time light (NLT) data (Imhoff et al., 1997; Henderson et al., 2003; Small et al., 2005; Zhou et al., 2014; Zhou et al., 2015), and combinations of these types (Schneider et al., 2003;

Gomez-Chova et al., 2006; Kasimu and Tateishi, 2008; Cao et al., 2009; Zhang et al., 2014; Duan et al., 2015; Jing et al., 2015; Salentinig and Gamba, 2015). The existing methods utilized various image features to classify urban and non-urban pixels on the images, based on the assumption that those features present some difference between urban and non-urban areas. These image features include geometrical, spectral and textural features.

The methods based on geometrical features assume that urban areas are dominated by objects with regular shapes, such as buildings, which can be extracted from high resolution areal images. Accordingly, corner or edge detectors are applied first to detect some feature points of regular shapes, which are considered the most urban points in the images. A surface is then constructed according to the distance to those feature points. Finally, a threshold is performed to separate urban and rural areas. This kind of methods includes the ones developed by Gamba et al. (2007), Sirmacek and Unsalan (2010), Kovacs and Sziranyi (2013) and Shi et al. (2015).

Most of the existing methods are based on spectral features, including spectral indices that are used to indicate certain kinds of land cover, such as normalized difference vegetation index (NDVI) and built-up index (NDBI). These methods apply various kinds of classifiers to separate urban and non-urban classes. For example, Ward et al. (2000) developed a hierarchical unsupervised image classification scheme applicable to Landsat Thematic Mapper (TM) data for identifying urban areas. Figure 2.5 shows this hierarchical image classification scheme. The first stage of the unsupervised classification process divides the image into vegetation, water and soil-impervious surface classes. NDVI, as reviewed in Section 2.2.2, band 5 and band 3 of the input TM data are used for vegetation classification. The unsupervised classification applies the Iterative Self-Organizing Data Analysis Technique (ISODATA) algorithm to a composite of the above three image layers to produce 20 classes. The vegetation class is further separated into woody and non-woody components. Composite images comprising band ratios associated with mineral and hydrothermal alteration properties are then created for further classifying the soil-impervious surface component. Finally, these classes are combined into four primary land cover types, including water, forest, cleared and urban areas.

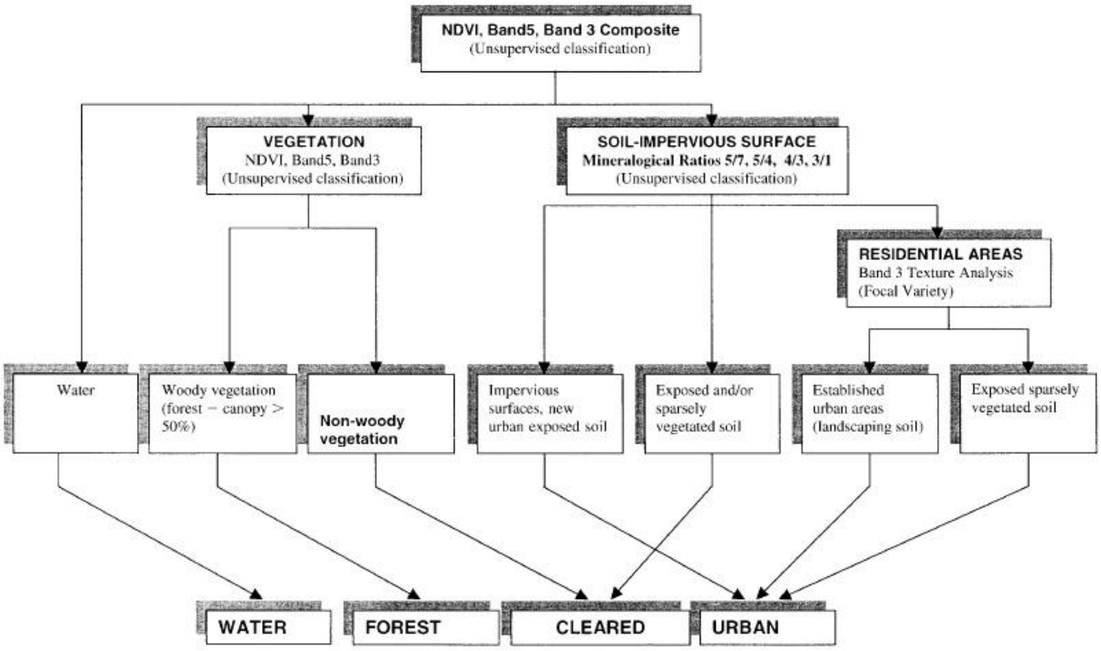


Figure 2.5 Hierarchical Image Classification Scheme for Urban Area Recognition (Source: Ward et al., 2000)

Zha et al. (2003) developed a method for automatically mapping urban areas based on the NDVI and NDBI, as reviewed in Section 2.2.2. Zha et al.'s method identifies urban areas through logical and arithmetic manipulations of the red, near-infrared and mid-infrared bands of multi-spectral images such as Landsat TM and SPOT images. Figure 2.6 shows an example of applying this method to a set of Landsat TM data to classify urban areas.

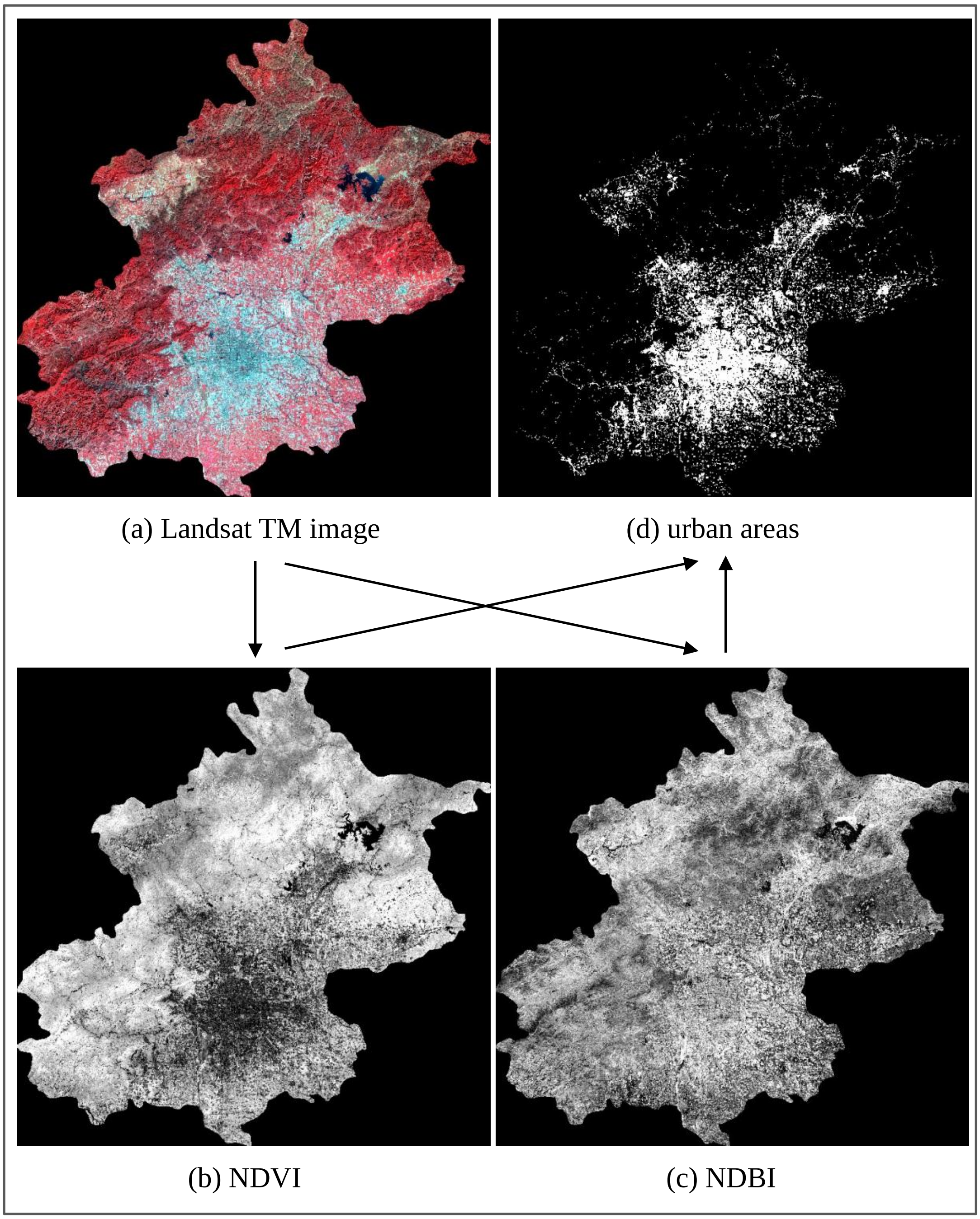


Figure 2.6 Urban Area Recognition using NDVI and NDBI Developed by Zha et al. (2003)

NDVI and NDBI images are firstly derived from the input TM image (Figure 2.6(b, c)). They are then recoded into binary images by assigning a certain positive value to pixels with positive values, and assigning 0 to other pixels. Subsequently, an image is produced by subtracting the recoded NDVI from the recoded NDBI to further exclude vegetated areas. In the output image, only pixels of built-up and barren areas have a positive value (Figure 2.6(d)). The advantage of this method is that the manipulations involved are quite simple and quick. It also maps urban areas quickly. When mapping large-scale areas (e.g. a full scene of Landsat TM data), its high efficiency is noticeable. However, when monitoring land cover change or urban growth, such high-speed data processing is not useful or relevant to its applications. Some disadvantages are found though. Firstly, it is unable to separate barren lands from urban areas. Even though it is used for mapping urban areas, its output urban areas still include barren lands, which usually appear in crop fields at the early stage of their growth. Secondly, it determines the extent of urbanization in each pixel by taking into consideration only each pixel's own spectral values and ignores the spatial configuration of pixels. According to the method, small vegetated areas in a city can result in rural holes in output urban areas. As a result, urban and non-urban pixels are widely mixed in its output. Thirdly, it requires the use of a spectral band of mid infrared, which is available in some satellite images (e.g. Landsat TM data band 5 and SPOT data band 4). But most mid infrared bands are not supported in higher resolution data (e.g. IKONOS, WorldView and QuickBird data), thus leading to the method's limited application to low or moderate resolution data.

Qiao et al. (2009) developed a decision tree model for extracting urban areas from both TM and SPOT data. This method is based on the V-I-S model, which classifies image pixels into four land cover types, namely vegetation, impervious surface, soil, and water. The V-I-S model is reviewed in Section 2.2.1. The method of Qiao et al. (2009) directly considers impervious surface as urban area. This method adopts an exclusion approach and extracts pixels of urban areas by removing pixels of the other three types one by one. The criterion for rejecting pixels relies on a spectral index related representatively to that land cover type. A threshold cut manipulation of index values is performed to decide whether a pixel should be excluded. Pixels with an index value over a given threshold are regarded as highly related to the corresponding type of vegetation, water, or soil, and thus rejected as non-urban. This logic is represented as a decision tree in Figure 2.7. After rejecting pixels of the other three types, the remaining pixels are considered as urban areas.

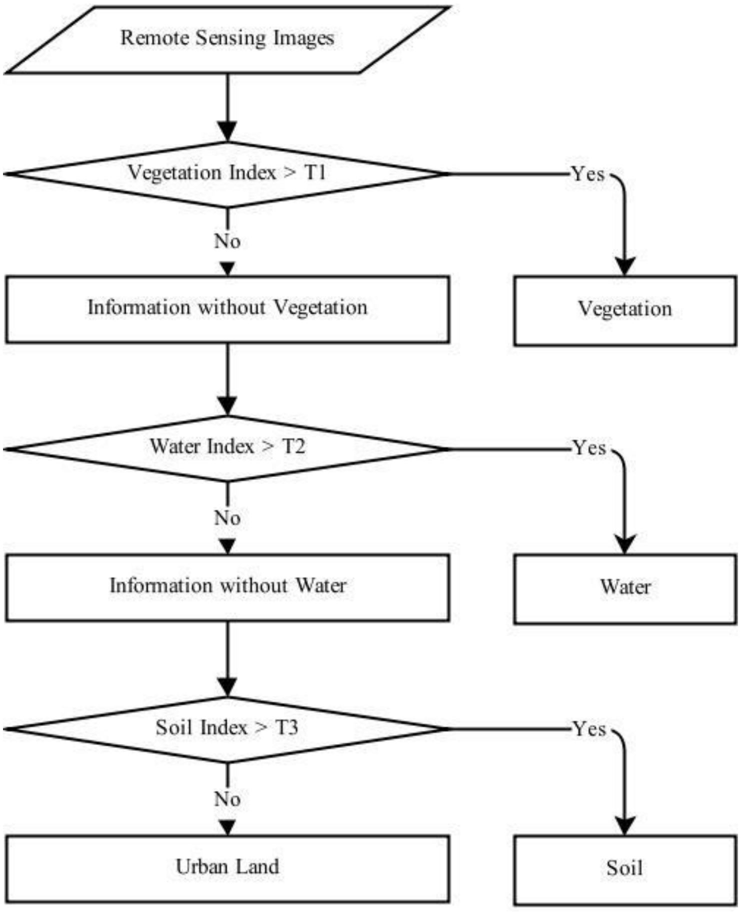


Figure 2.7 Decision Tree Model for Extracting Urban Areas developed by Qiao *et al.* (2009)

When extracting urban areas from TM data, the indices used as indicators for rejection at bifurcation points in the decision tree are the Soil Adjusted Vegetation Index (SAVI), Modified Normalized Difference Water Index (MNDWI), and

Normalized Difference Built-up Index (NDBI) respectively, which are reviewed in Section 2.2.2. In cases using SPOT data, due to a lack of mid-infrared bands, the MNDWI and NDBI cannot be applied. Instead, the Normalized Difference Water Index (NDWI) and a homogeneity index, which captures textural characteristics, are selected as water and soil indices respectively for rejecting pixels of those types. Compared with Zha et al.'s method, this method applies more spectral indices so that more information is utilized to form recognition rules. Combining several indices can produce more accurate results than relying on a single index. However, there are problems and limitations in this method. Theoretically, this method simply considers impervious surfaces equivalent to urban areas, and treats pixels of vegetation, soil and water as non-urban. This is an improper understanding of the concept of urban areas. Impervious surfaces, vegetation, soil, and water are land cover, which refer to physical materials distributed on the land surface. The extent of urbanization of a place should be determined by composition and configuration of various kinds of land cover in that place. Although urban areas are highly related to impervious surfaces, there must be pixels of impervious surfaces not representing urban areas, and pixels of the other three types not representing rural areas. Technically, this method is not fully automated or objective. Threshold values for deciding rejection of pixels of the other types (i.e. T1, T2, and T3) at bifurcation points in the decision tree (Figure 2.7) are determined by human experts, thus making the task highly difficult and subjective. In addition, the same as the method of Zha et al. (2003), it determines the extent of urbanization of each single pixel depending on the information from the pixel itself, and ignores its configuration with surrounding pixels, which gives rise to the same problem of the method of Zha et al. (2003), where urban and rural areas are heavily entwined in the results. Besides these methods, other classifiers and machine learning techniques are also applied in the methods based on spectral features, such as neutral network (Gamba et al., 2007), support vector machine (Cao et al., 2009) and random forests (Jing et al., 2015).

Textural features are also widely used to classify urban areas on remote sensing images, based on the fact that regular buildings present a unique texture that is different from the natural environment. The same as using spectral features, the principle is to classify each pixel of the image into urban or non-urban class. For example, the methods developed by Lorette et al. (2000), Dekker (2003), Corbane et al. (2009), Kayabol and Zerubia (2012), Aghababaee et al. (2013) and Chen et al. (2015) are of this type. In addition, some other existing methods utilized a combination of spectral and textural features, making use of both characteristics (Duan et al., 2015; Salentinig and Gamba, 2015).

The advantages in remote sensing based methods are obvious. As those methods are fully or semi-automated, they are more economical and efficient compared to traditional methods that rely on census and survey data. However, some disadvantages are found. Firstly, the existing methods reflect their local understanding of an urban area, which results in very different urban extents from the existing methods. It was reported by Potere et al. (2009) that the estimated global urban extent ranged from 276,000 to 3,532,000 $km^2$, by comparing eight global urban maps that were created using remotely sensed and census data. Secondly, the existing methods are pixel-based classification in nature. The classification process determines whether the area covered by the pixel is urban or not. However, an urban area should be a continuous space. Even those pixels of vegetation or water may be part of an urban area. Therefore, in order to use remote sensing images and techniques to recognize urban areas, there is still a gap between the current remote sensing based method and urban areas that are represented as geographical entities.

# Chapter 3 Remote Sensing Based Automated Urban Area Recognition: A New Strategy

The chapter describes a new strategy to develop an algorithm for automated recognition of urban areas using remote sensing data and techniques. Firstly, the urban-rural differences are formulated by summarizing the four urban characteristics identified in Section 2.1.3. Secondly, based on the urban-rural differences, relevant information and processes are selected for composing the algorithm. Finally, the study area used throughout the research is described in detail.

## 3.1 Urban-Rural Differences

In Section 2.1.3, four urban characteristics are identified by analyzing the current definitions of urban area. They are: 1) urban areas contain large and dense built-up areas; 2) urban areas contain heterogeneous elements; 3) urban areas are dominant by non-agricultural activities; and 4) urban areas are distinguishable from their surrounding rural areas. These four characteristics are true for describing urban areas. The goal is not only to describe urban areas, but to distinguish between urban and rural areas. Hence, these four urban characteristics are further revised in the following manner, to present the differences between urban and rural areas. They are 1) urban areas are composed of large and dense built-up areas, providing space for non-agricultural human activities, while rural areas are mainly composed of agricultural or natural lands, i.e. vegetated areas; 2) the physical elements of urban areas are more heterogeneous, while the ones of rural areas are more homogeneous; and 3) these differences are observable. These characteristics and differences are general and qualitative. In other to apply them to identify the extent of an urban area, they need to be described in a quantitative and measurable way.

## 3.2 Information and Processes for Characterizing Urban-Rural Differences

In order to develop an algorithm to urban area recognition as described in Section 3.2, two questions need to be answered: 1) what kinds of information, and 2) what kinds of processes are needed for characterizing the urban-rural difference. Information and processes are the two types of elements that are necessary for composing an algorithm.

### 3.2.1 Information for Representing Urban-Rural Differences

The urban-rural differences described in Section 3.1 are general and qualitative. In order to apply them to identify the extent of an urban area, they need to be described in a quantitative and measurable way. The first difference between urban and rural areas has been well realized and a well-known land cover composition model, i.e. the V-I-S model, has been developed to describe this urban-rural difference (Ridd, 1995; Ward et al., 2000). The V-I-S model is reviewed in Section 2.2.1. The proportional abundance of four types of land cover elements, i.e. vegetation, impervious surface, soil and water / shade, provides one kind of information for characterizing a place, which is referred to as land cover composition. The second difference can also be quantitatively described based on land cover. The distribution pattern of land cover can be observed as textures. Texture refers to the arrangement and frequency of tonal variation in particular areas of an image. Smooth textures are often the result of uniform and even surfaces, such as fields, asphalt or grasslands (Tempfli et al., 2009). A target with a rough surface and irregular structure results in a rough textured appearance. This kind of information is referred to as land cover configuration. These two kinds of information, i.e. land cover composition and configuration, can be derived from remote sensing data. Chapter 4 studies the use of eight remote sensing image features for characterizing urban and rural areas. Four proportional features correspond to land cover composition. Four textural features correspond to land cover configuration.

### 3.2.2 Process Chain for Urban Area Recognition

From the current urban definitions for census purpose, the whole process of urban recognition can be summarized as two steps, i.e. division and classification. The division is on the administrative basis. Administrative boundaries are imposed to divide a territory into administrative regions. All the administrative regions are then classified into urban and rural areas according to the census criteria. To automate such a process, four steps are proposed, they are, zoning, clustering, identification and merging. The construction of the four steps is based the urban characteristics extracted. The four steps are described as follows.

1) **Zoning**. It divides a territory into smaller regions. Different from administrative division, which is made with administrative decisions, the regions created by this process should reflect the urban characteristics. According to the fourth urban characteristic, an urban area is clearly distinguishable from its surrounding rural area, which means that the difference of the landscape between urban and rural areas,

implied by the other three urban characteristics, is observable. Hence, the zoning process is expected to divide a territory into regions that are different in the landscape.

2) **Clustering**. It clusters the divided regions into a number of groups according to a set of features. These groups are of no thematic meanings. Likewise, according to the fourth urban characteristic, these groups should be in such a manner that the similarity between groups is minimized and the similarity within groups is maximized. The features for characterizing regions should be identified based on the other three urban characteristics.

3) **Identification**. It identifies a group of regions that is certainly urban. Since the groups created by the clustering process are of no thematic meanings, a set of rules are needed for assigning the urban meaning to the group that is the most relevant to be urban. If such a group fails to be identified, then the process flow goes back to the clustering process, which should be adjusted and run again for the next identification. As a result, the clustering and identification loop until an urban group is successfully found. The expected rule set should also be based on the urban characteristics.

4) **Merging**. It merges all the regions into two areas, one of which is urban, and another is rural. According to the urban characteristics, the two areas should be different in the features related to those characteristics, and such a difference should be observable. Therefore, the dissimilarity of the two areas should be maximized.

An image segmentation algorithm is used for the zoning task, substituting the administrative partition, which is described in Chapter 5. Chapter 6 develops an iterative region clustering and merging algorithm to achieve the remaining three steps of the approach.

## 3.3 Study Area

The study area of this research is Beijing, the capital city of China. It ranges from 115°25´E to 117°30´E and from 39°26´N to 41°3´N. It covers an area of 16,410.54 $km^2$ (Ministry of Commerce PRC, 2007). Beijing is a city with a long history of over three thousand years, and is one of the largest world cities at present, ranking the eighth by Global Cities Index in 2014 (A.T. Kearney, 2014). Administratively, Beijing is divided into sixteen regions, including fourteen urban and suburban districts and two rural counties (Figure 3.1). Previously, there were eighteen administrative regions. Since 1st July 2010, Chongwen and Xuanwu Districts have been merged into Dongcheng and Xicheng Districts respectively (regions 1 and 2 in Figure 3.1).

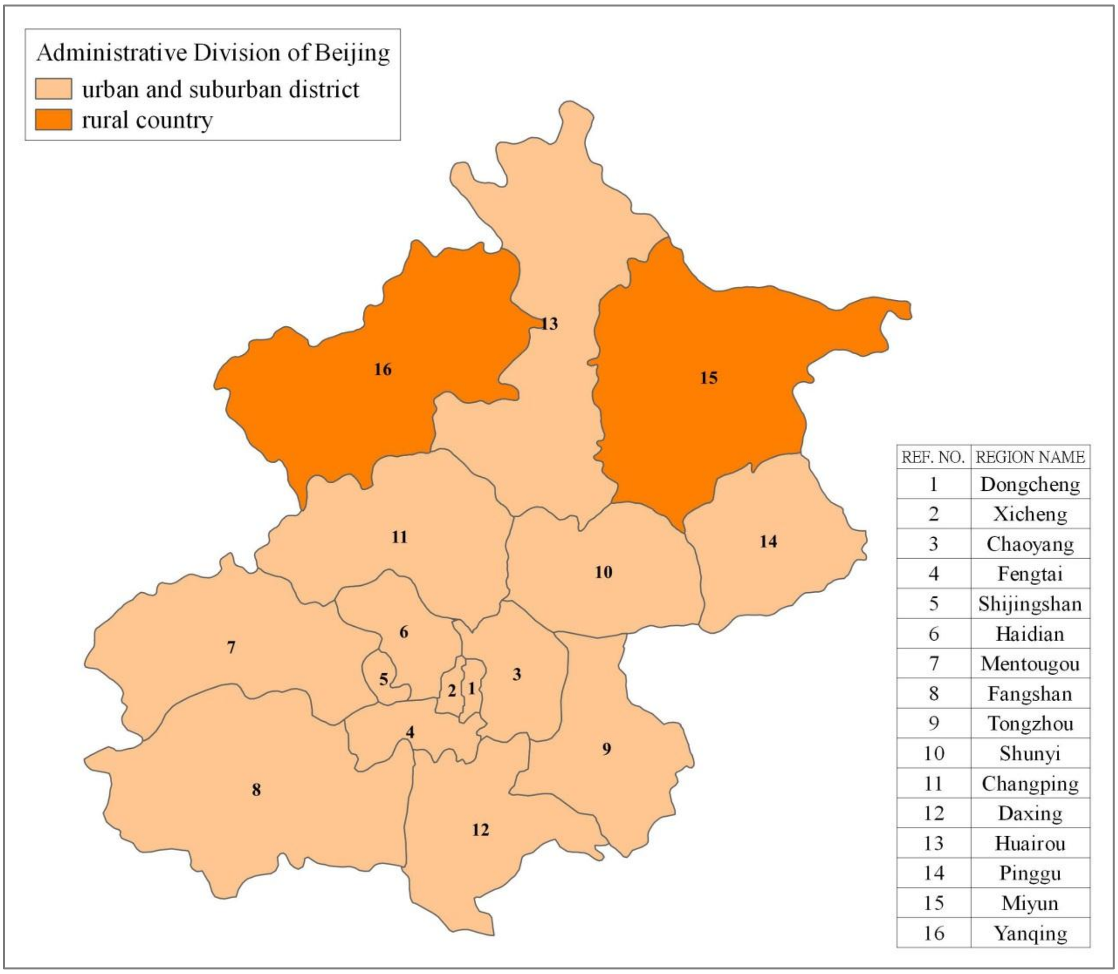


Figure 3.1 Administrative Division of Beijing

This spatial extent of Beijing has been formed since 1958. The administrative division and the administrative levels of the regions within this extent changed several times. The two urban districts, i.e. Dongcheng and Xicheng (regions 1 and 2 in Figure 3.1), form the urban core of Beijing, which occupy the old city region enclosed by city walls in the Qing Dynasty. After the foundation of the People's Republic of China, the accelerative urbanization process resulted in an increase of population and the city extent. The four neighboring regions to the two urban core regions, i.e. Chaoyang, Fengtai, Shijingshan and Haidian (regions 3-6 in Figure 3.1), have become suburban districts. These six regions together (regions 1-6 in Figure 3.1) are generally referred to as the urban area of Beijing (Tian et al., 2010). The other regions cover the most rural areas in Beijing. However, because of the urbanization process and urban planning purpose, the administrative levels of eight regions, i.e. Mentougou, Fangshan, Tongzhou, Shunyi, Changping, Daxing, Huanrou and Pinggu (regions 7-14 in Figure 3.1), has been upgraded from rural countries to municipal districts successively (Table 3.1). The other two regions, i.e. Miyun and Yanqing (regions 15 and 16 in Figure 3.1), are still rural countries in the administrative division. Hence, there are fourteen urban and suburban districts and two rural counties in the current administrative division of Beijing.

Table 3.1 Year of Administrative Upgrade of Beijing Regions

| Reference No. | Region Name | Year of Administrative Upgrade |
|---|---|---|
| 7 | Mentougou | 1958 |
| 8 | Fangshan | 1987 |
| 9 | Tongzhou | 1997 |
| 10 | Shunyi | 1998 |
| 11 | Changping | 1999 |
| 12 | Daxing | 2001 |
| 13 | Huairou | 2001 |
| 14 | Pinggu | 2001 |

Compared with population density data acquired in the sixth national census in 2010 (see Table 2.2), the population densities of the fourteen municipal districts range from 146 to 24,373 people/km$^2$, with a mean of 5808 people/km$^2$, and a standard deviation of 7933 people/km$^2$. This distribution shows that the population densities of municipal districts are dramatically different. Some districts, e.g. Huairou and Penggu, are more similar to rural countries than urban districts in population density, even if their administrative level has been upgraded. The comparison of population density ranges between municipal districts and countries is visualized in Figure 3.2. Consequently, the administrative division of Beijing does not reflect the realistic distinction between urban and rural areas. Some municipal districts include rural landscape and the realistic urban extent is smaller than the extent indicated by the administrative boundaries.

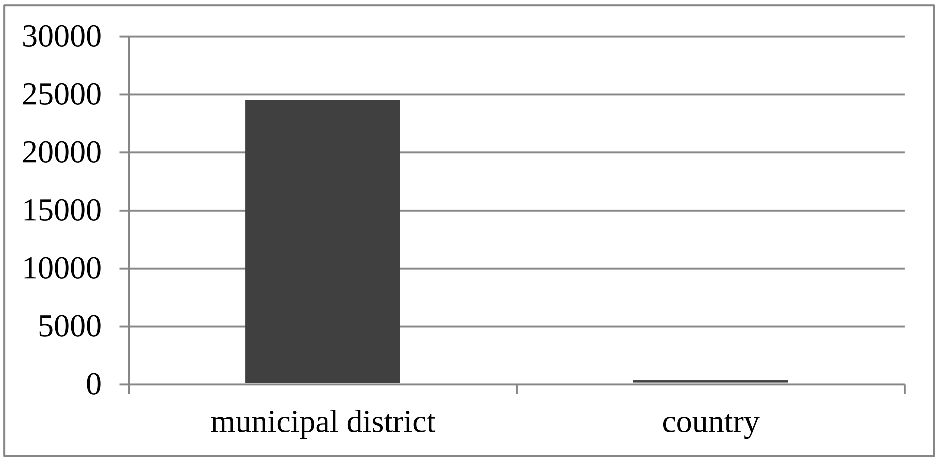


Figure 3.2 Population Ranges of District and Country of Beijing

In the main functional area planning of Beijing approved on 25th July 2012 by the Beijing government, the sixteen administrative regions are classified into four types according to their functional positioning, i.e. capital function core area, urban function expansion area, urban development new area and ecological conservation area (Figure 3.3) (Beijing Government, 2012).

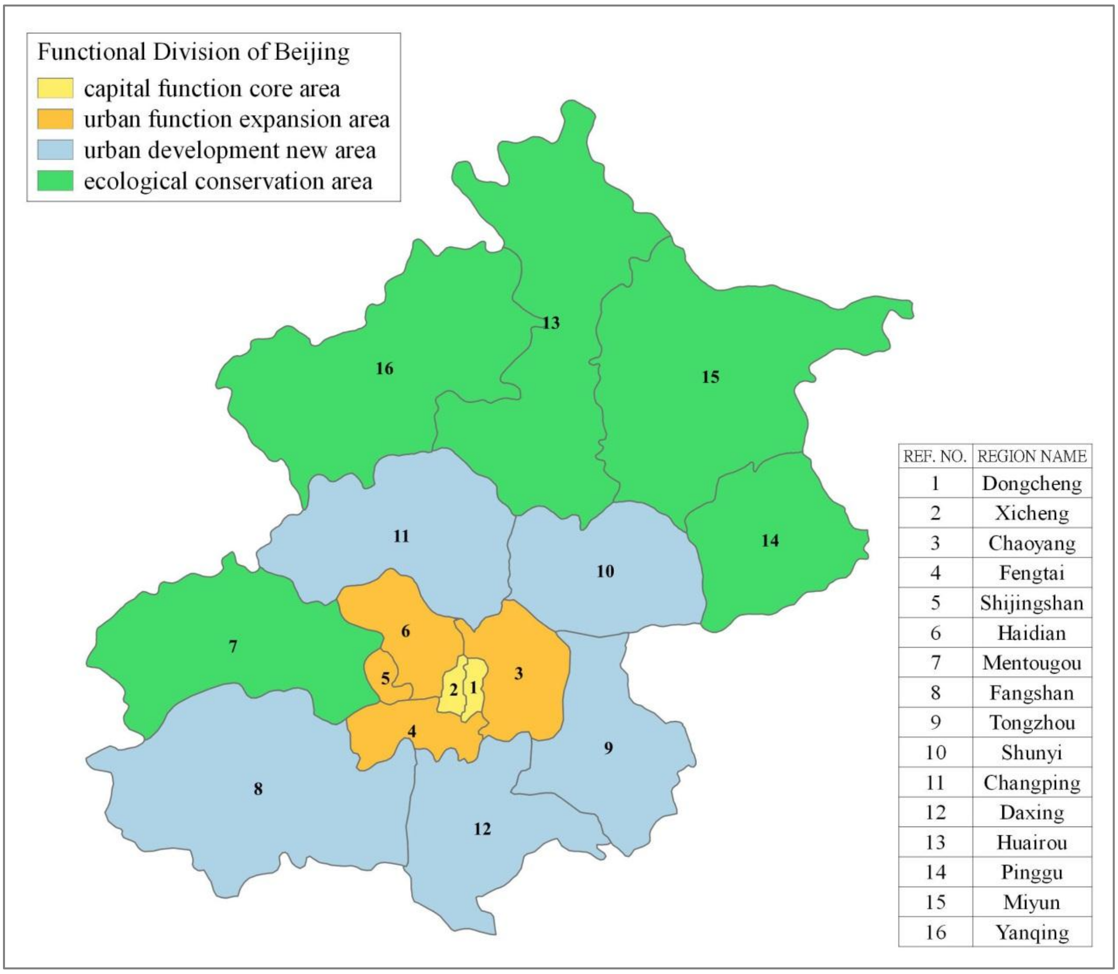


Figure 3.3 Functional Division of Beijing

The capital function core area comprises Dongcheng and Xicheng districts (regions 1 and 2 in Figure 3.3), which are fully urbanized areas. The main function of this type is optimization of development. The urban function expansion area is constituted of Chaoyang, Haidian, Fengtai and Shijingshan districts (regions 3-6 in Figure 3.3), which are highly but not fully urbanized areas. The main function of this type is high priority of development. The urban development new area is composed of Fangshan, Tongzhou, Shunyi, Changping and Daxing districts (regions 8-12 in Figure 3.3), which are of large potential to be developed. The main function of this type is development of new suburban areas. The ecological conservation area consists of Mentougou, Huairou and Pinggu districts, as well as Miyun and Yanqing countries (regions 7, 14-16 in Figure 3.3), which are of importance in natural resource conservation. The main function of this type is restriction of development (Beijing Government, 2012). It can be seen from such a functional division that the capital function core area and the urban function expansion area constitute the general urbanized area of Beijing; the urban development new area accounts for the urbanizing area of Beijing, surrounding the urbanized area, which shows a urban sprawl from the urbanized area into its surrounding environment; and the ecological conservation area is of importance in natural resource conservation, where strong urbanization is not allowed. This functional division accords with the pattern of population distribution in Beijing. Compared with population density data acquired in the sixth national census in 2010 (see Table 2.2), the two districts of the capital function core area have the highest population densities in Beijing, which are 21,881 and 24,373 people/km$^2$ respectively. The districts of the urban function expansion area are of relatively high population densities, from 6,860 to 7,702 people/km$^2$. The population densities in the urban development new area are considerably lower than the former two areas, from 506 to 1,361 people/km$^2$. In the ecological conservation area, population densities are evidently low, from 146 to 387 people/km$^2$. This comparison of population density ranges between the four types of areas is visualized in Figure 3.4.

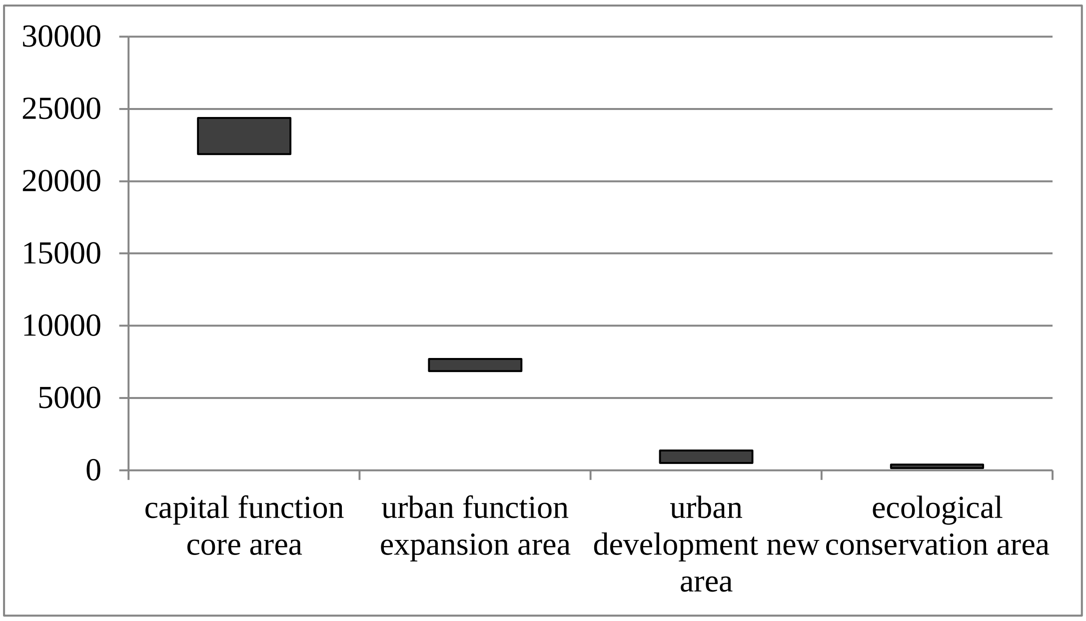


Figure 3.4 Population Ranges of Functional Areas of Beijing

Using the population data acquired from the fifth and sixth national censuses in 2000 and 2010 respectively, population densities in 2000 and 2010 are calculated for the four areas, as well as the absolute increase and increase rate between these two years, which are shown in Table 3.2.

Table 3.2 Population Density of Functional Areas of Beijing

| **Functional Type** | **Population Density in 2000** | **Population Density in 2010** | **Increase of Population Density** | **Increase Rate** |
|---|---|---|---|---|
| capital function core area | 22,742 | 23,247 | 505 | 2.22% |
| urban function expansion area | 4,949 | 7,402 | 2,453 | 49.57% |
| urban development new area | 554 | 979 | 425 | 76.71% |
| ecological conservation area | 178 | 201 | 23 | 12.92% |

The increase rates of the four areas show that the increase of population density in the capital function core area is the slowest (2.22%), due to the fact that this area has been highly urbanized; the urban function expansion area has a medium level of increase rate (49.57%), which reflects that this area is still under urbanization; the urban development new area presents the highest increase rate (76.71%), which indicates that the urbanization process is expanding to this area and it has a large potential to be further developed. The increase rate of the ecological conservation area is relatively low (12.92%), as it accounts for the rural area in Beijing, where the urbanization process is restricted and thus slow. Compared to the administrative division, this functional division by urban planners differentiates better between urbanized, urbanizing and rural areas.

Urban scholars, on the other hand, divide Beijing into four areas, i.e. inner center, outer center, inner periphery and outer periphery, according to the administrative boundaries and the underlying patterns (Tian et al., 2010). As shown in Figure 3.5, the inner center comprises Dongcheng and Xicheng districts (regions 1 and 2 in Figure 3.5), which equals the area inside the old walled city. Though the city walls no longer stand, they continue to retain geographical significance. Streets that once traversed the walls are still named “nei” (inner) or “wai” (outer) in relationship to whether the street sections are inside or outside the walls. The boundary of the inner city lies between the Second Ring Road and the Third Ring Road. The outer city encloses the inner city, comprising Chaoyang, Fengtai, Shijingshan and Haidian districts (regions 3-6 in Figure 3.5). It approximates the area between the Second Ring Road and the Fifth Ring Road. The inner periphery surrounds the outer city, composed of Mentougou, Fangshan, Tongzhou, Shunyi, Changping and Daxing districts (regions 7-12 in Figure 3.5). These districts are linked by the Sixth Ring Road. The outer periphery includes Penggu and Huairou districts, as well as Miyun and Yanqing countries (regions 14-16 in Figure 3.5). It is farther away from the inner and outer city regions.

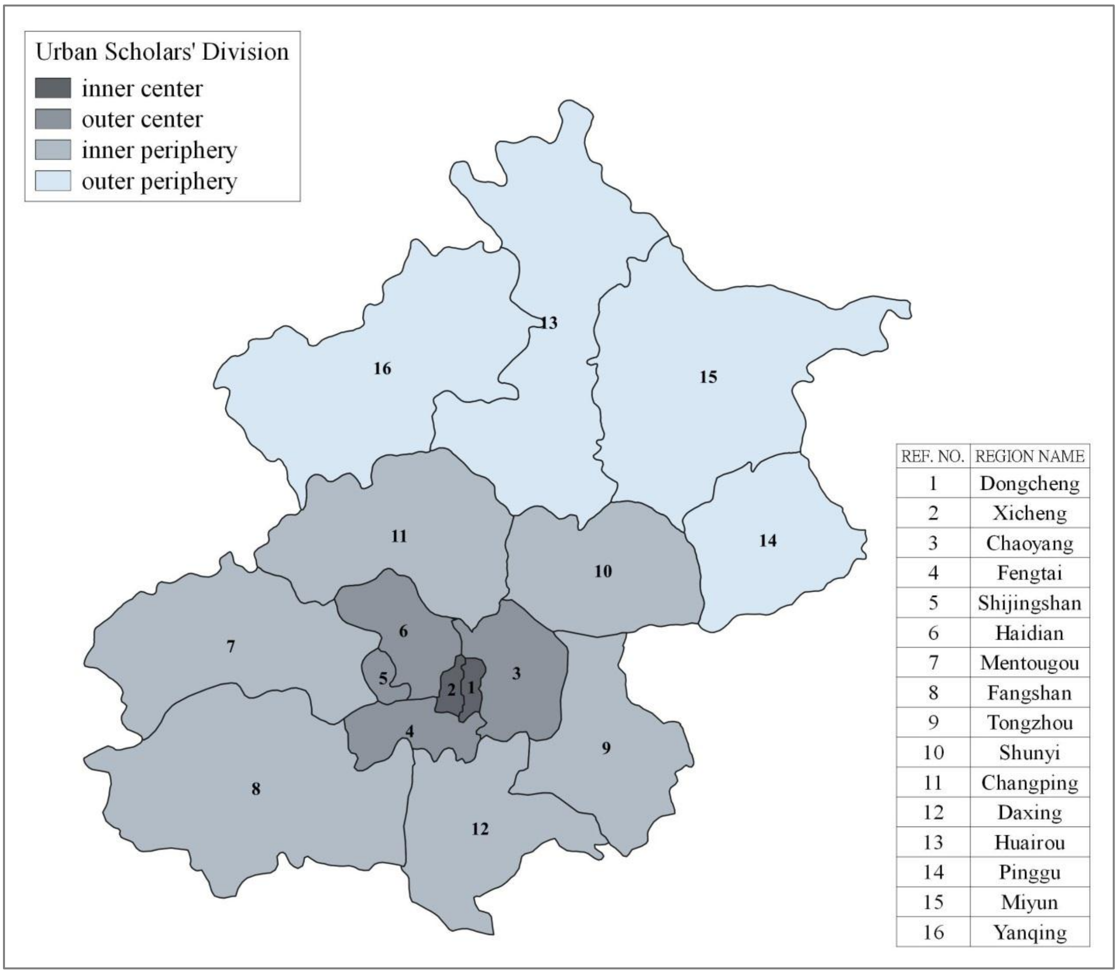


Figure 3.5 Analytical Division of Beijing

Compared with the functional division, the inner city equals the capital function core area; the outer city corresponds to the urban function expansion area; five of the six regions of the inner periphery compose the same area as the urban development new area; and the outer periphery is equivalent to four of the five regions of the ecological conservation area. The only difference is that in the functional division, Miyun district is regarded more similar to the other four areas of the ecological conservation area, even if it is not connected to them, while in the urban scholars' view, it is more close to the other five areas of the inner periphery, as they are spatially connected and enclose together the inner and outer city regions. The common view shared by urban planners and scholars is that the six districts, i.e. Dongcheng, Xicheng, Chaoyang, Fengtai, Shijingshan and Haidian compose the urban area of Beijing, based on the administrative boundaries.

Tian et al. (2010) proposed a new zoning method for Beijing based on the ring road system. The major road system, with ring roads and radial arteries, is a primary determinant of the urban spatial structure of Beijing. The ring roads and radial roads that have been developed over the past several decades give rise to the underlying pattern of urban growth of Beijing. The major road around the Forbidden City is named the first ring road. The concentric major roads beyond the first ring road are called the second, third, fourth, fifth and sixth ring roads in the order of the radial distance from the center of the city. Nowadays, the name of the first ring road is not used. Maps of Beijing do not indicate the first ring road (Figure 3.7). Only the names of the second to sixth ring roads are formally used. These five ring roads are depicted in yellow in Figure 3.6, on a base satellite image of Beijing. From inner to outer, the five rings correspond to the second to sixth ring roads. Tian et al. (2010) showed that these concentric ring roads provide a basic framework for the city's overall spatial pattern. They divided Beijing into five zones according to the ring road system. The first zone is the area inside the third ring road, which is regarded as the central business district (CBD) of Beijing. The second zone is the area between the third and fourth ring roads, which is dominant by office buildings, residential structures and commercial facilities. The third zone is the area between the fourth and fifth ring roads, regarded as manufacture-residence zone. The fourth zone is the area between the fifth and sixth ring roads, regarded as residence-manufacture zone. Compared with the third zone, more companies are located in the third zone while more residential areas are in the fourth zone. The fifth zone is the area outside the six ring roads, which includes suburbs and satellite cities. This zoning method does not attempt to draw a boundary between urban and rural areas, but it points out that the ring road order approximates the 'footprints' of urban growth, and the ring roads roughly indicates the location and extent of the urban area of Beijing.

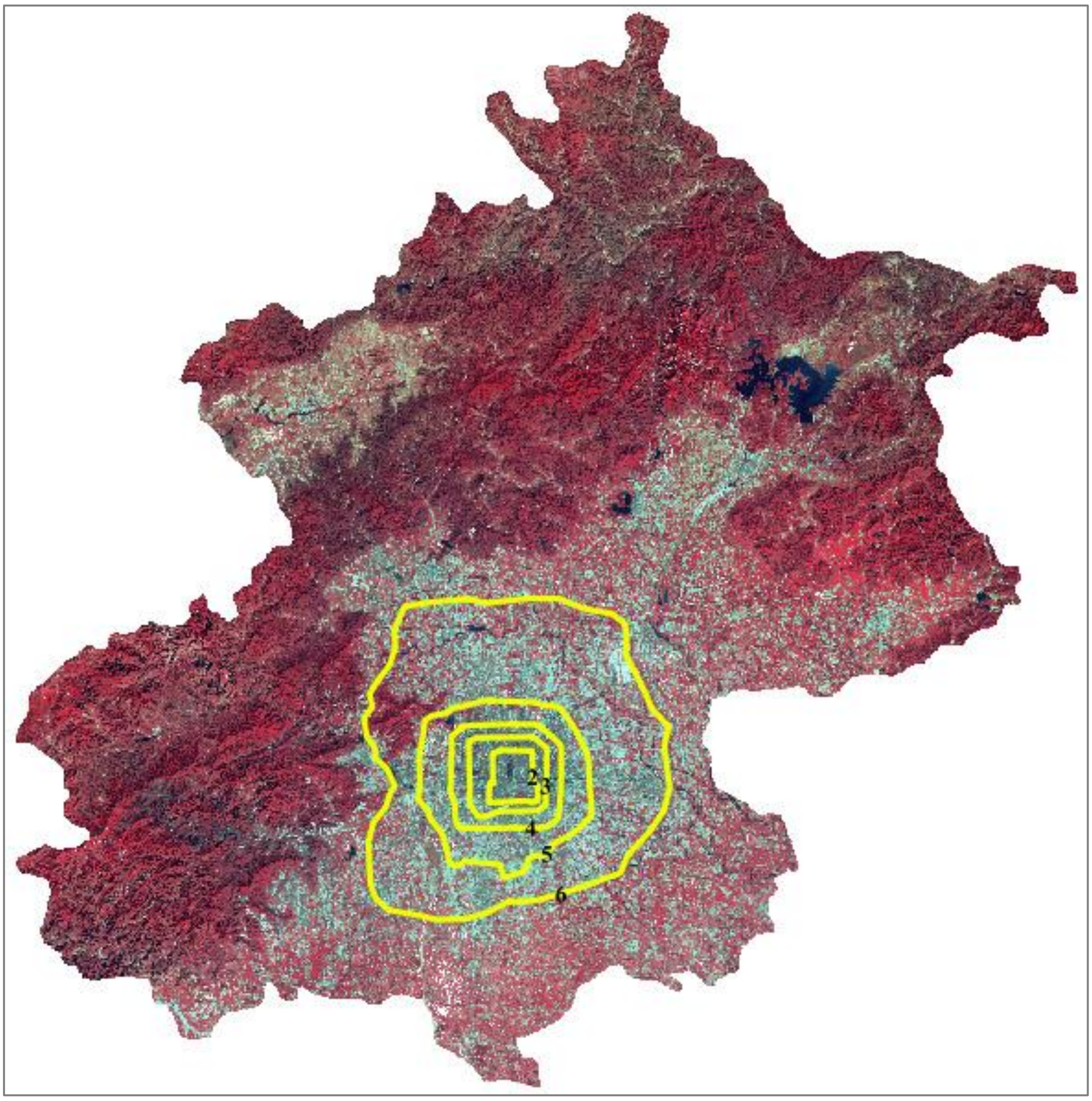


Figure 3.6 The Ring Road System of Beijing

This is consistent with the map of the urban area of Beijing in the Alas of Beijing, which was published by SinoMaps Press and audited by the Beijing Institute of Surveying and Mapping in 2008 (SinoMaps Press, 2008). SinoMaps Press is a public institution under the direct jurisdiction of the State Bureau of Surveying and Mapping.

It is the only national map publisher in China. The atlas contains a map of the urban area of Beijing (Figure 3.7). It does not indicate a definite extent of the urban area. It covers an area around from 116°3´E, 39°45´N to 116°44´E, 40°7´N. Such an area includes entire Dongcheng, Xicheng, ChaoYang, Fengtai, Shijingshan Districts and part of Haidian, Mentougou, Fangshan, Tongzhou, Shunyi, Changping, Daxing Districts. That is to say, it includes the entire inner center, almost the whole outer center and the inner part of the inner periphery. The four regions of the outer periphery are entirely outside the map extent. From the map's point of view, the urban area of Beijing is within such an extent. Moreover, consistent with the view of Tian et al. (2010), the concentric ring roads are located in the center of the map area. The second to fifth ring roads are entirely included and the sixth ring road is partly included.

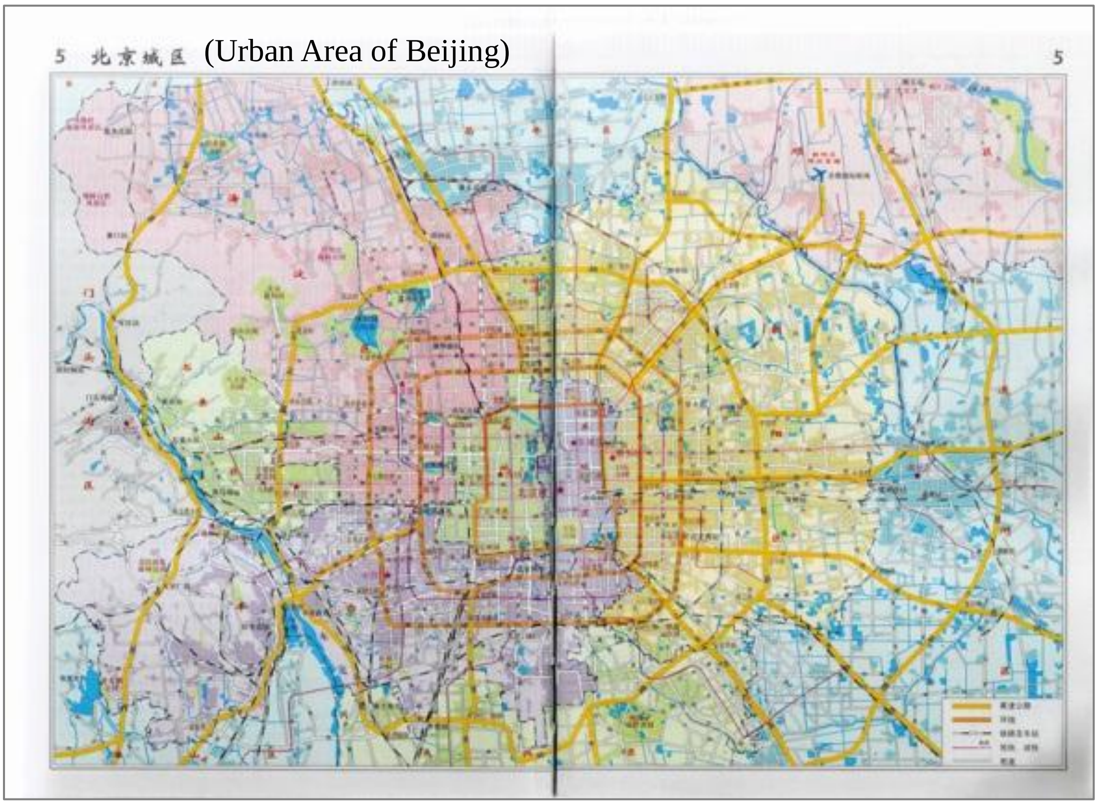


Figure 3.7 The Map of the Urban Area of Beijing

(Source: SinoMaps Press, 2008)

# Chapter 4 Evaluating Image Features for Characterizing Urban and Rural Areas

As discussed in Chapter 3, land cover composition and configuration can be used to characterize urban and rural areas, which can be described using a range of features derived from remote sensing images. This chapter introduces such a set of image features and evaluates if it presents a significant difference between urban and rural areas.

## 4.1 Remote Sensing Image Features Related to Urban Characteristics

A set of features is expected to represent two types of information, i.e. compositional and configurational information. The features for compositional information are straightforward. The V-I-S model presented that the composition of four types of land cover characterize different kinds of environment (Ridd, 1995). Based on the V-I-S model, a combination of the proportions of the four land cover types is used as the features for representing land cover composition. The four land cover types are vegetation, impervious surface, soil and water / shade. The features for configurational information are not so intuitive. The spatial distribution of land cover can be observed as textures. Texture is one of the key elements used for image interpretation (Tempfli et al., 2009). Texture refers to the arrangement and frequency of tonal variation in particular areas of an image. Smooth textures are often the result of uniform and even surfaces, such as fields, asphalt or grasslands. A target with a rough surface and irregular structure results in a rough textured appearance. Texture is a kind of structural information, which can be easily recognized by human eyes. As reviewed in Section 2.2.2.2, a set of image features has been developed for characterizing texture in a computational way, based on the so-called gray-level co-occurrence matrices (GLCM) (Haralick, 1973). Four of the GLCM textural features were further identified as optimal texture classifiers (Gotlieb and Kreyszig, 1990). This research uses these four textural features for representing land cover configuration. Altogether, a set of eight features is used to describe land cover. An analysis is made to evaluate if this feature set shows a significant difference between urban and rural environments and thus can be used to distinguish between urban and rural areas.

## 4.2 Experiments for Evaluation

Experiments are designed to test if the proposed eight features are effective to distinguish between urban and rural areas. As discussed in Section 3.3, based on the administrative boundaries of the study area, different urban-rural classifications are made by administrators, urban planners and scholars. Although differences are found in some regions, there are common urban and rural areas in the three divisions. Therefore, these three kinds of urban-rural division are used as reference data. The eight features are hence also calculated on an administrative division basis. They are calculated for all the sixteen administrative regions. Clustering analysis is performed to see if the eight features show a pattern that is consistent with the referenced data. The data and steps involved are described in detail as follows.

### 4.2.1 Data Sources

Two sets of Landsat-5 Thematic Mapper (TM) images of the study area are used in this study, which contain seven multi-spectral bands. The data are created by the U.S. Geological Survey (USGS) and stored in Geographic Tagged Image-File Format (GeoTIFF). They are downloaded from the Earth Science Data Interface (ESDI) at the Global Land Cover Facility (GLCF) of the University of Maryland. Landsat data are referenced using a Worldwide Reference System (WRS). In the WRS-2 of Landsat-5, the whole world is divided into 233 paths and 122 rows. Image data covering any portion of the world can be identified using the path and row numbers. The two sets of data used in this study are of path 123, row 32 and path 123, row 33 respectively. The combination of these two ranges covers the whole study area (the boundary of the study is delineated in yellow in Figure 4.1). Both of the two data sets were acquired on 22$^{nd}$ September 2009. A geo-referenced mosaicking is performed to combine the two sets of images. Figure 4.1 shows the image data in a false-color synthesis, by assigning the values of near-inferred, red and green bands to the red, green and blue channels respectively. The boundary of the study is delineated in yellow. The sensed energy intensity is recorded in 8-bit data, that is, there are 256 grey levels in each band of the image.

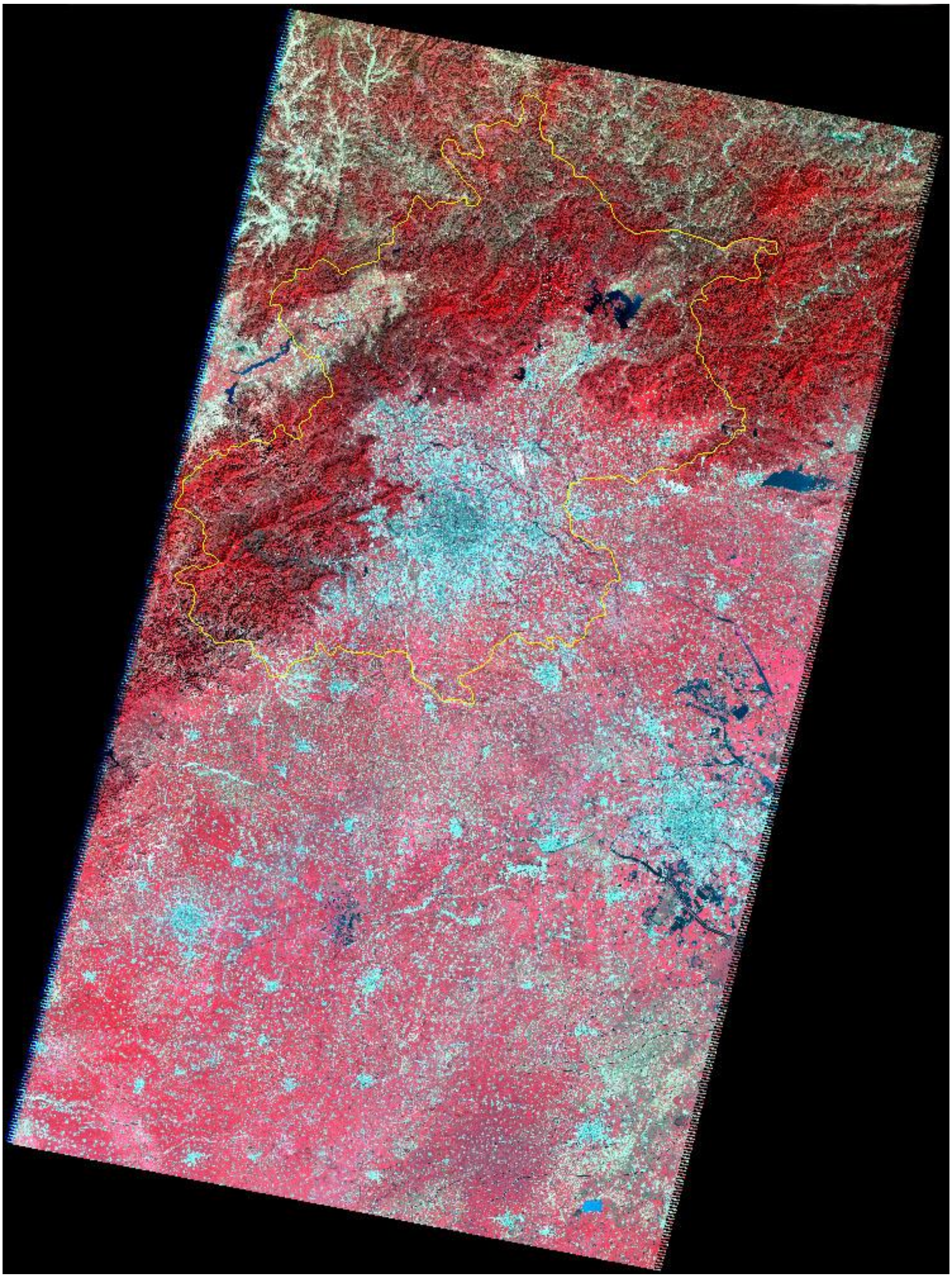

Figure 4.1 The Source Landsat TM Image Data

Another data set used in this study is the set of administrative boundaries of the study area, which is stored in a vector data format. It is downloaded from the GADM database of Global Administrative Areas. The administrative regions of Beijing are selected to be used, as shown in Figure 4.2.

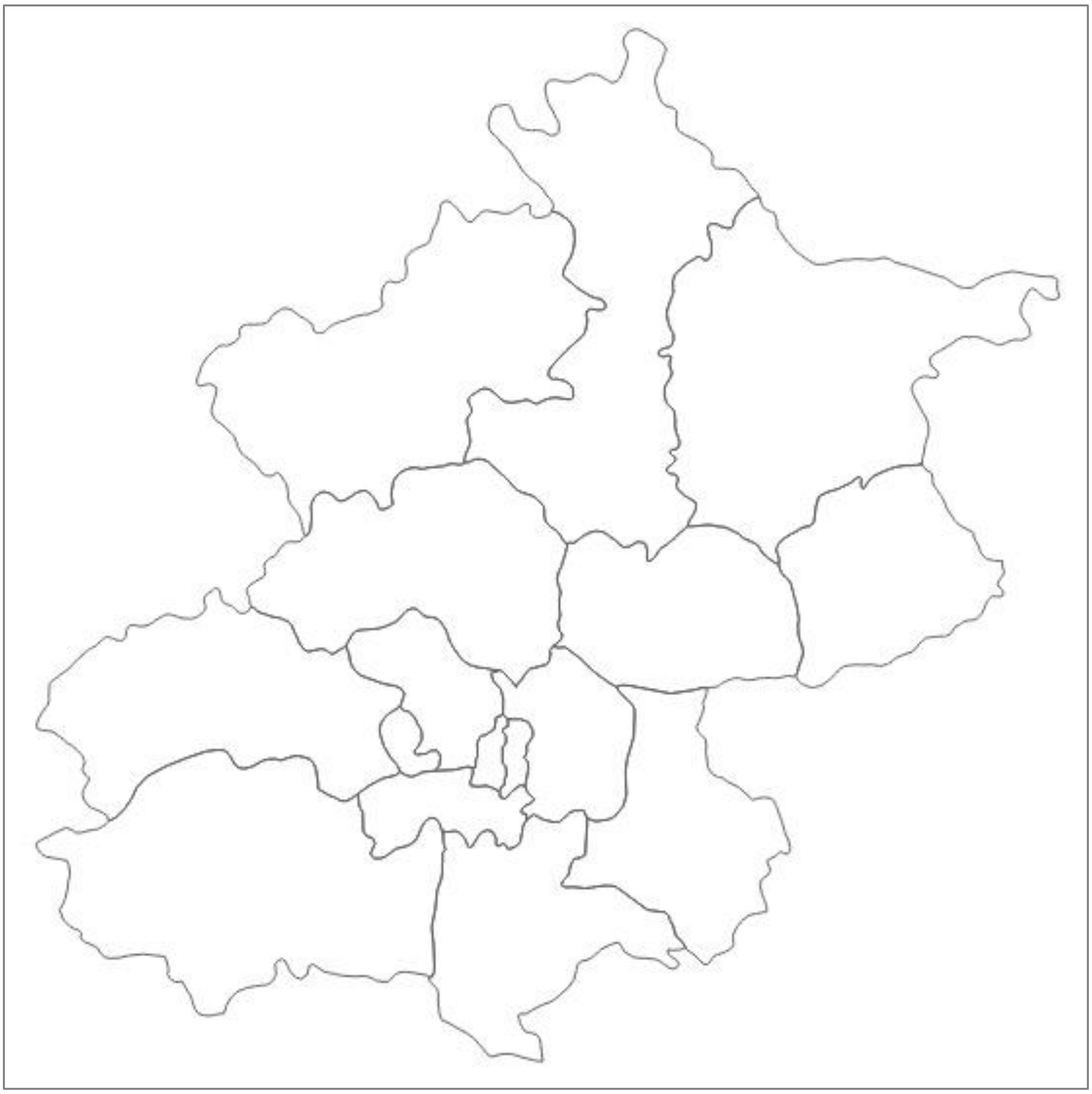

Figure 4.2 The Source Vector Data of Administrative Boundaries

By overlaying the vector data set on the image data set, the specific area of the image data corresponding to the study area is masked for later processing and analysis (Figure 4.3). The image area outside the study area is ignored in later processing and analysis. Figure 4.3 shows the masked image area in a false-color synthesis, by assigning the values of near-inferred, red and green bands to the red, green and blue channels respectively.

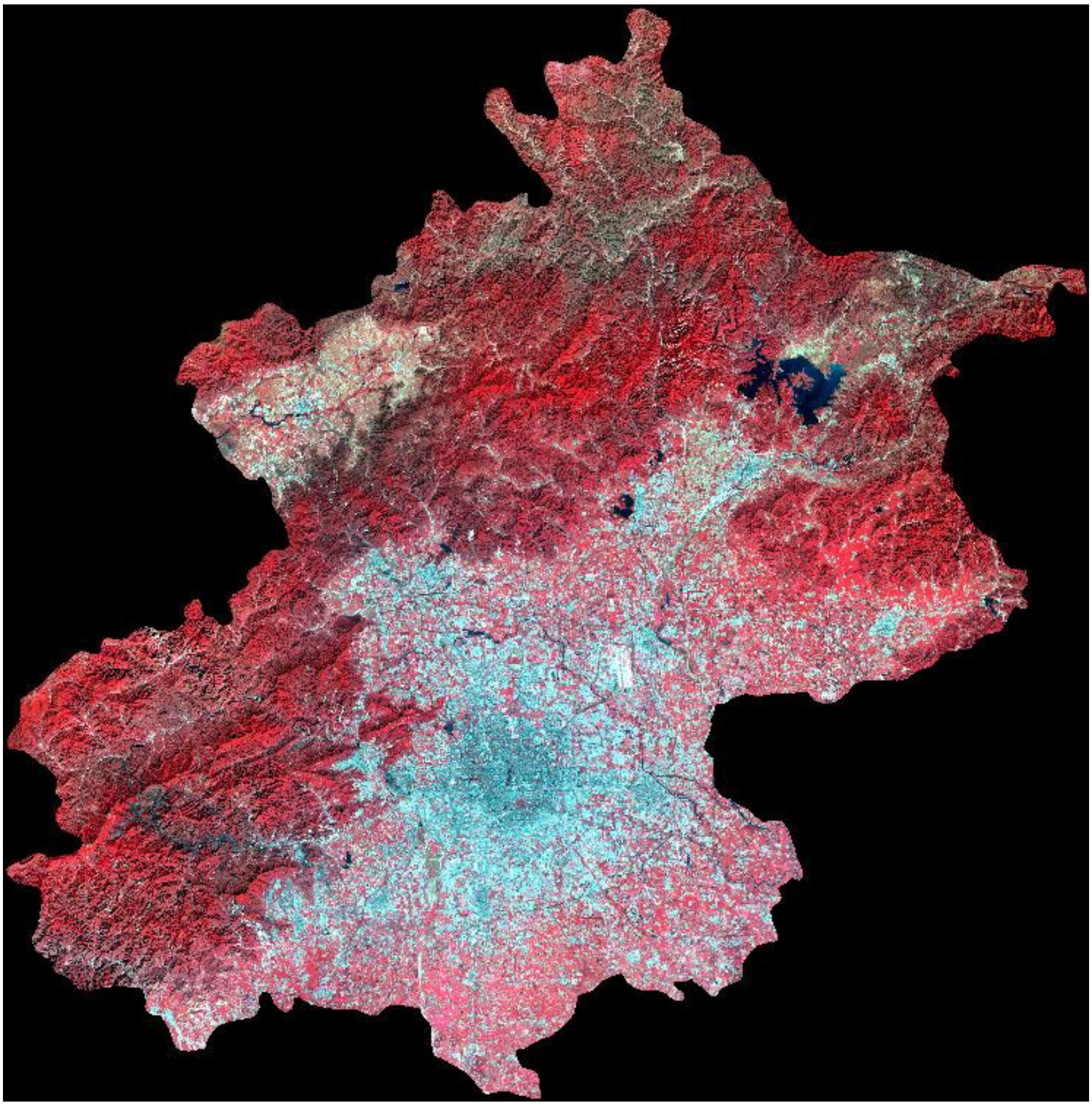

Figure 4.3 The Prepared Data of the Study Area for Analysis

### 4.2.2 Extraction of the Eight Features

In urban remote sensing, linear spectral unmixing is widely used to extract the proportions of land cover in each image pixel. As reviewed in Section 2.2.3, this process involves a selection of representative pixels of each land cover type, which are called endmembers. In this study, endmembers are selected manually from the image. Vegetation endmembers are selected from vegetated hillsides exposed to sun light. Impervious surface endmembers are selected from large building roofs, road crosses and airport runways. Soil endmembers are selected from bare farm lands. Water endmembers are selected from lakes. The separability of the selected endmembers can be evaluated prior to the unmixing process, using the Jeffries-Matusita and Transformed Divergence separability measures (Richards and Jia, 2005). Both the measures range from 0 to 2 and indicate how well the pairs of endmembers of any two of the four land cover types are statistically separable. Values greater than 1.9 indicate good separability. The endmembers with good separability are then used to unmix each image pixel. Four proportions, corresponding to the four land cover types, are calculated for every pixel. Before the unmixing results are used to extract the eight features, they are evaluated in three ways. Firstly, the four proportions are visualized as grey-level images to see if the proportion distribution pattern is consistent with the prior knowledge about the study area. Secondly, the root mean square (RMS) error is calculated for every pixel. A small RMS error indicates that the linear mixture model constructed is mathematically good. Lastly, the unmixed land cover fractions are used to produce a hard classification for comparison, by assigning each pixel to the land cover type with the highest proportion in the pixel. The confusion matrix is then produced.

After obtaining the per-pixel unmixing results, the eight features can be extracted for each administrative region. The proportions of the four land cover classes in a region are calculated by averaging the proportions in the pixels in that region. The textural features are calculated from the hard classification produced from the unmixing results. Summarily, the eight features are calculated for the sixteen administrative regions of the study area, they are:

$f_1$: the proportion of vegetation

$f_2$: the proportion of impervious surface

$f_3$: the proportion of soil

$f_4$: the proportion of water/shade

$f_5$: angular second moment

$f_6$: inverse difference moment

$f_7$: constrast

$f_8$: entropy

The following analysis verifies if the combination of these eight features is effective to characterize urban and rural areas.

### 4.2.3 A Clustering Analysis of the Eight Features

The purpose of this analysis is to test if the proposed eight features are effective to characterize urban and rural areas. Urban and rural areas are expected to show a difference in the feature space composed of the eight features. In order to detect and determine if a difference exists, this study utilizes an automated clustering algorithm. A k-means clustering is performed to classify the sixteen regions in the feature space (MacQueen, 1967). The clustering is a process that groups a set of data such that the similarity within classes is maximized and the similarity between classes is minimized. If two regions are similar with regard to the eight features, they are put to the same class. Otherwise, if two regions are distant in the feature space, they are separated into different classes. According to the three referenced divisions of the study area, numbers of classes of 2, 3 and 4 are tested. In addition, in order to see if the spatial locations of the regions influence the classification, the clustering process is performed twice for each test. At the first time, only the eight features are taken as input to the process, while at the second time, the spatial locations of the regions, represented by their geometrical centroids, are also input to the process. The clustering results are then compared with the referenced divisions. If the clustering results show a pattern consistent with the reference divisions, then the eight features are verified to be useful to characterize different kinds of areas. The results are presented in the next section.

## 4.3 Results and Analysis

The results of linear spectral unmixing of Landsat TM multi-spectral data of the study area are shown in Figure 4.4. Each pixel of the image is unmixed into four proportions, of vegetation, impervious surface, soil and water / shade respectively. These proportions are visualized as images in Figure 4.4. Brighter pixels indicates higher proportions of the corresponding land cover types. Visually, the distribution of the four types of land cover is consistent with the prior knowledge of the study area. Vegetation is mainly distributed in hills and farm lands. The proportions of vegetation are obviously low in the urban area, around the six city regions of the study area (Figure 4.4a). The distribution of impervious surface shows a clear pattern that the proportions are high in the urban area and low in the hill areas. The distinction is easily observed (Figure 4.4b). Soil dose not present such an apparent distinction as vegetation and impervious surface. But it can still be seen that higher proportions are distributed in rural places (Figure 4.4c). High proportions of water / shade correspond to rivers, lakes and building shades (Figure 4.4d).

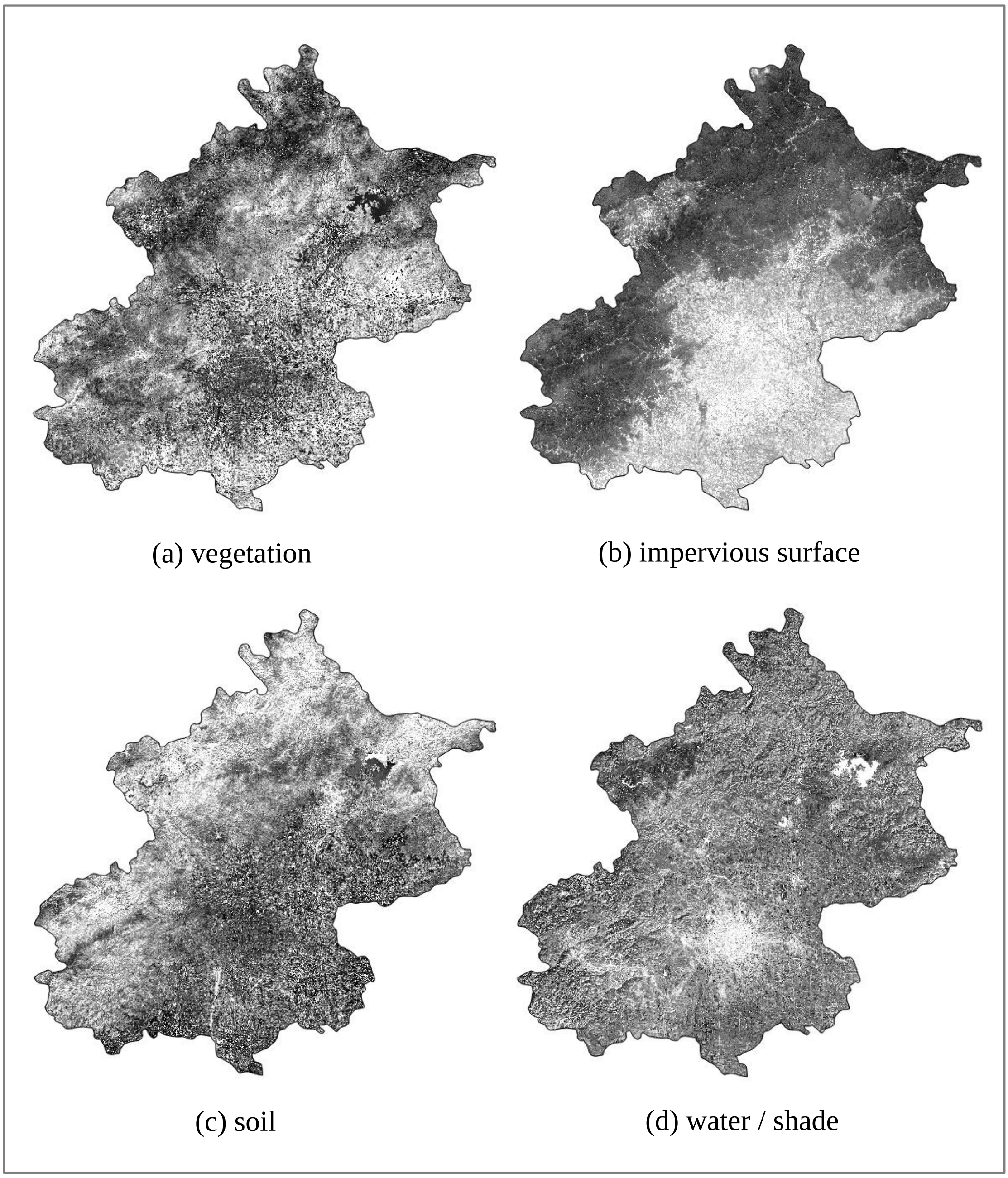


Figure 4.4 Land Cover Proportion Images of the Unmixing Result

The RMS error is calculated for every pixel individually. Some statistics of all RMS errors are computed. The min, max, mean and standard deviation are 0, 5.56, 0.03 and 0.06 respectively. Compared to the 256 grey levels, the RMS errors are small. In addition, 99.9% of the RMS errors are below 0.55. The RMS errors show that the linear mixture model constructed is mathematically good. A hard classification is then produced from the unmixing results, which shown in Figure 4.5. Vegetation, impervious surface, soil and water are indicated in green, red, yellow and blue respectively.

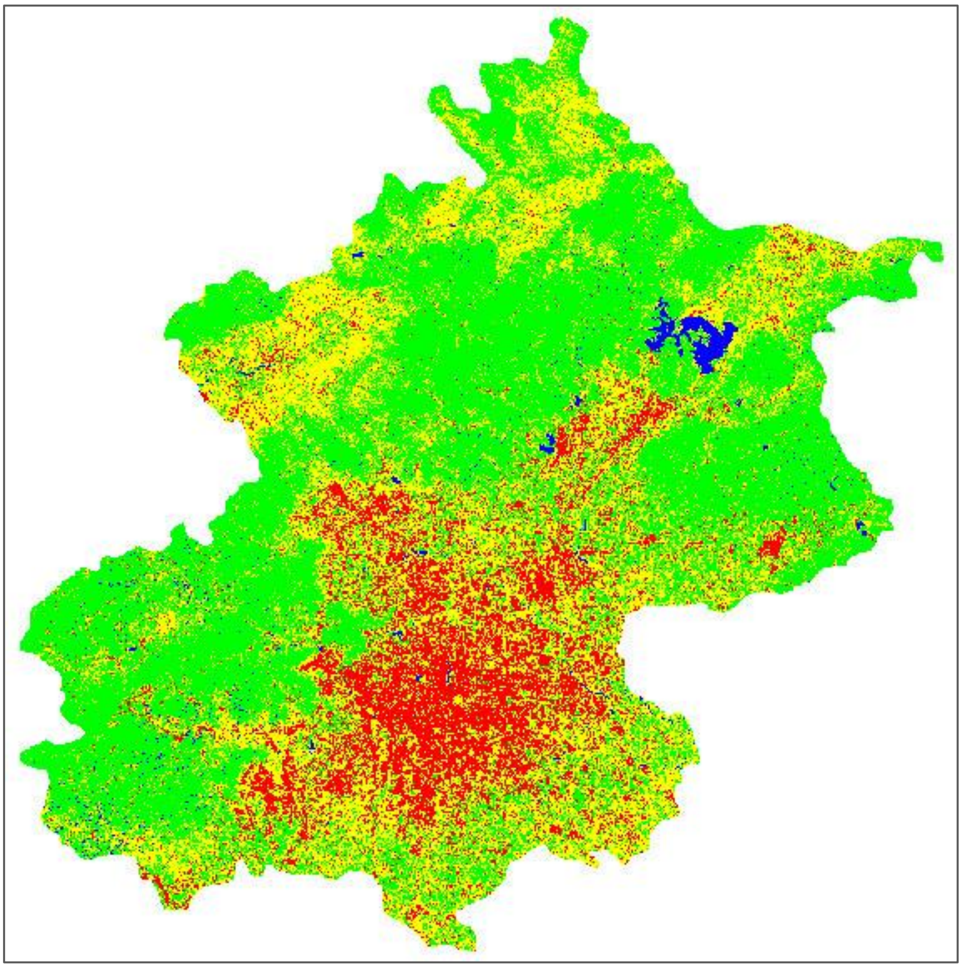

Figure 4.5 Land Cover Classification of the Study Area

The classification accuracy is assessed by comparing the classification data with the visual interpretation of a number of sample pixels. As a rule of thumb, Congalton (1991) suggested at least 50 samples per class, and at least 75-100 samples per class if the area exceeds 500 $km^2$ or the number of classes is more than 12. This coincides with those suggested by Hay (1979) and Fenstermaker (1991). In this study, 500 samples are randomly selected from the study area. The confusion matrix is presented in Table 4.1, including the producer’s accuracy, user’s accuracy of each class, overall accuracy and kappa coefficient.

Table 4.1 Accuracy Report of the Classification Result

| | | Reference Data | | | | | |
|---|---|---|---|---|---|---|---|
| | | V | I | S | W | Σ | user's acc. |
| Classified Data | V | 159 | 5 | 3 | 5 | 172 | 92.40% |
| | I | 8 | 144 | 5 | 0 | 157 | 91.70% |
| | S | 10 | 8 | 77 | 1 | 96 | 80.20% |
| | W | 1 | 2 | 1 | 71 | 75 | 94.70% |
| | Σ | 178 | 159 | 86 | 77 | 500 | |
| | prod. acc. | 89.30% | 90.60% | 89.50% | 92.20% | | |
| | overall accuracy 90.2% | | kappa coefficient 0.86 | | | | |

### 4.3.1 The Eight Features

Based on the unmixing results, the four proportional features, i.e. $f_1 - f_4$ described in Section 4.2.2, are extracted for the sixteen administrative regions of the study area. The results are shown in Table 4.2. The reference numbers of the regions corresponds to the numbers in Figure 3.2.

Table 4.2 The Proportional Features of the Sixteen Administrative Regions

| Ref. No. | Proportion of Vegetation | Proportion of Impervious Surface | Proportion of Soil | Proportion of Water / Shade |
|---|---|---|---|---|
| 1 | 0.00881 | 0.74873 | 0.22155 | 0.02091 |
| 2 | 0.01317 | 0.76361 | 0.21492 | 0.00830 |
| 3 | 0.05841 | 0.56468 | 0.37305 | 0.00386 |
| 4 | 0.09036 | 0.59532 | 0.31338 | 0.00095 |
| 5 | 0.32072 | 0.42957 | 0.24791 | 0.00179 |
| 6 | 0.27448 | 0.35485 | 0.36358 | 0.00708 |
| 7 | 0.79712 | 0.04134 | 0.15040 | 0.01115 |
| 8 | 0.51963 | 0.13291 | 0.33219 | 0.01527 |

| | | | | |
|---|---|---|---|---|
| 9 | 0.23060 | 0.25642 | 0.50313 | 0.00985 |
| 10 | 0.36041 | 0.19605 | 0.44067 | 0.00287 |
| 11 | 0.48841 | 0.16751 | 0.33702 | 0.00706 |
| 12 | 0.26014 | 0.28652 | 0.45314 | 0.00020 |
| 13 | 0.67076 | 0.03600 | 0.28597 | 0.00727 |
| 14 | 0.75477 | 0.05479 | 0.18296 | 0.00748 |
| 15 | 0.61936 | 0.05003 | 0.28802 | 0.04259 |
| 16 | 0.55277 | 0.03627 | 0.40462 | 0.00634 |

It can be seen that the lowest proportions of vegetation appear in regions 1 and 2, which are around 1%. At the same time, these two regions have the highest proportions of impervious surface, which are over 70%. These two regions are Dongcheng and Xicheng districts, which are the most urbanized area of the study area. In the functional division, they compose the capital function core area (Figure 3.4). In the analytical division, they are the inner center of the study area (Figure 3.6). The lowest proportions of impervious surface appear in regions 7, 13 – 16, which are below 10%. These regions also contain the highest proportions of vegetation, which are above 60%. These regions equal to the ecological conservations area in the function division, which are the most rural regions of the study area (Figure 3.4). The regions 3 – 6 have proportions of impervious surface between 30% and 60%, which correspond to the urban function expansion area in the functional division and outer center in the analytical division (Figures 3.4 and 3.6). Regions 8 – 12 take up the proportions of impervious surface between 10% and 30%, which constitute the same area as the urban development new area in the functional division (Figure 3.6). For the ease of observing the pattern, the land cover proportions of the sixteen regions are visualized in Figure 4.6. Brighter colors indicates higher proportions. Comparing to the divisions of the study area from both urban planners and scholars (Figure 3.4 and 3.6), it can be seen that the proportions of vegetation and impervious show a clear pattern that distinguishes between urban and rural areas (Figure 4.6(a, b)).

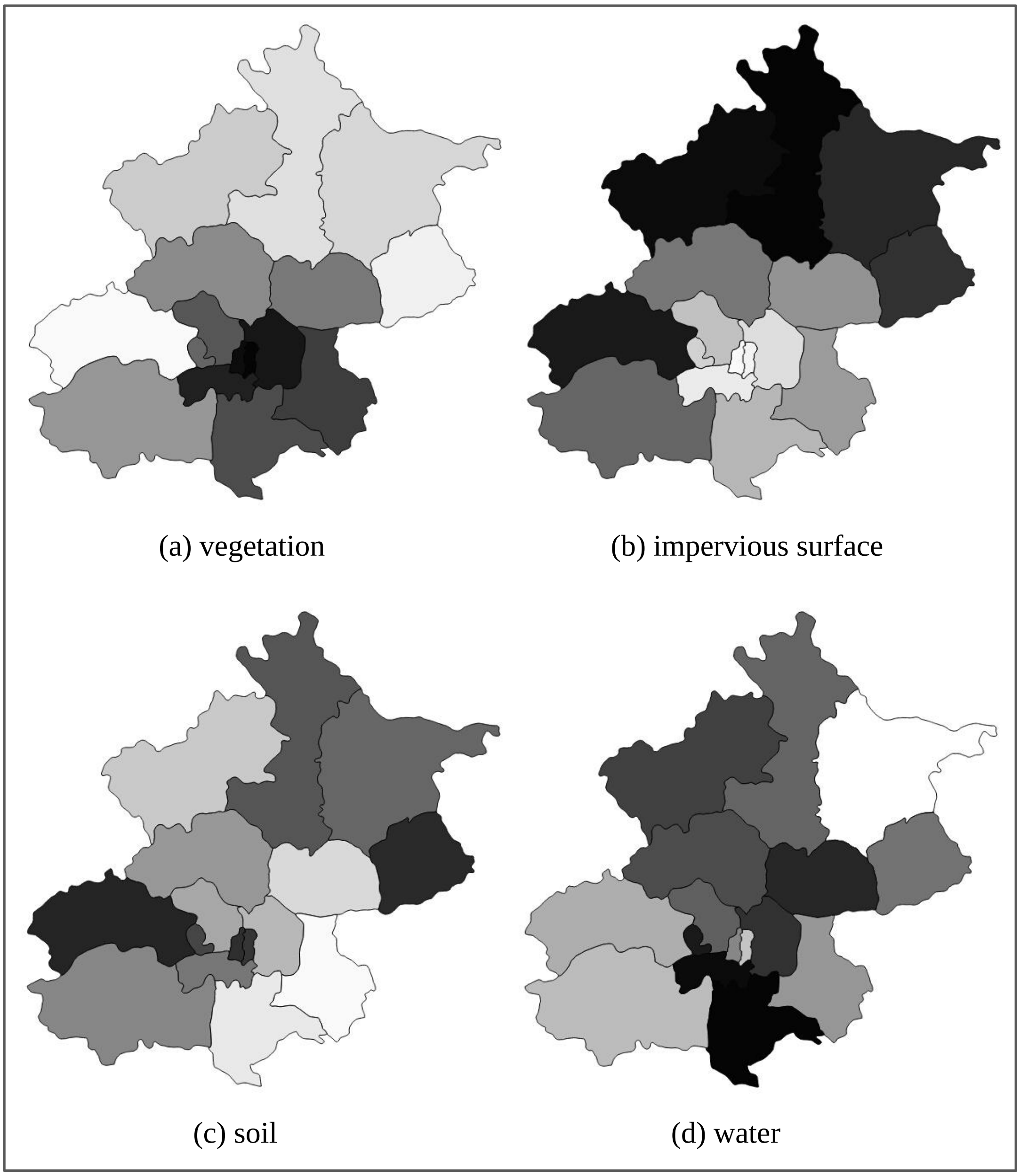

(a) vegetation (b) impervious surface

(c) soil (d) water

Figure 4.6 Comparison of Proportional Features between Administrative Regions

Based on the classification, the four textural features, i.e. $f_5 - f_8$ described in Section 4.2.2, are extracted for the sixteen administrative regions of the study area. The results are shown in Table 4.3. The reference numbers of the regions corresponds to the numbers in Figure 4.7.

Table 4.3 The Textural Features of the Sixteen Administrative Regions

| Ref. No. | Angular Second Moment | Inverse Difference Moment | Contrast | Entropy |
|---|---|---|---|---|
| 1 | 0.44188 | 0.90117 | 0.19767 | 1.05758 |
| 2 | 0.42838 | 0.88247 | 0.23506 | 1.08669 |
| 3 | 0.33336 | 0.88852 | 0.22296 | 1.21524 |
| 4 | 0.34404 | 0.89108 | 0.21783 | 1.19871 |
| 5 | 0.35384 | 0.90468 | 0.19064 | 1.17020 |
| 6 | 0.36904 | 0.89596 | 0.20809 | 1.16104 |
| 7 | 0.84831 | 0.97341 | 0.05319 | 0.36710 |
| 8 | 0.64173 | 0.94448 | 0.11105 | 0.73362 |
| 9 | 0.45683 | 0.91404 | 0.17191 | 1.02570 |
| 10 | 0.53044 | 0.92491 | 0.15018 | 0.91346 |
| 11 | 0.59391 | 0.94213 | 0.11574 | 0.80578 |
| 12 | 0.42406 | 0.90731 | 0.18537 | 1.07660 |
| 13 | 0.87546 | 0.98012 | 0.03977 | 0.31188 |
| 14 | 0.81486 | 0.96931 | 0.06138 | 0.43160 |
| 15 | 0.82704 | 0.97094 | 0.05811 | 0.40846 |
| 16 | 0.85646 | 0.97313 | 0.05374 | 0.35055 |

It can be seen that the lowest values of angular second moment appears in regions 1 – 6, which are between 0.33 and 0.44. The highest values appear in regions 7, 13 – 16, which are between 0.81 and 0.88. The other regions 8 – 12 take up the values between 0.42 and 0.64. Similarly, these three groups of regions hold the values of inverse difference moment of different and not overlapping ranges, between 0.88 and 0.90, 0.97 and 0.98, 0.91 and 0.94 respectively. On the contrary, the regions 1 – 6 show the highest values of both contrast and entropy, from 0.19 to 0.24 and from 1.06 to 1.22 respectively. The medium levels of contrast and entropy appear in regions 8 – 12, which are between 0.11 and 0.19, 0.73 and 1.08 respectively. The lowest ranges appear in regions 7, 13 – 16, which are from 0.04 to 0.06 and from 0.31 to 0.43 respectively. The four textural features of the sixteen regions are visualized in Figure

4.7. Brighter colors indicate higher values. It can be seen that all the four features show a good accordance with the functional division of the study area (Figure 3.4).

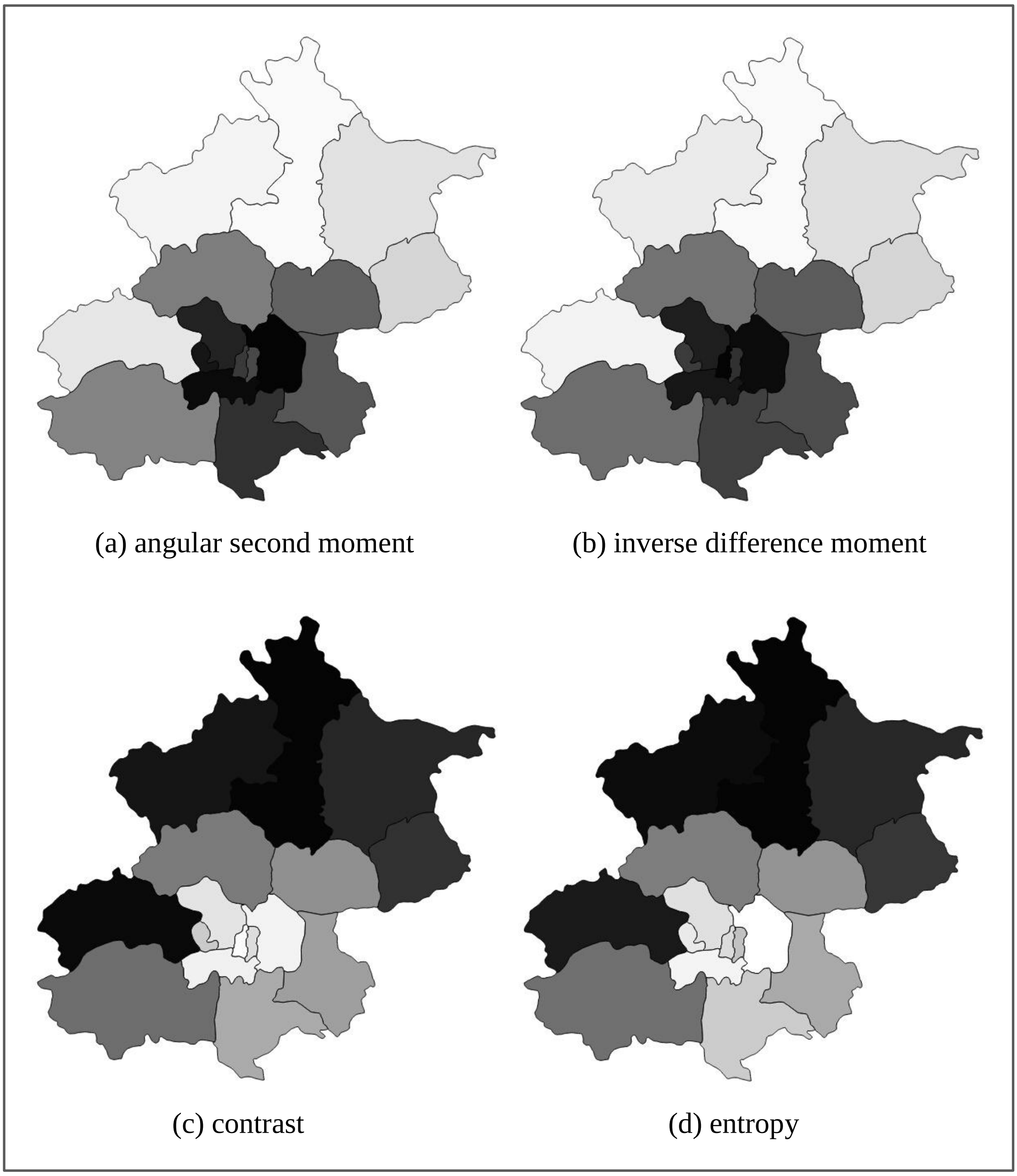


Figure 4.7 Comparison of Textural Features between Administrative Regions

### 4.3.2 Clustering Results and Analysis

A clustering analysis is then made to test if the difference between the sixteen regions in the feature space can be identified in an automated manner. The sixteen regions are clustered into two, three and four classes. The clustering process is performed twice for each. The first time only the eight features are used as input, referred to as non-spatial clustering, while the second time the spatial locations of the regions are also considered, referred to as spatial clustering. All the classes identified are of no thematic meaning. The purpose is to observe their spatial patterns and the patterns characterized by the eight features. The results are presented as follows.

Figure 4.8 shows the results of clustering of the sixteen regions into two classes. Figure 4.8(a) shows the clustering result by the eight features. The result shows that one class, indicated in yellow, includes the whole center area and half of the inner periphery area, while the other class, indicated in orange, includes the whole outer periphery and half of the inner periphery, as compared to the Figure 3.6. Taking the spatial locations into consideration, as shown in Figure 4.8(b), the result accords well with the functional division (Figure 3.4). The yellow class includes exactly the capital function core area and the urban function expansion area. The orange class includes exactly the urban development new area and the ecological conservation area.

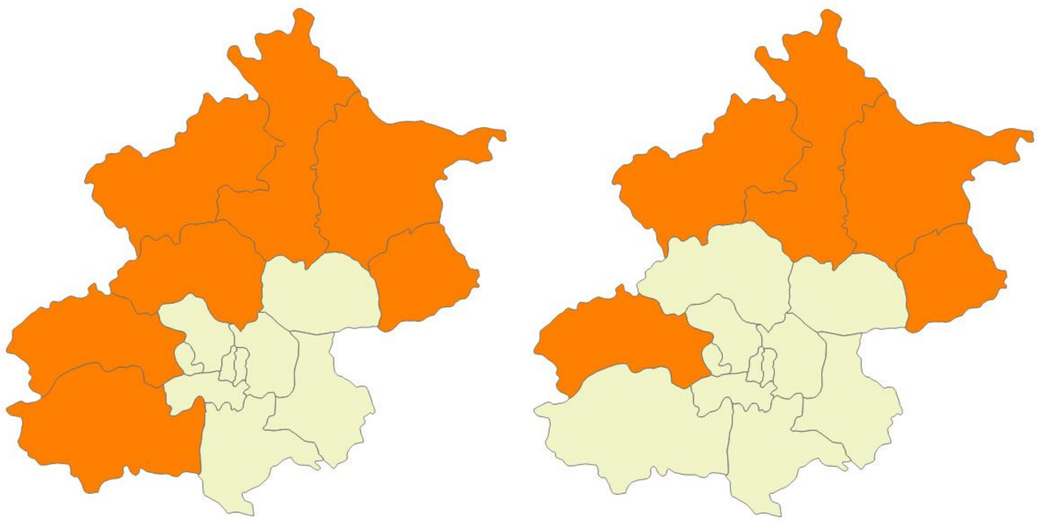

(a) non-spatial (b) spatial

Figure 4.8 Clustering of Administrative Regions into Two Groups

According to Tables 4.2 and 4.3, the same difference between the two classes in the feature space is found in both non-spatial and spatial clustering results. The yellow regions have the proportions of vegetation and values of contrast and entropy that are higher than those of the orange regions. Also, the yellow regions have the proportions of impervious surface and values of angular second moment and inverse difference moment that are lower than those of the orange regions.

Figure 4.9 shows the results of clustering of the sixteen regions into three classes. Compared with the Figure 4.9(a) shows that the non-spatial clustering identifies three classes that approximate the functional division of the study area (Figure 3.4). The spatial clustering result fits the functional division better (Figure 4.9(b)). The green regions equal to the ecological conservation area. The orange regions are identical to the urban development new area. The yellow regions include exactly the capital function core area and the urban function expansion area in the functional division

(Figure 3.4), which are equivalent to the inner and outer center areas in the urban scholar's division (Figure 3.6). According to Table 4.2, the yellow regions have the highest proportions of impervious and lowest proportions of vegetation. On the contrary, the green regions have the lowest proportion of impervious and the highest proportions of vegetation.

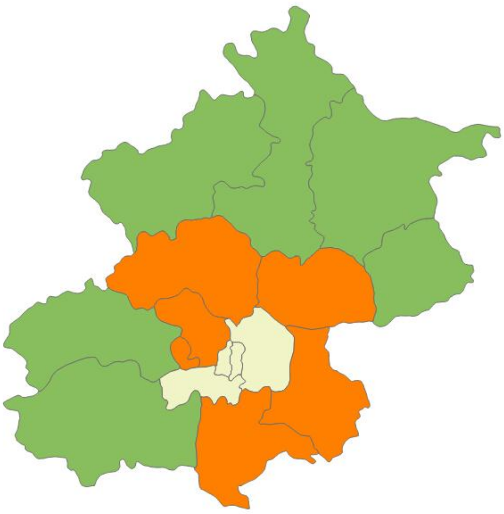

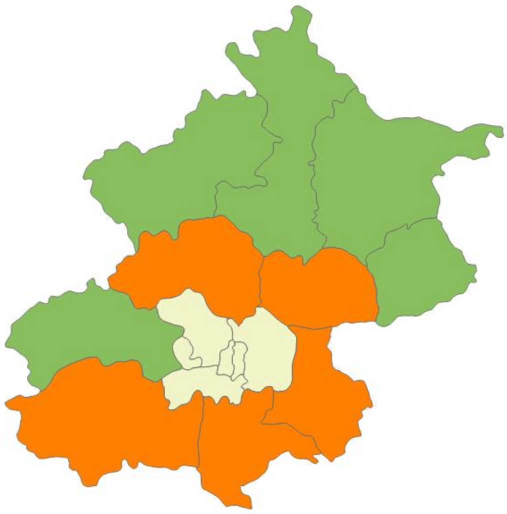

(a) non-spatial (b) spatial

Figure 4.9 Clustering of Administrative Regions into Three Groups

Figure 4.10 shows the results of clustering of the sixteen regions into four classes. Figure 4.10(a) shows that the non-spatial clustering identifies almost the same classification as the functional division (Figure 3.4). The yellow regions equal to the capital function core area. The orange regions are identical to the urban function expansion area. The blue regions include five of the six regions of the urban development new area. The green regions include the whole ecological conservation area and one region of the urban development new area. The spatial clustering also identifies a very similar pattern corresponding the functional division (Figure 4.10(b)). The green regions include exactly the regions of ecological conservation area. The blue regions are exactly the urban development new area. The yellow regions include the whole capital function core area. Two regions of the urban function expansion area are included in the yellow class by the spatial clustering, because they are closer in their locations.

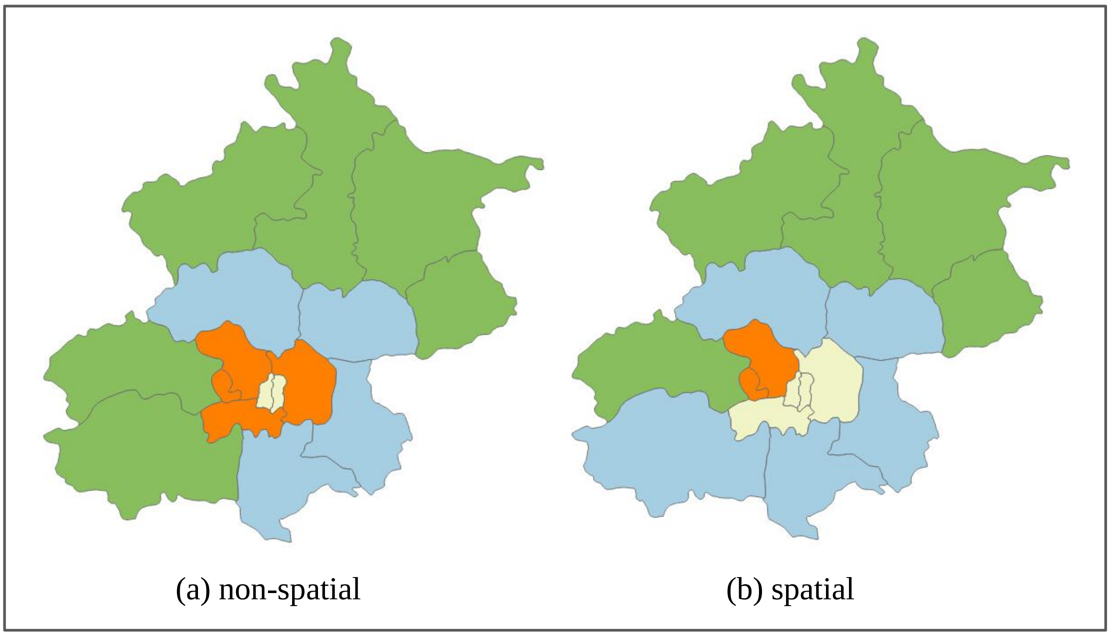


Figure 4.10 Clustering of Administrative Regions into Four Groups

According to Table 4.2 , the yellow regions have the highest proportions of impervious and lowest proportions of vegetation. On the contrary, the green regions have the lowest proportion of impervious and the highest proportions of vegetation. Also, the yellow regions have lower values of angular second moment and inverse difference moment and higher values of constrast and entropy than green regions (Table 4.3).

As discussed in Section 3.3, the common urban areas of the three referenced divisions include the regions 1 – 6 in Figure 3.2. The common rural areas include the regions 15 and 16 in Figure 3.2. By comparing the clustering results the common urban and rural areas in the referenced divisions, it can be seen that urban and rural areas are successfully differentiated by all the clustering processes.

Two conclusions are drawn from the analysis. Firstly, the combination of the eight features is valid for characterizing different kinds of areas, they are, the four proportions of vegetation, impervious surface, soil and water / shade, and the four textural features including angular second moment, inverse difference moment, contrast and entropy. Urban and rural areas present a distinction in these features. The combination of these features is effective for distinguishing between urban and rural areas. Secondly, urban areas present higher proportions of impervious surface and lower proportions of vegetation than rural areas. These two proportional features are useful for assigning thematic meanings to the classes of the regions.

# 5 Division of a City Region for Urban-Rural Classification

From the current urban definitions for census purpose, the whole process of urban recognition can be summarized as two steps, i.e. division and classification. The division is on the administrative basis. Administrative boundaries are imposed to divide a territory into administrative regions. All the administrative regions are then classified into urban and rural areas according to the census criteria. Likewise, other classification schemes can be applied. For administrative purpose, the regions are classified into municipal district and country. For planning purpose, the regions are classified into capital function core area, urban function expansion area, urban development new area and ecological conservation area. For analytical purpose, the regions are classified into inner center, outer center, inner periphery and outer periphery. All these classifications are made on the regions that are divided by administrative boundaries. Before an urban-rural classification can be made, a territory must be divided into smaller regions, as the spatial unit for assigning a thematic meaning, e.g. urban and rural. One kind of division is the administrative division. However, administrative boundaries do not accord with the boundaries of physical landscape, and they are fixed and do not change according to the urbanization process. Therefore, a zoning method is needed to divide a territory into smaller regions. These regions should be divided by boundaries that reflect the boundaries of landscape. This study addresses the zoning issue.

## 5.1 Division of a City Region: Administrative vs Homogeneous

A city region per se is an administrative region. Municipal districts and countries are sub-regions at a lower administrative level than the city region. There are two problems of classification of urban and rural areas based on an administrative division. Firstly, administrative boundaries do not accord with the boundaries of physical landscape. Secondly, administrative boundaries do not change according to the change of physical landscape. Cities are sprawling into their surrounding landscapes. The process of urbanization keeps transforming the natural and agricultural environments into built environments. As a result, urban boundaries keep moving outwards. Hence, the fixed administrative division is not appropriate for dividing urban and rural areas. Instead, a zoning method is needed for divide a city region into sub-regions that accord with the physical landscape. This can be achieved using remote sensing data and techniques.

According to the fourth urban characteristic, an urban area is clearly distinguishable from its surrounding rural area, which means that the difference of the landscape between urban and rural areas, implied by the other three urban characteristics, is observable. Hence, the zoning process is expected to divide a territory into regions that are different in the landscape. The multi-resolution image segmentation technique, which is reviewed in Section 3.2.2, fits the requirement of the zoning task. This algorithm is an optimization procedure that minimizes the average heterogeneity and maximizes the respective homogeneity of resulting segments. As reviewed in Section 2.2.4, the stop criterion for the optimization procedure is an input scale parameter.

Prior to the merge of two segments, the resulting increase of a defined heterogeneity is calculated. If the resulting increase exceeds threshold determined by the scale parameter, then the merge is not performed and the segmentation process stops. The scale parameter is an abstract term that determines the maximum allowed heterogeneity for the resulting image segments. By changing its value, the sizes of resulting segments can be varied. However, it is more useful to control the segmentation process by a parameter with physical meaning, e.g. the average area of the resulting segments. The administrative division can be used as a reference. The segmentation is performed to produce such sub-regions that their average area is the closest to area of the smallest administrative region. The resulting regions are referred to as homogeneous regions. An experiment is designed to test if this method can better separate different landscapes than the administrative division.

## 5.2 Experimental Design for Comparing Administrative and Homogeneous Divisions

The experiment is designed to see how remote sensing data and techniques can be used to achieve a division of a city region, and how it differs from the administrative division.

### 5.2.1 Data Sources

The source data is the same as the ones used in the experiments described in Chapter 4. Two sets of Landsat-5 Thematic Mapper (TM) images of the study area are used in this study, which contain seven multi-spectral bands. The sensed energy intensity is recorded in 8-bit data, that is, there are 256 grey levels in each band of the image. Another data set used in this study is the set of administrative boundaries of the study area, which is stored in a vector data format. A geo-referenced mosaicking is performed to combine the two sets of images. By overlaying the vector data set on the image data set, the specific area of the image data corresponding to the study area is masked for later processing and analysis.

### 5.2.2 A Continuous Region Splitting Analysis

The multi-resolution segmentation is a bottom-up region merging technique. It starts with individual pixels, which form the smallest segments. In subsequent steps, pairs of image segments are merged into larger regions by minimizing the defined weighted heterogeneity of resulting regions. The process stops when the smallest growth exceeds the threshold specified by a scale parameter. By increasing the scale parameter, more times of merge are allowed to produce larger segments. The largest possible segment is the whole input image region. However, in order to observe how a region is continuously divided into sub-regions, a top-down region split process is used to create a series of segmentation results. Each step can be viewed as a further split than the previous step.

The TM data of the study area are input to the segmentation process. The vector data of the administrative boundaries of the study area are also input as a constraint. By imposing the administrative boundary constraint, the input image is firstly split according to the administrative boundaries, so at least sixteen regions must be output from the segmentation process. By decreasing the scale parameter, changes of output segments are found. Each time of change can be viewed as a further split of the previous segmentation result, and is referred to as a splitting step. The splitting process stops when the average size of the resulting regions becomes lower than the smallest administrative region.

The purpose of the segmentation process is to identify homogenous regions. If a region includes homogenous landscape, its grey-level variation in the image channels is relatively small. The grey-level variation of a region in a spectral band is measured by the range of the grey-level of the region. The grey-level range is calculated as the difference between the maximum and the minimum grey-level values. If a region is split into several homogenous sub-regions, the average grey-level range of the sub-regions should be lower than their super-region. Otherwise, the region is split into sub-regions that are not more homogeneous than it. The average grey-level ranges of all regions in the seven multi-spectral bands all calculated for each step, in order to see if a decrease of the average ranges occurs along the continuous splitting.

### 5.2.3 Homogeneous Division without Administrative Boundary Constraint

The administrative boundaries are imposed as a constraint for the observation of the splitting process. The purpose of a zoning method is to divide a territory into regions according to the physical landscape rather than the administrative consideration. Therefore, the segmentation is performed with the same input but removing the administrative boundary constraint. The expected result is that the segmentation produces more homogeneous regions than those produced with the administrative boundary constraint.

## 5.3 Results and Analysis

This section presents the experiment results.

### 5.3.1 Splitting Results and Analysis

The results of the continuous splitting process are shown in Figure 5.1. At the beginning, the input image is split into sixteen regions according to the administrative boundaries. No new segment is produced, as large growth of heterogeneity is allowed. This administrative division of the input image is regarded as the source status of the subsequent splitting steps (Figure 5.1(a)). The regions produced in the subsequent steps are sub-regions of the sixteen administrative regions. The areas of the sixteen administrative regions range from 42 $km^2$ to 2557.3 $km^2$. By reducing the scale parameter, smaller sub-regions are produced. Each change of the segmentation result is recorded as a step. The number of regions increases along the splitting steps (Figure 5.1(b-j)). The splitting process stops when the average size of the resulting regions becomes lower than the smallest administrative region. At the ninth change of the segmentation result, a total of 373 regions are produced, with an average area of 39.7 $km^2$ (Figure 5.1(j)). The numbers of the sub-regions of the sixteen administrative regions produced in the splitting steps are listed in Table 5.1. The reference numbers of the sixteen administrative are the same as those in Table 3.2. It can be seen that the earliest splits occur in regions 6, 13, 15 and 16, which means that these regions contain different landscapes that are the most distinguishable. Regions 1 and 2 keep unchanged until the steps 7 and 8 respectively, which means they contain a homogeneous landscape.

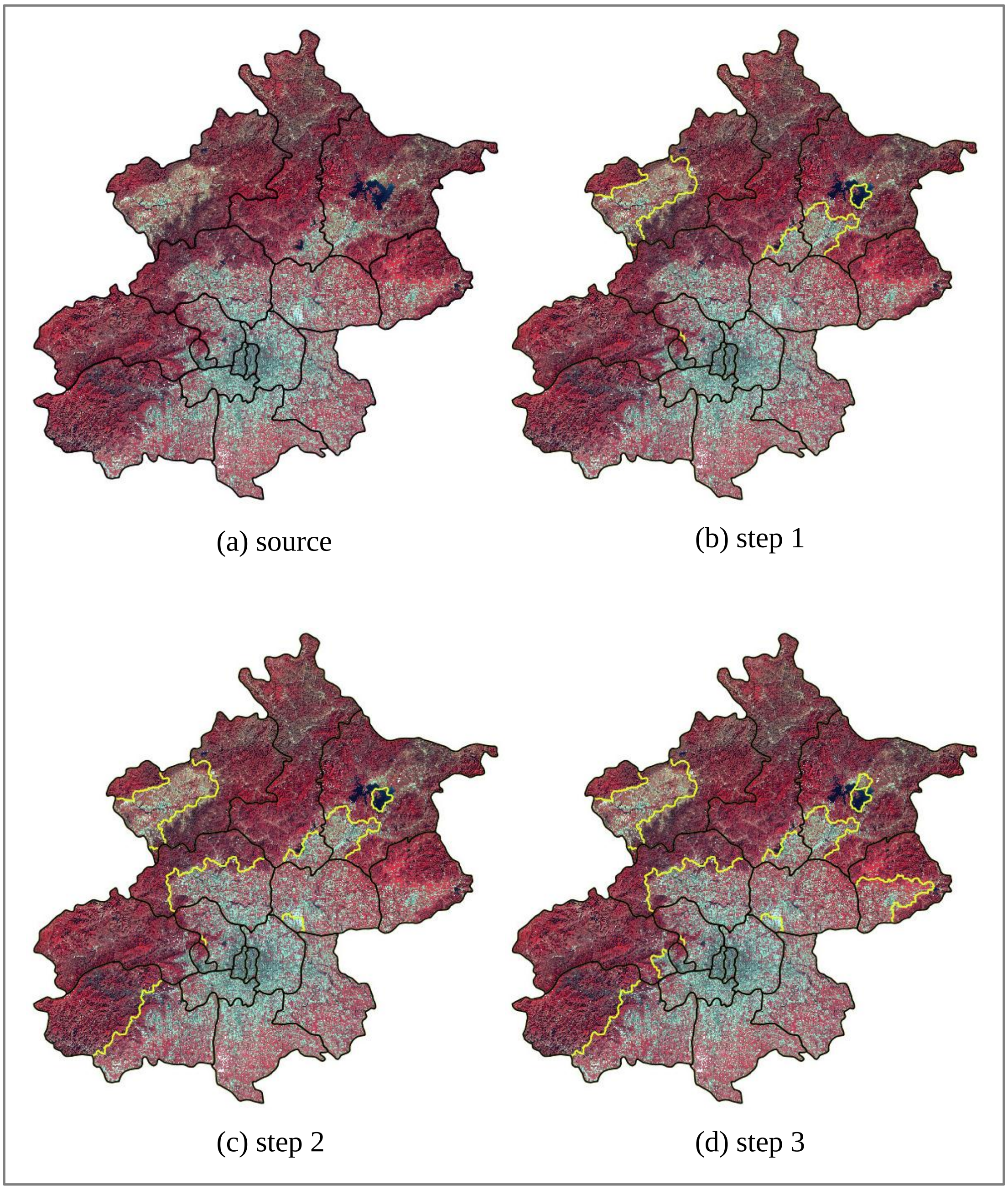


Figure 5.1 Splitting Process using Multi-Resolution Image Segmentation

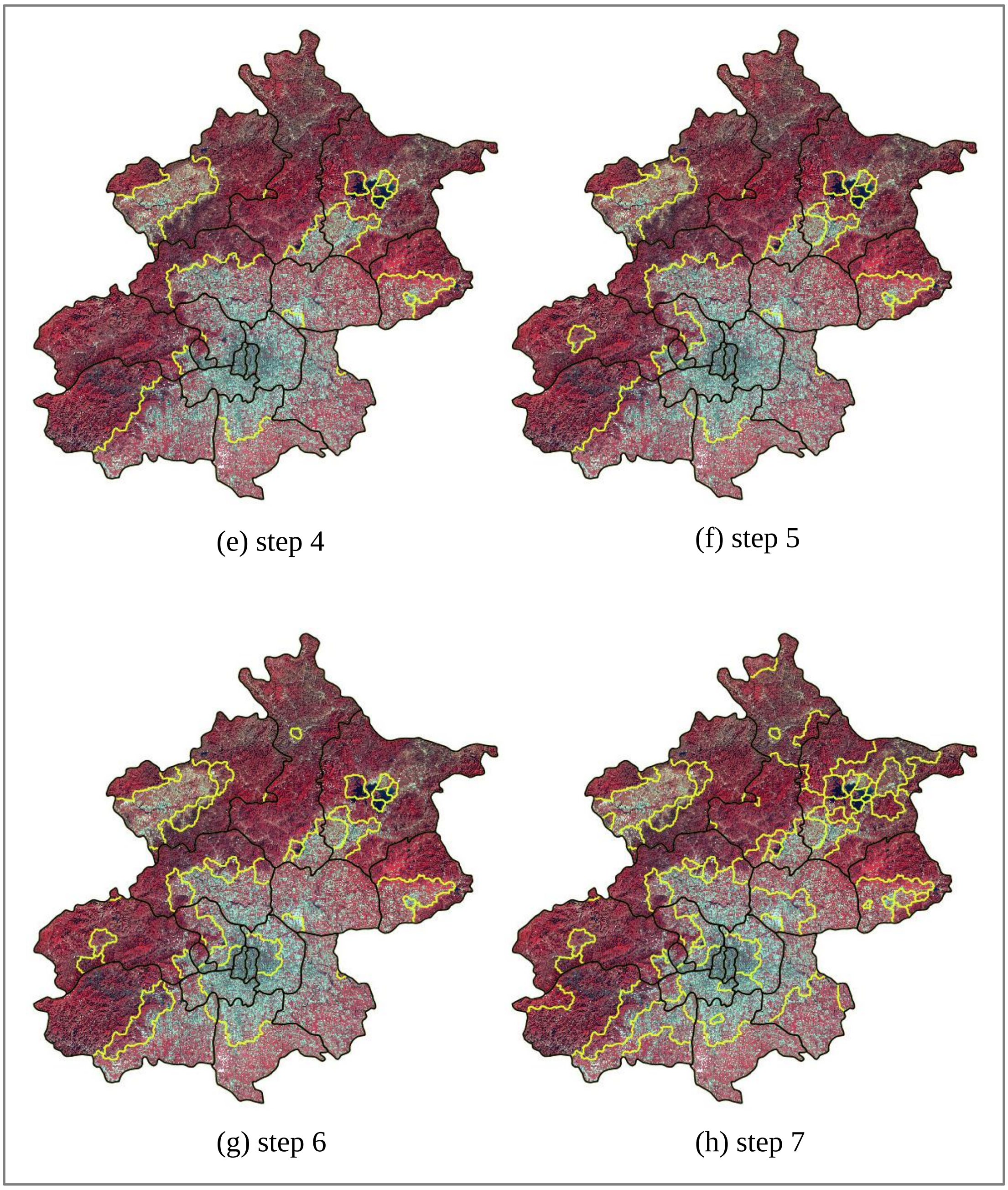


Figure 5.1 Splitting Process using Multi-Resolution Image Segmentation (cont'd)

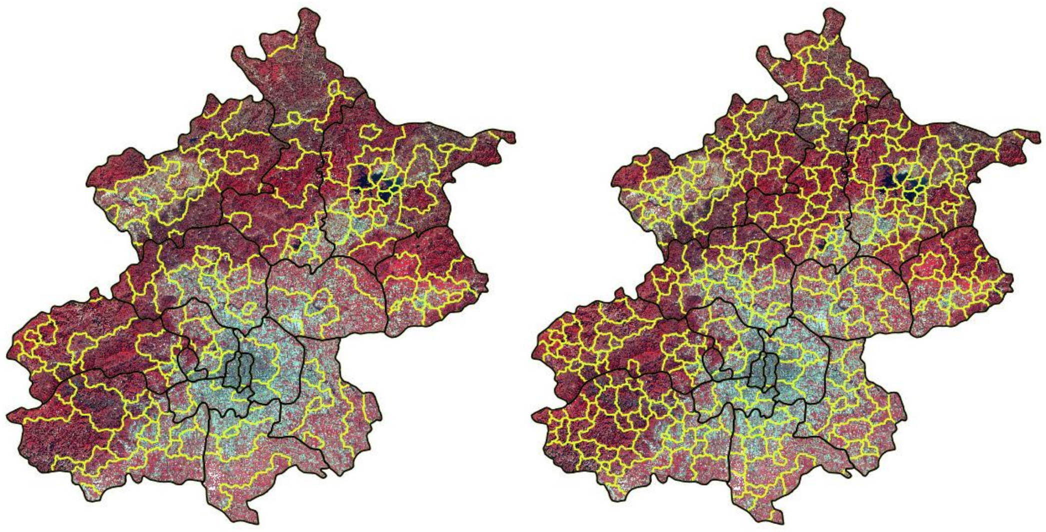

(i) step 8 (j) step 9

Figure 5.1 Splitting Process using Multi-Resolution Image Segmentation (cont'd)

Table 5.1 Number of Resulting Sub-Regions in Administrative Regions

| | **number of resulting sub-regions** | | | | | | | | |
|---|---|---|---|---|---|---|---|---|---|
| **ref. no.** | **step 1** | **step 2** | **step 3** | **step 4** | **step 5** | **step 6** | **step 7** | **step 8** | **step 9** |
| **1** | 1 | 1 | 1 | 1 | 1 | 1 | 1 | 2 | 2 |
| **2** | 1 | 1 | 1 | 1 | 1 | 1 | 1 | 1 | 2 |
| **3** | 1 | 1 | 1 | 1 | 1 | 3 | 4 | 4 | 8 |
| **4** | 1 | 1 | 1 | 1 | 1 | 2 | 4 | 5 | 9 |
| **5** | 1 | 1 | 1 | 1 | 2 | 2 | 2 | 2 | 2 |
| **6** | 2 | 2 | 2 | 2 | 3 | 4 | 6 | 10 | 11 |
| **7** | 1 | 1 | 2 | 2 | 3 | 5 | 6 | 19 | 34 |
| **8** | 1 | 2 | 2 | 2 | 3 | 4 | 6 | 20 | 45 |
| **9** | 1 | 1 | 1 | 2 | 2 | 2 | 4 | 8 | 20 |
| **10** | 1 | 2 | 2 | 2 | 2 | 2 | 3 | 5 | 17 |
| **11** | 1 | 2 | 2 | 2 | 2 | 5 | 7 | 15 | 33 |
| **12** | 1 | 1 | 1 | 2 | 2 | 2 | 3 | 7 | 20 |
| **13** | 2 | 2 | 2 | 2 | 3 | 6 | 12 | 20 | 48 |
| **14** | 1 | 1 | 2 | 3 | 3 | 3 | 7 | 13 | 21 |
| **15** | 3 | 3 | 4 | 7 | 8 | 8 | 19 | 31 | 57 |
| **16** | 4 | 4 | 4 | 5 | 6 | 8 | 10 | 20 | 44 |
| **Σ** | 23 | 26 | 29 | 36 | 43 | 58 | 95 | 182 | 373 |
| **mean area ($km^2$)** | 643.2 | 569 | 510.1 | 410.9 | 344 | 255.1 | 155.7 | 81.3 | 39.7 |

The average grey-level ranges of the seven spectral bands are calculated for the segmentation results, which are listed in Table 5.2. The changes of the average grey-level ranges are visualized in Figure 5.2. It can be seen that all the seven spectral bands show a decrease in the average grey-level range. In each step, the segmentation algorithm produces sub-regions that are more homogeneous than their super-regions.

Table 5.2 Change of Average Grey-Level Ranges in Spectral Bands

| | **average grey-level range** | | | | | | |
|---|---|---|---|---|---|---|---|
| **step** | **band 1** | **band 2** | **band 3** | **band 4** | **band 5** | **band 6** | **band 7** |
| **source** | 174.38 | 128.06 | 163.38 | 162.81 | 239.00 | 54.19 | 239.06 |
| **1** | 149.39 | 106.57 | 138.43 | 142.52 | 214.70 | 47.48 | 203.43 |
| **2** | 147.23 | 103.50 | 135.31 | 138.73 | 212.23 | 46.65 | 202.65 |
| **3** | 146.72 | 101.07 | 132.55 | 136.72 | 212.03 | 44.69 | 201.66 |
| **4** | 132.78 | 90.89 | 120.28 | 129.39 | 198.17 | 40.36 | 185.03 |
| **5** | 130.63 | 89.51 | 117.77 | 128.09 | 195.02 | 38.88 | 179.98 |
| **6** | 122.48 | 83.26 | 110.59 | 119.22 | 188.53 | 37.02 | 165.00 |
| **7** | 109.25 | 72.80 | 98.20 | 109.03 | 181.03 | 33.68 | 159.38 |
| **8** | 102.04 | 66.67 | 90.80 | 101.93 | 172.18 | 31.65 | 146.53 |
| **9** | 89.39 | 57.95 | 80.46 | 92.88 | 158.50 | 29.83 | 128.97 |

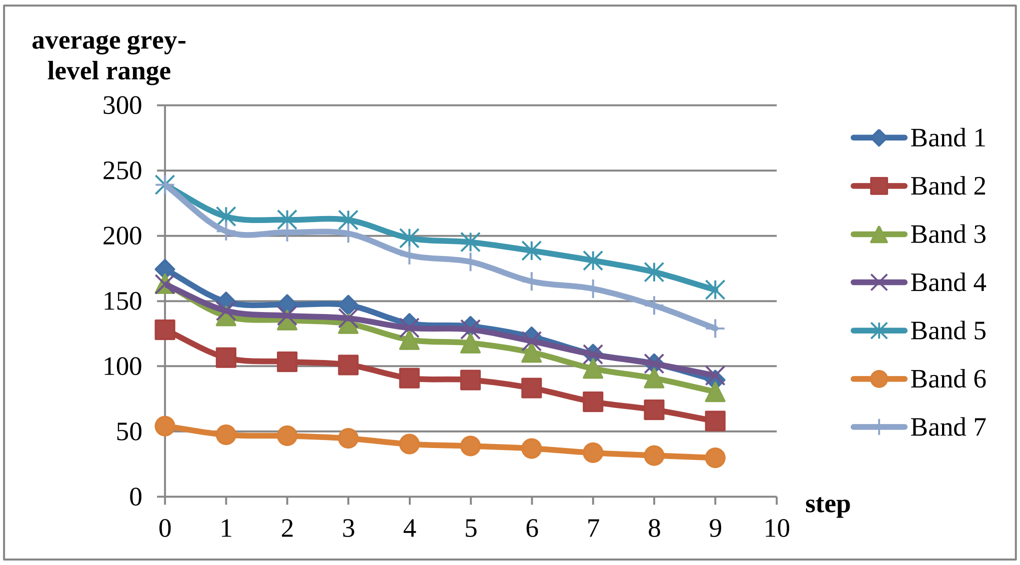


Figure 5.2 Change of Average Grey-Level Ranges in Spectral Bands

### 5.3.2 Homogeneous Division of a City Region for Urban-Rural Classification

The same input as in the ninth step is used to split the image of the study area into sub-regions, but the input of the administrative boundaries is removed. The segmentation is made according only the grey-level variation of the image. As a result, the output is different from that produced with the administrative boundary constraint (Figure 5.3). To compare this result with the one produced with the administrative boundary constraint and the administrative division, the average grey-level ranges of the seven bands of these three kinds of division are listed in Table 5.3.

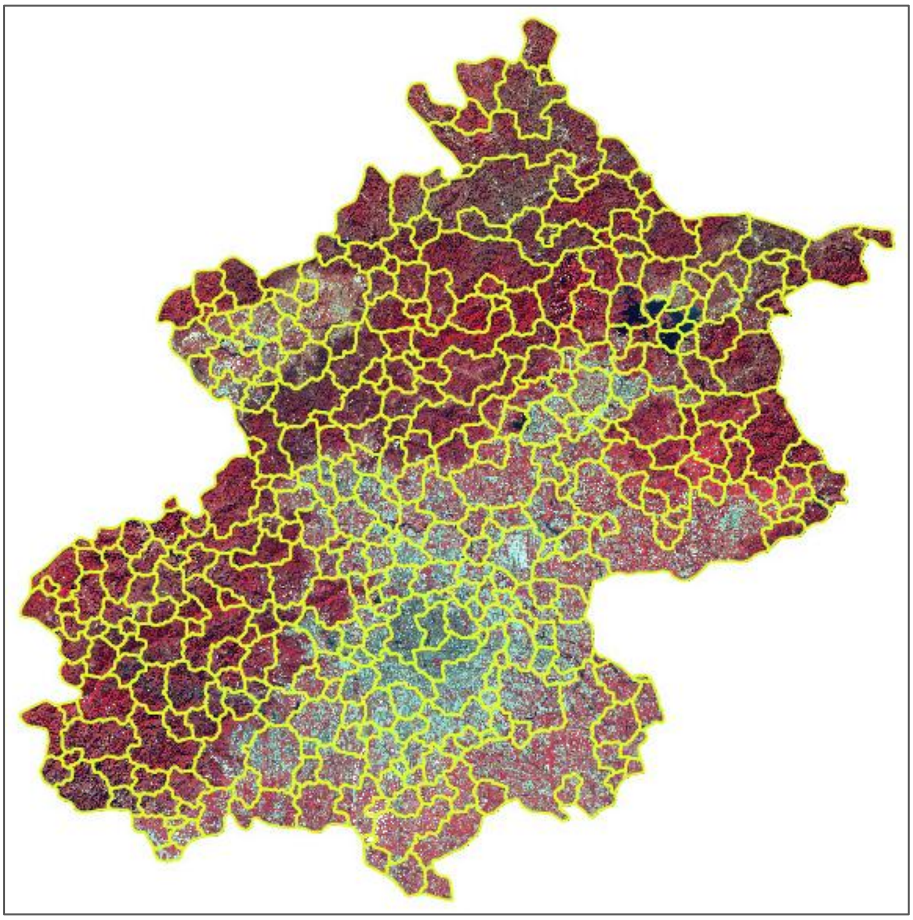

Figure 5.3 Homogeneous Division without Administrative Boundary Constraint

Table 5.3 Comparison of Average Grey-Level Ranges

| | **average grey-level range** | | | | | | |
|---|---|---|---|---|---|---|---|
| | **band 1** | **band 2** | **band 3** | **band 4** | **band 5** | **band 6** | **band 7** |
| **administrative** | 174.38 | 128.06 | 163.38 | 162.81 | 239.00 | 54.19 | 239.06 |
| **constrained** | 89.39 | 57.95 | 80.46 | 92.88 | 158.50 | 29.83 | 128.97 |
| **unconstrained** | 88.64 | 57.80 | 80.23 | 93.03 | 158.47 | 29.59 | 128.22 |

Except the band 4, the average grey-level ranges in the other six bands are further reduced by removing the administrative boundary constraint. It is concluded that the multi-resolution segmentation algorithm is able to divide a territory into regions that are different in the landscape. Therefore, it is appropriate to be used as the zoning method for the proposed approach to urban area recognition.

# Chapter 6 An Iterative Clustering and Merging Algorithm for Urban Area Recognition

Chapter 4 evaluates the eight features for characterizing different kinds of areas. Chapter 5 describes the multi-resolution segmentation as the zoning method for dividing a territory according to the physical landscape. These two chapters address the issue about what kinds of data are used. This addresses the issue about what kinds of processes are needed for urban area recognition.

## 6.1 From Urban Characteristics to an Iterative Clustering and Merging Algorithm

The purpose of the algorithm is to separate a city region into two sub-regions. One corresponds to the urban area, and the other corresponds to the rural area. Chapter 3 proposes a four-step approach to the recognition of urban areas. The first step is addressed in Chapter 5. The algorithm described in this Chapter is developed for achieving the remaining three steps, i.e. clustering, identification and merging. Clustering and identification are achieved by an iterative clustering analysis. Merging is achieved by an iterative merging analysis. These two sub-processes are described in the following sub-sections respectively.

### 6.1.1 Iterative Clustering for Identifying an Urban Area

According the first three urban characteristics, urban and rural areas are different in land cover composition and configuration. A set of compositional and configurational features is identified for characterizing places, which is described in Chapter 4. According to the fourth urban characteristic, the difference between urban and rural areas is observable. Consequently, a clustering process should be able to distinguish between different kinds of areas using those features. The resulting groups of an automated clustering process are of no thematic meanings. Hence, an identification step is needed to find a group of the urban meaning from the clustering result. This group should satisfy some conditions that reflect the urban characteristics. Firstly, an urban area is a single connected area, rather than a union of several scattered regions. Even if there are some satellite suburbs in many cities, there must be a main urban area of the cities. Secondly, according to the first two urban characteristics, urban areas are composed of large and dense built-up areas, providing space for non-agricultural human activities, while rural areas are mainly composed of agricultural or natural lands, i.e. vegetated areas. Reflected by the compositional features, an urban area should be high in the proportion of impervious surface and low in the proportion of vegetation, compared with other non-urban areas.

Accordingly, the clustering and identification process adopts an iterative strategy. The input number of cluster is adjusted and the clustering is repeated until the expected area appears. At the beginning, the input regions are clustered into two groups. One group must be higher in the proportion of impervious surface and lower in the proportion of vegetation than the other one. It should contain the expected urban area. However, it also includes some regions that are not very urban, as the group size is large. Also, the condition of connectedness is usually not satisfied. The spatial locations of the regions can be used as additional input, so that the regions in each cluster are also close in spatial distance, but this does not guarantee that the regions within clusters are adjacent. If the expected area is not identified in a clustering result, the number of clusters is increased by one and input regions are re-clustered. Different kinds of landscapes are further separated. The similarity within each group is increased. A series of results are produced. Without a stop condition, the maximum number of clusters equals to the number of input regions. This is the most separated case that each input region forms a cluster. The expected area should appear at a certain step in the result series before the end is reached. The expected area should also be stable, keeping unchanged for some steps after it appears. If it is not stable, it still includes not similar elements. The steps after the expected area is identified are not useful, as the regions are over separated. Hence, a stop condition should be imposed. The overall steps of the iterative clustering process are described as follows.

1) Begin the process by clustering the input regions into two groups;

2) Check if the stop condition is satisfied. If satisfied go to step 4, otherwise go to step 3;

3) Increase the number of clusters by one, and re-cluster the input regions, and go to step 2;

4) Remove the holes of the output area if there is any.

The stop condition of the process is that such an area is found that satisfies the following:

1) It is a single connected area;

2) It is of the highest proportion of impervious surface among the areas satisfying (1);

3) It is of the lowest proportion of vegetation among the areas satisfying (1).

4) It is unchanged in more than three following steps.

5) If an area that satisfies (2) – (4) but not satisfies (1), the largest connected component of the area is selected as the expected output.

After the clustering and identification process, a set of regions are identified to form an area that can be determinately labelled as urban, but the remaining regions are still unclassified.

### 6.1.2 Iterative Merging for an Urban-Rural Division

The final step of the proposed approach to urban area recognition is merging. It merges all the regions into two areas, one of which is urban, and another is rural. The urban and rural areas form an urban-rural division of the city extent. The output of the previous step is a connected area comprising a cluster of regions that are determined as urban. In the real world, there is no physical boundary between urban and rural areas. There is a transition of landscape between urban and rural areas. Accordingly, the remaining regions that are not determined as urban are also not definitely rural. Some regions close to the urban area are more possible to be classified as urban as well. According to the first three urban characteristics, the urban and rural areas are different in the features related to those characteristics. According to the fourth urban characteristic, such a difference should be observable. Hence, the dissimilarity of the resulting urban and rural areas should be maximized. In other to find such an urban-rural division, an iterative merging strategy is adopted. The merging process is described as follows.

1) At the beginning, the output urban regions from the clustering and identification process are merged as an urban area. The features of the merged area are calculated as

the means of the features of its region components. In other words, in the feature space, the merged area is represented by the mean center of its components.

2) From the remaining regions, the one that is adjacent to the merged area and is the closest to the merged area in the feature space, i.e. the nearest neighbor, is merged into the urban area. As a result, the resulting area is expanded, and its mean center is changed.

3) The step 2 is repeated until all the regions are merged as one area. If there are $n$ regions produced by the segmentation process, and a cluster of $m$ regions is output by the clustering and identification process, then there are $n – m+1$ merging steps.

4) In each merging step, the remaining regions are also merged in to an area, representing a rural area. As a result, two areas are formed. The distance between the mean centers of these two areas in the feature space is calculated. The distance changes along the merging steps. The urban area in the step of the largest distance is identified as the final output, because in that step the urban and rural areas are in the most dissimilar status. In other to see if the proposed iterative clustering and merging algorithm works as expected, experiments are designed to test the algorithm.

## 6.2 Experimental Design for Testing the Algorithm

This section describes the data and processes for testing the proposed iterative clustering and merging algorithm.

### 6.2.1 Data Input

The input of the iterative clustering process is the output regions from the segmentation process described in Chapter 5. The regions are represented by the eight proportional and textural features described in Chapter 4. Totally 379 regions are produced by the segmentation process. The eight features are calculated for all regions. The regions are visualized as thematic maps using the eight features respectively. Figure 6.1 shows the four proportional features of the regions respectively, and Figure 6.2 shows the four textural features of the regions respectively. In both figures, brighter tones indicate higher values of the corresponding features.

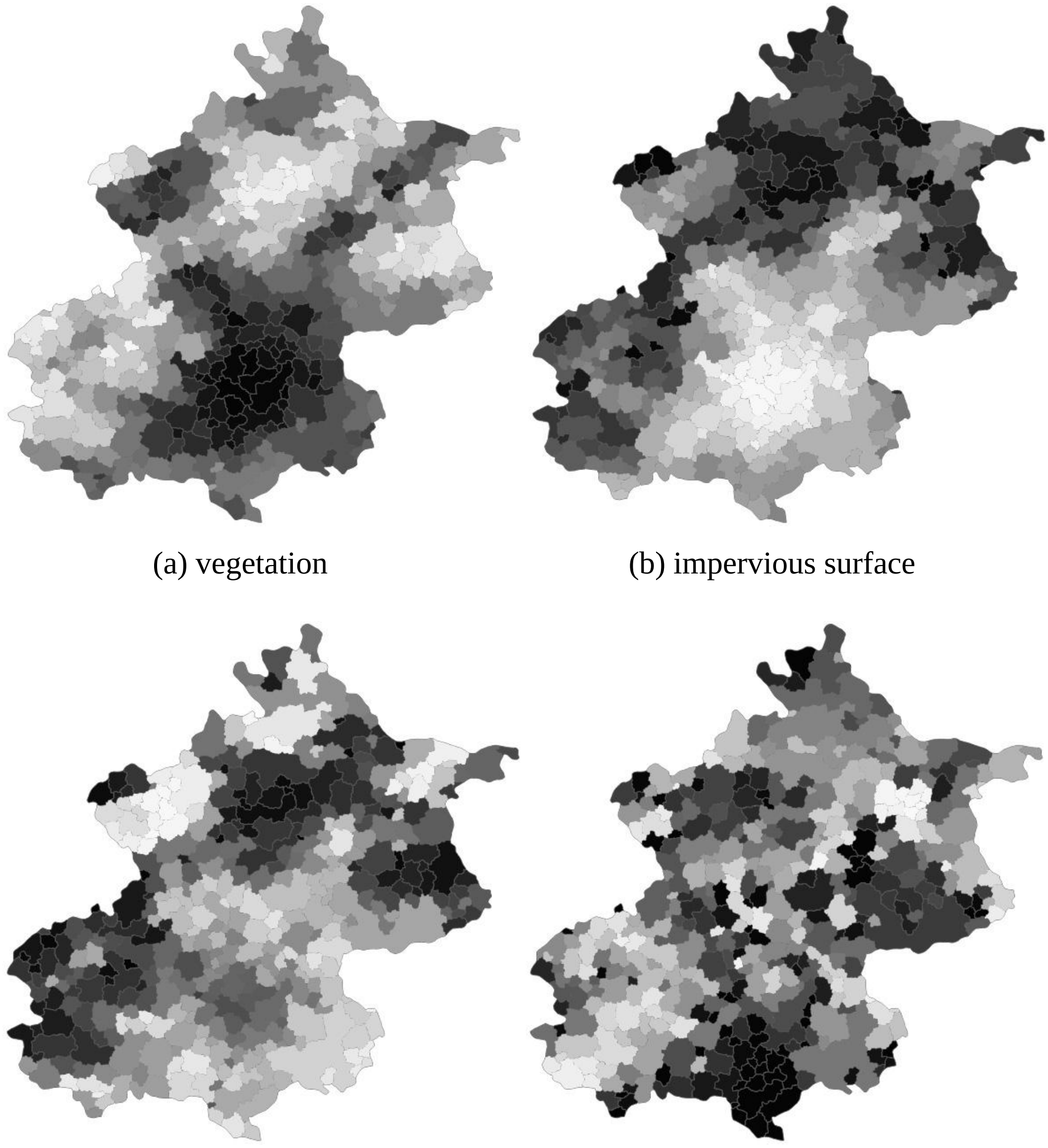

(a) vegetation (b) impervious surface

(c) soil (d) water

Figure 6.1 Visualization of Input Regions with Proportional Features

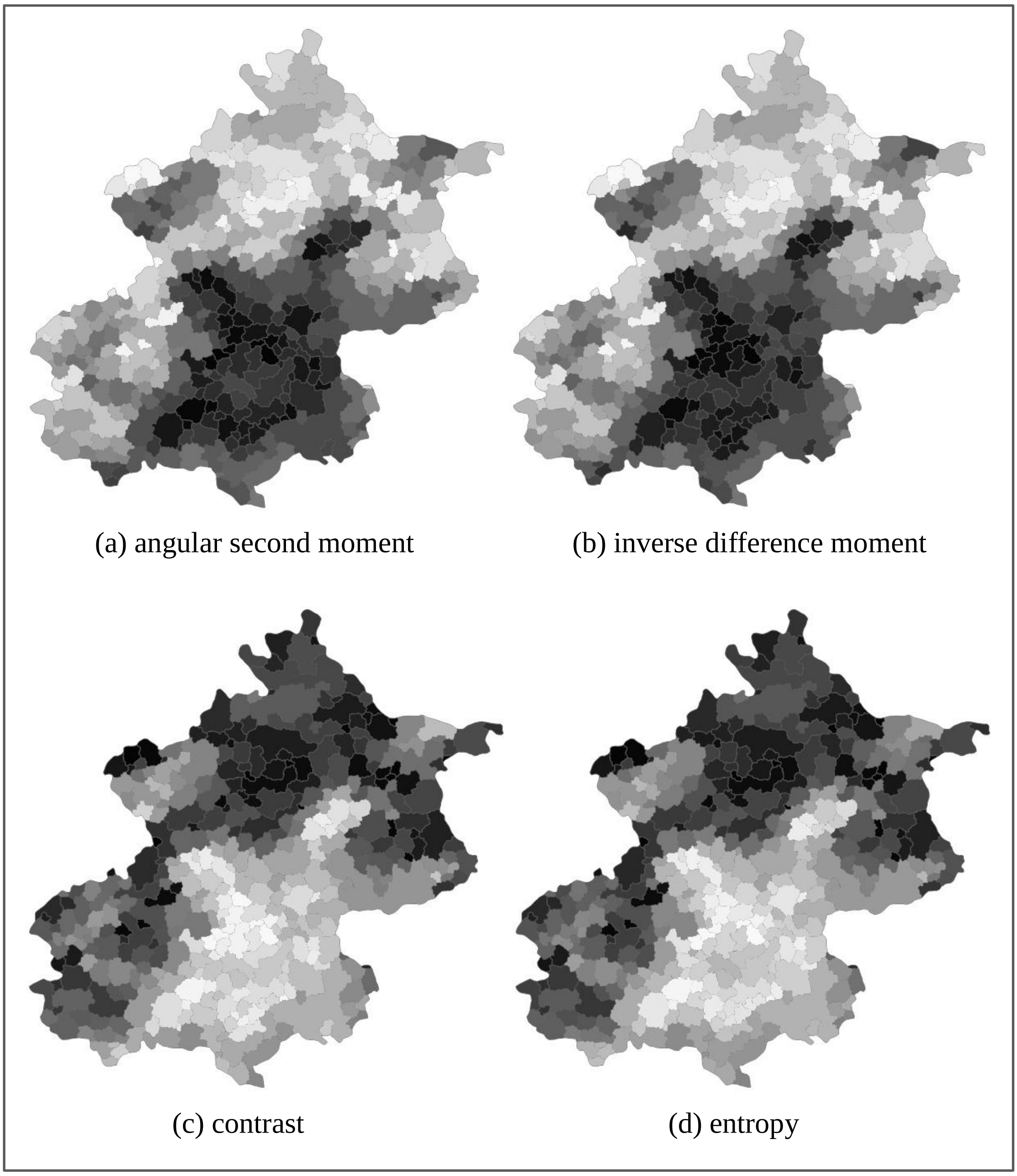

(a) angular second moment (b) inverse difference moment

(c) contrast (d) entropy

Figure 6.2 Visualization of Input Regions with Textural Features

### 6.2.2 A Clustering Analysis

An experiment is designed for observing the change of output clusters along a series of clustering operations, in order to see if the expected urban area can be identified during the clustering. The k-means clustering algorithm is applied. The input number of expected clusters is initiated as 2. The number is increased by one in each following clustering, until it reaches the maximum of the total number of the input regions. There are 379 input regions, so from 2 to 379 there are totally 378 times of clustering to be performed. Each time of clustering is referred to as a step of the iterative clustering process. In each time of clustering, the regions of each output cluster are united as one region. For each united region, the eight features, the mean center of the united region in the feature space, the mean and standard deviation of the distances of the compositional regions to the united region in the feature space, and the number of connected components are computed. In each time of clustering, a new cluster is produced, which means that some existing clusters are further split and become smaller, but some may remain unchanged if their internal similarity is large enough. The expected result is that a cluster satisfying the conditions described in Section 6.1.1 is found during the clustering process.

### 6.2.3 A Merging Analysis

The second experiment is designed to test the iterative merging process. The input of the merging process is the output of the clustering process, including the expected cluster of urban regions, and the remaining unclassified regions. The merging begins with the cluster of urban regions, which are merged into an urban area as a starting point. In the successive merges, the nearest neighbor of the existing urban area is selected from the remaining unclassified regions, and merged into the existing urban area. The remaining unmerged regions are then united as a rural region. Hence, in each merge, all regions are merged into two areas, one of which represents an urban area, and the other one presents a rural area. The eight proportional and textural features, the mean center in the feature space, the mean and standard deviation of the distances of the compositional regions to the merged area in the feature space are computed for both the areas. Also, the distance between the mean centers of the two areas in the feature space is computed. If the output urban cluster of the clustering process contains $n$ regions, there are totally 379-$n$+1 times of merge. Each time of merge is referred to as an iterative merging step. Along the merging steps, the resulting urban area become larger, while the rural area become smaller, until all the regions are merged into one urban area. The change of the distance between the mean centers of the two areas is visualized using a scatter plot graph. It is expected a maximum of the distance between the two mean centers exists during the merging process. The change of the distance is expected to present one of the two possible patterns. If the output urban cluster of the clustering process already includes the whole urban area, the distance between the urban area and the rural area comprising the remaining regions is already the largest. The successive merging process keeps merging the rural regions into the urban area, which reduces their distance as they become similar (Figure 6.3(a)). If the clustering output only contains the very urban part of the urban area, the merging process then finds more regions that are better to be merged into the urban area than to be classified as rural. These merging steps give rise to an increase of the distance between the urban and rural areas. After the whole urban area is produced, the successive merging steps go on merging the remaining regions that are better to be merged into the rural area instead. As a result, the distance decreases after it reaches a peak (Figure 6.3(b)). According to the urban characteristics, urban and rural areas are best differentiated when their dissimilarity is maximized. Therefore, the final result of the urban area is identified at the step where the maximum of urban-rural distance appears.

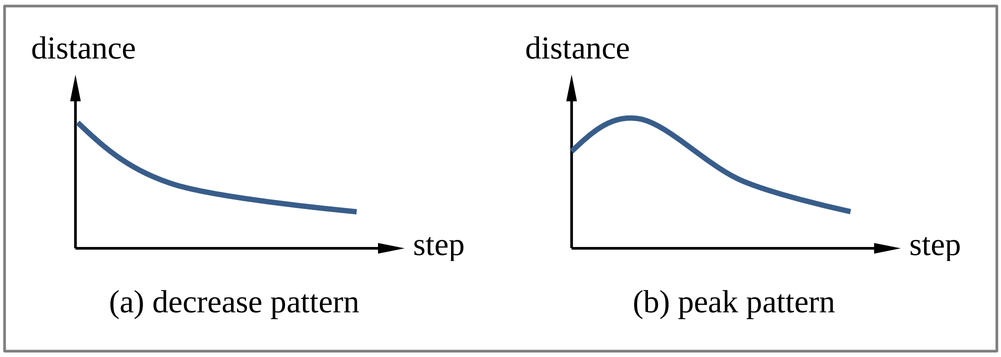


Figure 6.3 Expected Pattern of Distance Change

## 6.3 Results and Analysis

This section presents the results of the experiments described in Section 6.2.

### 6.3.1 Clustering Analysis Results

As described in Section 6.2.2, there are 378 times of clustering until all the regions are totally separated. From all the clustering results, a subset is selected to present here. According to the conditions that the expected urban cluster should satisfied, as described in Section 6.1.1, the cluster with the highest proportion of impervious surface and lowest proportion of vegetation is traced. The results presented here include those key steps at which such a target cluster changes, until the stop conditions are satisfied. The steps where no change of the target cluster is observed and the steps after the stop conditions are satisfied are omitted. As a result, the results of 12 key steps are presented in Table 6.1, in which the reference number is used to be referred to by Figure 3.2, the columns f1 to f8 show the values of the eight proportional and textural features described in Chapter 4. The column of n-connected indicates the number of connected components of a cluster. The columns of mean and standard deviation show the mean and standard deviation of the distances of the regions to the mean center of the cluster in the feature space. The maximum of the reference number is the number of clusters produced in those steps. It is used to number the steps. Step *n* refers to the step at which *n* clusters are generated.

Table 6.1 The Results of the Key Steps of the Iterative Clustering Process

(a) step 2

| ref. no. | f1 | f2 | f3 | f4 | f5 | f6 | f7 | f8 | n connected | mean | standard deviation |
|---|---|---|---|---|---|---|---|---|---|---|---|
| **1** | 0.7176 | 0.0219 | 0.2430 | 0.0175 | 0.9100 | 0.9823 | 0.0354 | 0.2227 | 7 | 0.3248 | 0.1781 |
| **2** | 0.2325 | 0.3090 | 0.4533 | 0.0053 | 0.4791 | 0.9071 | 0.1857 | 0.9948 | 4 | 0.3327 | 0.1406 |

(b) step 3

| ref. no. | f1 | f2 | f3 | f4 | f5 | f6 | f7 | f8 | n connected | mean | standard deviation |
|---|---|---|---|---|---|---|---|---|---|---|---|
| **1** | 0.4025 | 0.1019 | 0.4873 | 0.0082 | 0.6915 | 0.9439 | 0.1121 | 0.6447 | 17 | 0.2900 | 0.1099 |
| **2** | 0.1456 | 0.4185 | 0.4300 | 0.0059 | 0.3952 | 0.8921 | 0.2157 | 1.1273 | 5 | 0.2310 | 0.1004 |
| **3** | 0.7916 | 0.0128 | 0.1769 | 0.0187 | 0.9412 | 0.9881 | 0.0239 | 0.1575 | 4 | 0.2328 | 0.1580 |

(c) step 4

| ref. no. | f1 | f2 | f3 | f4 | f5 | f6 | f7 | f8 | n connected | mean | standard deviation |
|---|---|---|---|---|---|---|---|---|---|---|---|
| **1** | 0.4539 | 0.0686 | 0.4620 | 0.0155 | 0.7684 | 0.9573 | 0.0854 | 0.5081 | 23 | 0.2783 | 0.1257 |
| **2** | 0.0877 | 0.5305 | 0.3773 | 0.0045 | 0.3547 | 0.8837 | 0.2325 | 1.1896 | 3 | 0.1713 | 0.0862 |
| **3** | 0.8148 | 0.0112 | 0.1572 | 0.0168 | 0.9480 | 0.9895 | 0.0211 | 0.1426 | 4 | 0.2058 | 0.1463 |
| **4** | 0.2848 | 0.2002 | 0.5095 | 0.0054 | 0.5139 | 0.9137 | 0.1726 | 0.9425 | 11 | 0.1995 | 0.0816 |

(d) step 6

| ref. no. | f1 | f2 | f3 | f4 | f5 | f6 | f7 | f8 | n connected | mean | standard deviation |
|---|---|---|---|---|---|---|---|---|---|---|---|
| **1** | 0.4114 | 0.0319 | 0.5210 | 0.0357 | 0.8677 | 0.9735 | 0.0531 | 0.3171 | 9 | 0.3263 | 0.1935 |
| **2** | 0.0811 | 0.5496 | 0.3657 | 0.0037 | 0.3520 | 0.8817 | 0.2365 | 1.1949 | 3 | 0.1693 | 0.0867 |
| **3** | 0.8220 | 0.0099 | 0.1560 | 0.0121 | 0.9561 | 0.9915 | 0.0170 | 0.1235 | 7 | 0.1746 | 0.0772 |
| **4** | 0.2699 | 0.2130 | 0.5110 | 0.0061 | 0.5014 | 0.9124 | 0.1752 | 0.9612 | 8 | 0.1969 | 0.0777 |
| **5** | 0.8406 | 0.0162 | 0.1285 | 0.0147 | 0.9217 | 0.9833 | 0.0335 | 0.2011 | 3 | 0.1837 | 0.0892 |
| **6** | 0.4816 | 0.0975 | 0.4128 | 0.0081 | 0.6990 | 0.9471 | 0.1059 | 0.6366 | 21 | 0.2145 | 0.0888 |

(e) step 8

| ref. no. | f1 | f2 | f3 | f4 | f5 | f6 | f7 | f8 | n connected | mean | standard deviation |
|---|---|---|---|---|---|---|---|---|---|---|---|
| **1** | 0.2486 | 0.0875 | 0.6563 | 0.0076 | 0.7025 | 0.9409 | 0.1183 | 0.6298 | 6 | 0.2227 | 0.0926 |
| **2** | 0.0767 | 0.5615 | 0.3581 | 0.0038 | 0.3512 | 0.8810 | 0.2380 | 1.1966 | 3 | 0.1624 | 0.0846 |
| **3** | 0.5229 | 0.0116 | 0.4200 | 0.0455 | 0.9397 | 0.9869 | 0.0262 | 0.1645 | 7 | 0.3176 | 0.1816 |
| **4** | 0.2451 | 0.2397 | 0.5085 | 0.0068 | 0.4698 | 0.9079 | 0.1842 | 1.0106 | 13 | 0.1666 | 0.0712 |
| **5** | 0.8287 | 0.0194 | 0.1368 | 0.0150 | 0.9117 | 0.9817 | 0.0366 | 0.2231 | 3 | 0.1868 | 0.0948 |
| **6** | 0.4527 | 0.1178 | 0.4237 | 0.0057 | 0.6569 | 0.9400 | 0.1199 | 0.7072 | 15 | 0.2173 | 0.0954 |
| **7** | 0.5861 | 0.0475 | 0.3482 | 0.0182 | 0.8297 | 0.9694 | 0.0612 | 0.3972 | 13 | 0.2328 | 0.0893 |
| **8** | 0.8713 | 0.0083 | 0.1135 | 0.0070 | 0.9634 | 0.9930 | 0.0141 | 0.1053 | 10 | 0.1248 | 0.0613 |

(f) step 9

| ref. no. | f1 | f2 | f3 | f4 | f5 | f6 | f7 | f8 | n connected | mean | standard deviation |
|---|---|---|---|---|---|---|---|---|---|---|---|
| **1** | 0.2499 | 0.0887 | 0.6559 | 0.0054 | 0.6990 | 0.9401 | 0.1198 | 0.6362 | 5 | 0.2190 | 0.0939 |
| **2** | 0.0767 | 0.5615 | 0.3581 | 0.0038 | 0.3512 | 0.8810 | 0.2380 | 1.1966 | 3 | 0.1624 | 0.0846 |
| **3** | 0.3292 | 0.0219 | 0.5678 | 0.0811 | 0.9024 | 0.9802 | 0.0397 | 0.2457 | 7 | 0.3815 | 0.1671 |
| **4** | 0.2451 | 0.2397 | 0.5085 | 0.0068 | 0.4698 | 0.9079 | 0.1842 | 1.0106 | 13 | 0.1666 | 0.0712 |
| **5** | 0.8287 | 0.0194 | 0.1368 | 0.0150 | 0.9117 | 0.9817 | 0.0366 | 0.2231 | 3 | 0.1868 | 0.0948 |
| **6** | 0.4546 | 0.1164 | 0.4231 | 0.0059 | 0.6611 | 0.9410 | 0.1180 | 0.6999 | 15 | 0.2188 | 0.0937 |
| **7** | 0.6697 | 0.0380 | 0.2773 | 0.0150 | 0.8582 | 0.9740 | 0.0520 | 0.3402 | 8 | 0.2225 | 0.0850 |
| **8** | 0.9001 | 0.0054 | 0.0871 | 0.0073 | 0.9745 | 0.9950 | 0.0101 | 0.0778 | 12 | 0.0947 | 0.0448 |
| **9** | 0.6363 | 0.0098 | 0.3345 | 0.0194 | 0.9496 | 0.9892 | 0.0215 | 0.1421 | 9 | 0.1389 | 0.0919 |

(g) step 10

| ref. no. | f1 | f2 | f3 | f4 | f5 | f6 | f7 | f8 | n connected | mean | standard deviation |
|---|---|---|---|---|---|---|---|---|---|---|---|
| **1** | 0.2552 | 0.0728 | 0.6660 | 0.0059 | 0.7378 | 0.9478 | 0.1044 | 0.5684 | 3 | 0.2023 | 0.0883 |
| **2** | 0.0448 | 0.6284 | 0.3232 | 0.0036 | 0.3598 | 0.8807 | 0.2386 | 1.1848 | 3 | 0.1390 | 0.0749 |
| **3** | 0.3263 | 0.0215 | 0.5668 | 0.0854 | 0.9043 | 0.9806 | 0.0387 | 0.2413 | 6 | 0.3923 | 0.1586 |
| **4** | 0.3232 | 0.1749 | 0.4974 | 0.0046 | 0.5511 | 0.9213 | 0.1575 | 0.8837 | 12 | 0.1580 | 0.0659 |
| **5** | 0.8322 | 0.0172 | 0.1351 | 0.0155 | 0.9173 | 0.9824 | 0.0352 | 0.2118 | 2 | 0.1833 | 0.0914 |
| **6** | 0.4780 | 0.1082 | 0.4063 | 0.0075 | 0.6808 | 0.9444 | 0.1112 | 0.6648 | 12 | 0.2207 | 0.0915 |
| **7** | 0.6697 | 0.0380 | 0.2773 | 0.0150 | 0.8582 | 0.9740 | 0.0520 | 0.3402 | 8 | 0.2225 | 0.0850 |

| | | | | | | | | | | | |
|---|---|---|---|---|---|---|---|---|---|---|---|
| **8** | 0.9001 | 0.0054 | 0.0871 | 0.0073 | 0.9745 | 0.9950 | 0.0101 | 0.0778 | 12 | 0.0947 | 0.0448 |
| **9** | 0.6363 | 0.0098 | 0.3345 | 0.0194 | 0.9496 | 0.9892 | 0.0215 | 0.1421 | 9 | 0.1389 | 0.0919 |
| **10** | 0.1732 | 0.3442 | 0.4762 | 0.0064 | 0.3775 | 0.8909 | 0.2181 | 1.1526 | 11 | 0.1442 | 0.0555 |

(h) step 12

| **ref. no.** | **f1** | **f2** | **f3** | **f4** | **f5** | **f6** | **f7** | **f8** | **n connected** | **mean** | **standard deviation** |
|---|---|---|---|---|---|---|---|---|---|---|---|
| **1** | 0.2369 | 0.0839 | 0.6727 | 0.0064 | 0.7097 | 0.9428 | 0.1144 | 0.6198 | 1 | 0.1788 | 0.0636 |
| **2** | 0.0486 | 0.6270 | 0.3204 | 0.0039 | 0.3597 | 0.8806 | 0.2389 | 1.1850 | 4 | 0.1398 | 0.0751 |
| **3** | 0.3259 | 0.0042 | 0.1661 | 0.5038 | 0.9863 | 0.9981 | 0.0037 | 0.0417 | 1 | 0.2575 | 0.1257 |
| **4** | 0.2655 | 0.2170 | 0.5104 | 0.0072 | 0.4941 | 0.9120 | 0.1761 | 0.9734 | 12 | 0.1720 | 0.0778 |
| **5** | 0.8058 | 0.0252 | 0.1525 | 0.0165 | 0.8920 | 0.9782 | 0.0436 | 0.2660 | 2 | 0.1893 | 0.1024 |
| **6** | 0.4187 | 0.1220 | 0.4520 | 0.0073 | 0.6450 | 0.9363 | 0.1275 | 0.7260 | 10 | 0.2243 | 0.0958 |
| **7** | 0.8443 | 0.0124 | 0.1334 | 0.0098 | 0.9459 | 0.9896 | 0.0208 | 0.1493 | 4 | 0.1481 | 0.0566 |
| **8** | 0.9027 | 0.0042 | 0.0890 | 0.0041 | 0.9795 | 0.9959 | 0.0083 | 0.0647 | 9 | 0.0844 | 0.0446 |
| **9** | 0.6429 | 0.0131 | 0.3392 | 0.0048 | 0.9387 | 0.9876 | 0.0249 | 0.1673 | 10 | 0.1373 | 0.0793 |
| **10** | 0.1591 | 0.3637 | 0.4729 | 0.0044 | 0.3663 | 0.8893 | 0.2215 | 1.1693 | 9 | 0.1431 | 0.0677 |
| **11** | 0.5090 | 0.0988 | 0.3773 | 0.0149 | 0.6941 | 0.9458 | 0.1084 | 0.6466 | 5 | 0.1826 | 0.0686 |
| **12** | 0.3815 | 0.0345 | 0.5752 | 0.0088 | 0.8621 | 0.9735 | 0.0531 | 0.3322 | 13 | 0.1716 | 0.898 |

(i) step 17

| ref. no. | f1 | f2 | f3 | f4 | f5 | f6 | f7 | f8 | n connected | mean | standard deviation |
|---|---|---|---|---|---|---|---|---|---|---|---|
| **1** | 0.1531 | 0.1206 | 0.7254 | 0.0009 | 0.6186 | 0.9244 | 0.1512 | 0.7777 | 2 | 0.0710 | 0.0352 |
| **2** | 0.0268 | 0.6946 | 0.2749 | 0.0036 | 0.3928 | 0.8876 | 0.2249 | 1.1336 | 2 | 0.1155 | 0.0695 |
| **3** | 0.3259 | 0.0042 | 0.1661 | 0.5038 | 0.9863 | 0.9981 | 0.0037 | 0.0417 | 1 | 0.2575 | 0.1257 |
| **4** | 0.1993 | 0.2888 | 0.5016 | 0.0103 | 0.4231 | 0.9014 | 0.1971 | 1.0804 | 10 | 0.1477 | 0.0808 |
| **5** | 0.8789 | 0.0128 | 0.0968 | 0.0115 | 0.9357 | 0.9862 | 0.0275 | 0.1722 | 1 | 0.1334 | 0.0561 |
| **6** | 0.2720 | 0.0680 | 0.6521 | 0.0079 | 0.7506 | 0.9506 | 0.0987 | 0.5469 | 1 | 0.1714 | 0.0823 |
| **7** | 0.8656 | 0.0081 | 0.1154 | 0.0109 | 0.9616 | 0.9923 | 0.0154 | 0.1118 | 6 | 0.1174 | 0.0554 |
| **8** | 0.8957 | 0.0043 | 0.0958 | 0.0042 | 0.9795 | 0.9959 | 0.0081 | 0.0649 | 5 | 0.0832 | 0.0402 |
| **9** | 0.6388 | 0.0095 | 0.3469 | 0.0049 | 0.9499 | 0.9892 | 0.0217 | 0.1417 | 9 | 0.1173 | 0.0712 |
| **10** | 0.2233 | 0.2537 | 0.5184 | 0.0046 | 0.4379 | 0.8959 | 0.2081 | 1.0640 | 7 | 0.1537 | 0.0568 |
| **11** | 0.5057 | 0.0995 | 0.3798 | 0.0151 | 0.6926 | 0.9456 | 0.1089 | 0.6494 | 5 | 0.1725 | 0.0602 |
| **12** | 0.3607 | 0.0295 | 0.6026 | 0.0072 | 0.8743 | 0.9747 | 0.0506 | 0.3069 | 7 | 0.1807 | 0.0756 |
| **13** | 0.7442 | 0.0281 | 0.2219 | 0.0059 | 0.8908 | 0.9804 | 0.0391 | 0.2787 | 10 | 0.1025 | 0.0537 |
| **14** | 0.6448 | 0.0557 | 0.2789 | 0.0206 | 0.7967 | 0.9615 | 0.0771 | 0.4572 | 9 | 0.1964 | 0.0622 |
| **15** | 0.3847 | 0.0792 | 0.5242 | 0.0119 | 0.7335 | 0.9507 | 0.0985 | 0.5775 | 6 | 0.1470 | 0.0615 |
| **16** | 0.3456 | 0.1743 | 0.4772 | 0.0030 | 0.5527 | 0.9230 | 0.1540 | 0.8803 | 13 | 0.1274 | 0.0721 |
| **17** | 0.1007 | 0.4839 | 0.4114 | 0.0040 | 0.3206 | 0.8750 | 0.2499 | 1.2439 | 9 | 0.1030 | 0.0406 |

(j) step 21

| ref. no. | f1 | f2 | f3 | f4 | f5 | f6 | f7 | f8 | n connected | mean | standard deviation |
|---|---|---|---|---|---|---|---|---|---|---|---|
| **1** | 0.1531 | 0.1206 | 0.7254 | 0.0009 | 0.6186 | 0.9244 | 0.1512 | 0.7777 | 2 | 0.0710 | 0.0352 |
| **2** | 0.0259 | 0.7009 | 0.2694 | 0.0038 | 0.3952 | 0.8872 | 0.2256 | 1.1306 | 3 | 0.1084 | 0.0675 |
| **3** | 0.6455 | 0.0122 | 0.3155 | 0.0267 | 0.9427 | 0.9885 | 0.0231 | 0.1601 | 7 | 0.1326 | 0.0898 |
| **4** | 0.1340 | 0.4077 | 0.4536 | 0.0048 | 0.3504 | 0.8916 | 0.2167 | 1.1892 | 8 | 0.1048 | 0.0459 |
| **5** | 0.8715 | 0.0142 | 0.1013 | 0.0130 | 0.9291 | 0.9849 | 0.0303 | 0.1883 | 1 | 0.1322 | 0.0542 |
| **6** | 0.2720 | 0.0680 | 0.6521 | 0.0079 | 0.7506 | 0.9506 | 0.0987 | 0.5469 | 1 | 0.1714 | 0.0823 |
| **7** | 0.9090 | 0.0061 | 0.0707 | 0.0142 | 0.9716 | 0.9944 | 0.0112 | 0.0868 | 7 | 0.0953 | 0.0431 |
| **8** | 0.8928 | 0.0053 | 0.0985 | 0.0033 | 0.9749 | 0.9950 | 0.0099 | 0.0774 | 5 | 0.0853 | 0.0360 |
| **9** | 0.9019 | 0.0036 | 0.0886 | 0.0058 | 0.9811 | 0.9960 | 0.0080 | 0.0600 | 3 | 0.0792 | 0.0427 |
| **10** | 0.2678 | 0.2042 | 0.5234 | 0.0046 | 0.4951 | 0.9049 | 0.1903 | 0.9747 | 6 | 0.1670 | 0.0489 |
| **11** | 0.4960 | 0.0953 | 0.3921 | 0.0167 | 0.7031 | 0.9474 | 0.1052 | 0.6307 | 7 | 0.1930 | 0.0832 |
| **12** | 0.3607 | 0.0295 | 0.6026 | 0.0072 | 0.8743 | 0.9747 | 0.0506 | 0.3069 | 7 | 0.1807 | 0.0756 |
| **13** | 0.7878 | 0.0234 | 0.1822 | 0.0066 | 0.9044 | 0.9823 | 0.0355 | 0.2490 | 4 | 0.0936 | 0.0453 |
| **14** | 0.6603 | 0.0536 | 0.2630 | 0.0232 | 0.8067 | 0.9643 | 0.0713 | 0.4390 | 10 | 0.1768 | 0.0469 |
| **15** | 0.4339 | 0.1134 | 0.4470 | 0.0058 | 0.6659 | 0.9407 | 0.1186 | 0.6890 | 10 | 0.2061 | 0.0961 |
| **16** | 0.3132 | 0.1815 | 0.5023 | 0.0029 | 0.5401 | 0.9207 | 0.1585 | 0.9020 | 10 | 0.1113 | 0.0601 |
| **17** | 0.0846 | 0.5096 | 0.4007 | 0.0051 | 0.3154 | 0.8704 | 0.2592 | 1.2548 | 7 | 0.0903 | 0.0359 |
| **18** | 0.6146 | 0.0092 | 0.3685 | 0.0078 | 0.9483 | 0.9883 | 0.0233 | 0.1441 | 6 | 0.1283 | 0.0588 |
| **19** | 0.1541 | 0.0061 | 0.2148 | 0.6250 | 0.9812 | 0.9977 | 0.0047 | 0.0527 | 1 | 0.2114 | 0.0926 |

| | | | | | | | | | | | |
|---|---|---|---|---|---|---|---|---|---|---|---|
| **20** | 0.7239 | 0.0261 | 0.2427 | 0.0072 | 0.8978 | 0.9816 | 0.0369 | 0.2617 | 3 | 0.1007 | 0.0382 |
| **21** | 0.2250 | 0.2578 | 0.5071 | 0.0101 | 0.4440 | 0.9020 | 0.1961 | 1.0512 | 14 | 0.1410 | 0.0792 |

(k) step 23

| ref. no. | f1 | f2 | f3 | f4 | f5 | f6 | f7 | f8 | n connected | mean | standard deviation |
|---|---|---|---|---|---|---|---|---|---|---|---|
| **1** | 0.1488 | 0.1059 | 0.7442 | 0.0011 | 0.6515 | 0.9301 | 0.1398 | 0.7204 | 1 | 0.1429 | 0.0826 |
| **2** | 0.0250 | 0.7069 | 0.2641 | 0.0040 | 0.3969 | 0.8860 | 0.2280 | 1.1294 | 3 | 0.1012 | 0.0690 |
| **3** | 0.6842 | 0.0118 | 0.2675 | 0.0364 | 0.9456 | 0.9892 | 0.0216 | 0.1527 | 7 | 0.1338 | 0.0855 |
| **4** | 0.1159 | 0.4195 | 0.4572 | 0.0074 | 0.3626 | 0.9000 | 0.2000 | 1.1645 | 7 | 0.1092 | 0.0438 |
| **5** | 0.8745 | 0.0134 | 0.0984 | 0.0136 | 0.9314 | 0.9852 | 0.0295 | 0.1835 | 3 | 0.1156 | 0.0463 |
| **6** | 0.3048 | 0.1089 | 0.5643 | 0.0219 | 0.6579 | 0.9363 | 0.1274 | 0.7113 | 3 | 0.1093 | 0.0479 |
| **7** | 0.9168 | 0.0061 | 0.0685 | 0.0086 | 0.9714 | 0.9944 | 0.0113 | 0.0870 | 6 | 0.0852 | 0.0295 |
| **8** | 0.8974 | 0.0045 | 0.0937 | 0.0045 | 0.9787 | 0.9958 | 0.0084 | 0.0674 | 1 | 0.0840 | 0.0358 |
| **9** | 0.8878 | 0.0052 | 0.1009 | 0.0061 | 0.9737 | 0.9945 | 0.0110 | 0.0799 | 2 | 0.0838 | 0.0482 |
| **10** | 0.1946 | 0.3180 | 0.4865 | 0.0010 | 0.3870 | 0.8860 | 0.2279 | 1.1432 | 5 | 0.1482 | 0.0471 |
| **11** | 0.4931 | 0.0616 | 0.4212 | 0.0242 | 0.7819 | 0.9600 | 0.0800 | 0.4912 | 8 | 0.2201 | 0.0985 |
| **12** | 0.3398 | 0.0526 | 0.5990 | 0.0086 | 0.8002 | 0.9617 | 0.0766 | 0.4563 | 7 | 0.1796 | 0.0647 |
| **13** | 0.8004 | 0.0269 | 0.1658 | 0.0069 | 0.8934 | 0.9806 | 0.0388 | 0.2736 | 3 | 0.0884 | 0.0425 |
| **14** | 0.6862 | 0.0501 | 0.2410 | 0.0227 | 0.8137 | 0.9647 | 0.0705 | 0.4254 | 9 | 0.1690 | 0.0551 |
| **15** | 0.4219 | 0.0894 | 0.4817 | 0.0070 | 0.7128 | 0.9478 | 0.1043 | 0.6092 | 10 | 0.1720 | 0.0880 |
| **16** | 0.3810 | 0.1425 | 0.4737 | 0.0029 | 0.6017 | 0.9293 | 0.1413 | 0.8031 | 8 | 0.1499 | 0.0869 |
| **17** | 0.0888 | 0.5011 | 0.4055 | 0.0046 | 0.3168 | 0.8722 | 0.2557 | 1.2514 | 7 | 0.0970 | 0.0414 |

| | | | | | | | | | | | |
|---|---|---|---|---|---|---|---|---|---|---|---|
| **18** | 0.5083 | 0.0128 | 0.4735 | 0.0054 | 0.9316 | 0.9849 | 0.0302 | 0.1845 | 6 | 0.1798 | 0.0738 |
| **19** | 0.1541 | 0.0061 | 0.2148 | 0.6250 | 0.9812 | 0.9977 | 0.0047 | 0.0527 | 1 | 0.2114 | 0.0926 |
| **20** | 0.7134 | 0.0226 | 0.2575 | 0.0065 | 0.9094 | 0.9834 | 0.0333 | 0.2357 | 3 | 0.1066 | 0.0378 |
| **21** | 0.2233 | 0.2686 | 0.4971 | 0.0110 | 0.4323 | 0.9014 | 0.1973 | 1.0695 | 11 | 0.1214 | 0.0460 |
| **22** | 0.9133 | 0.0033 | 0.0804 | 0.0030 | 0.9827 | 0.9964 | 0.0073 | 0.0550 | 6 | 0.0756 | 0.0493 |
| **23** | 0.3403 | 0.1820 | 0.4737 | 0.0040 | 0.5393 | 0.9197 | 0.1606 | 0.9016 | 6 | 0.1790 | 0.0912 |

(l) step 32

| ref. no. | f1 | f2 | f3 | f4 | f5 | f6 | f7 | f8 | n connected | mean | standard deviation |
|---|---|---|---|---|---|---|---|---|---|---|---|
| **1** | 0.1488 | 0.1059 | 0.7442 | 0.0011 | 0.6515 | 0.9301 | 0.1398 | 0.7204 | 1 | 0.1429 | 0.0826 |
| **2** | 0.0268 | 0.6952 | 0.2746 | 0.0033 | 0.3938 | 0.8880 | 0.2240 | 1.1318 | 1 | 0.1172 | 0.0701 |
| **3** | 0.6975 | 0.0129 | 0.2415 | 0.0481 | 0.9421 | 0.9887 | 0.0226 | 0.1608 | 5 | 0.1463 | 0.0897 |
| **4** | 0.1431 | 0.3693 | 0.4795 | 0.0081 | 0.3727 | 0.9010 | 0.1981 | 1.1504 | 6 | 0.0799 | 0.0323 |
| **5** | 0.8683 | 0.0146 | 0.1038 | 0.0133 | 0.9271 | 0.9844 | 0.0311 | 0.1936 | 1 | 0.1239 | 0.0471 |
| **6** | 0.2931 | 0.1015 | 0.5824 | 0.0230 | 0.6710 | 0.9379 | 0.1241 | 0.6896 | 1 | 0.0602 | 0.0238 |
| **7** | 0.9191 | 0.0069 | 0.0656 | 0.0083 | 0.9681 | 0.9938 | 0.0125 | 0.0950 | 5 | 0.0873 | 0.0367 |
| **8** | 0.9085 | 0.0048 | 0.0791 | 0.0076 | 0.9756 | 0.9949 | 0.0102 | 0.0744 | 3 | 0.0754 | 0.0368 |
| **9** | 0.8917 | 0.0049 | 0.0997 | 0.0037 | 0.9770 | 0.9955 | 0.0090 | 0.0722 | 1 | 0.0852 | 0.0308 |
| **10** | 0.1951 | 0.3238 | 0.4801 | 0.0010 | 0.3824 | 0.8855 | 0.2289 | 1.1500 | 4 | 0.1413 | 0.0476 |
| **11** | 0.5947 | 0.0714 | 0.2889 | 0.0449 | 0.7592 | 0.9571 | 0.0858 | 0.5335 | 5 | 0.1629 | 0.0656 |
| **12** | 0.3519 | 0.0539 | 0.5895 | 0.0047 | 0.7972 | 0.9613 | 0.0773 | 0.4622 | 5 | 0.1715 | 0.0558 |
| **13** | 0.7737 | 0.0252 | 0.1799 | 0.0212 | 0.8914 | 0.9786 | 0.0428 | 0.2762 | 2 | 0.0992 | 0.0260 |

| | | | | | | | | | | | |
|---|---|---|---|---|---|---|---|---|---|---|---|
| **14** | 0.6834 | 0.0477 | 0.2451 | 0.0238 | 0.8176 | 0.9649 | 0.0703 | 0.4182 | 10 | 0.1635 | 0.0487 |
| **15** | 0.4614 | 0.0918 | 0.4337 | 0.0131 | 0.7117 | 0.9485 | 0.1030 | 0.6088 | 7 | 0.2094 | 0.0938 |
| **16** | 0.2485 | 0.1902 | 0.5586 | 0.0027 | 0.5224 | 0.9158 | 0.1684 | 0.9302 | 4 | 0.1049 | 0.0256 |
| **17** | 0.1126 | 0.4456 | 0.4337 | 0.0082 | 0.3231 | 0.8784 | 0.2433 | 1.2382 | 4 | 0.0905 | 0.0535 |
| **18** | 0.6504 | 0.0086 | 0.3368 | 0.0042 | 0.9549 | 0.9903 | 0.0193 | 0.1302 | 6 | 0.0952 | 0.0480 |
| **19** | 0.3988 | 0.0543 | 0.5364 | 0.0105 | 0.7972 | 0.9615 | 0.0769 | 0.4628 | 2 | 0.1559 | 0.0583 |
| **20** | 0.7729 | 0.0304 | 0.1924 | 0.0043 | 0.8859 | 0.9802 | 0.0396 | 0.2896 | 4 | 0.0795 | 0.0336 |
| **21** | 0.2224 | 0.2604 | 0.5008 | 0.0163 | 0.4439 | 0.9061 | 0.1879 | 1.0498 | 10 | 0.1075 | 0.0371 |
| **22** | 0.6951 | 0.0147 | 0.2862 | 0.0040 | 0.9328 | 0.9865 | 0.0269 | 0.1831 | 3 | 0.1157 | 0.0595 |
| **23** | 0.3901 | 0.1570 | 0.4504 | 0.0025 | 0.5720 | 0.9226 | 0.1548 | 0.8496 | 5 | 0.1711 | 0.1199 |
| **24** | 0.1541 | 0.0061 | 0.2148 | 0.6250 | 0.9812 | 0.9977 | 0.0047 | 0.0527 | 1 | 0.2114 | 0.0926 |
| **25** | 0.3408 | 0.1958 | 0.4604 | 0.0030 | 0.5267 | 0.9218 | 0.1564 | 0.9207 | 4 | 0.1039 | 0.0476 |
| **26** | 0.9411 | 0.0020 | 0.0535 | 0.0034 | 0.9880 | 0.9973 | 0.0055 | 0.0393 | 7 | 0.0591 | 0.0351 |
| **27** | 0.3930 | 0.0413 | 0.5386 | 0.0271 | 0.8477 | 0.9728 | 0.0544 | 0.3649 | 2 | 0.1745 | 0.0541 |
| **28** | 0.4078 | 0.0940 | 0.4900 | 0.0082 | 0.6991 | 0.9459 | 0.1082 | 0.6406 | 3 | 0.1060 | 0.0411 |
| **29** | 0.2290 | 0.3004 | 0.4679 | 0.0027 | 0.3915 | 0.8859 | 0.2283 | 1.1375 | 3 | 0.1492 | 0.0992 |
| **30** | 0.3761 | 0.0161 | 0.6024 | 0.0055 | 0.9138 | 0.9807 | 0.0385 | 0.2244 | 4 | 0.1466 | 0.0833 |
| **31** | 0.4282 | 0.1348 | 0.4354 | 0.0016 | 0.6171 | 0.9328 | 0.1343 | 0.7786 | 4 | 0.1001 | 0.0380 |
| **32** | 0.0684 | 0.5419 | 0.3862 | 0.0035 | 0.3149 | 0.8703 | 0.2595 | 1.2554 | 7 | 0.0733 | 0.0327 |

In table 6.1(a), all the regions are clustered into 2 groups. One has a higher proportion of impervious surface (30.9%), a lower proportion of vegetation (23.3%) and more heterogeneous texture than the other. The expected urban regions are contained in this cluster (ref. no. = 2). The other cluster contains more rural regions. In the following step shown in Table 6.1(b), both the regions are further split and a new cluster is generated. The shrunk urban cluster has a higher proportion of impervious surface and a lower proportion of vegetation than in the previous step. In the steps shown in Table 6.1(c-l), more different kinds of landscapes are differentiated. An increase of impervious surface proportion and a decrease of vegetation proportion are observed. In Table 6.1(l), the impervious surface and vegetation proportions of the target cluster become 69.5% and 2.7% respectively (still ref. no. = 2). Moreover, the target cluster becomes a connected area at this step. That is to say, the conditions of connectedness, highest proportion of impervious surface and lowest proportion of vegetation are satisfied. By observing the successive steps, it is found that this cluster remains unchanged in the following 13 steps until the number of clusters increases to 46. This means the condition of stability is also satisfied. As a result, the cluster of the reference number 2 is the expected output of the iterative clustering and identification process, which contains 23 regions that are definitely labelled as urban. The clustering results in those key steps are visualized in Figure 6.4. Clusters are indicated using different colors. Regions of the same color belong to the same cluster. Figure 6.4(m) shows the color-reference number mapping, in which the reference number is used to refer to the clusters in Table 6.1. The color scheme is used throughout the steps in Figure 6.4(a-l).

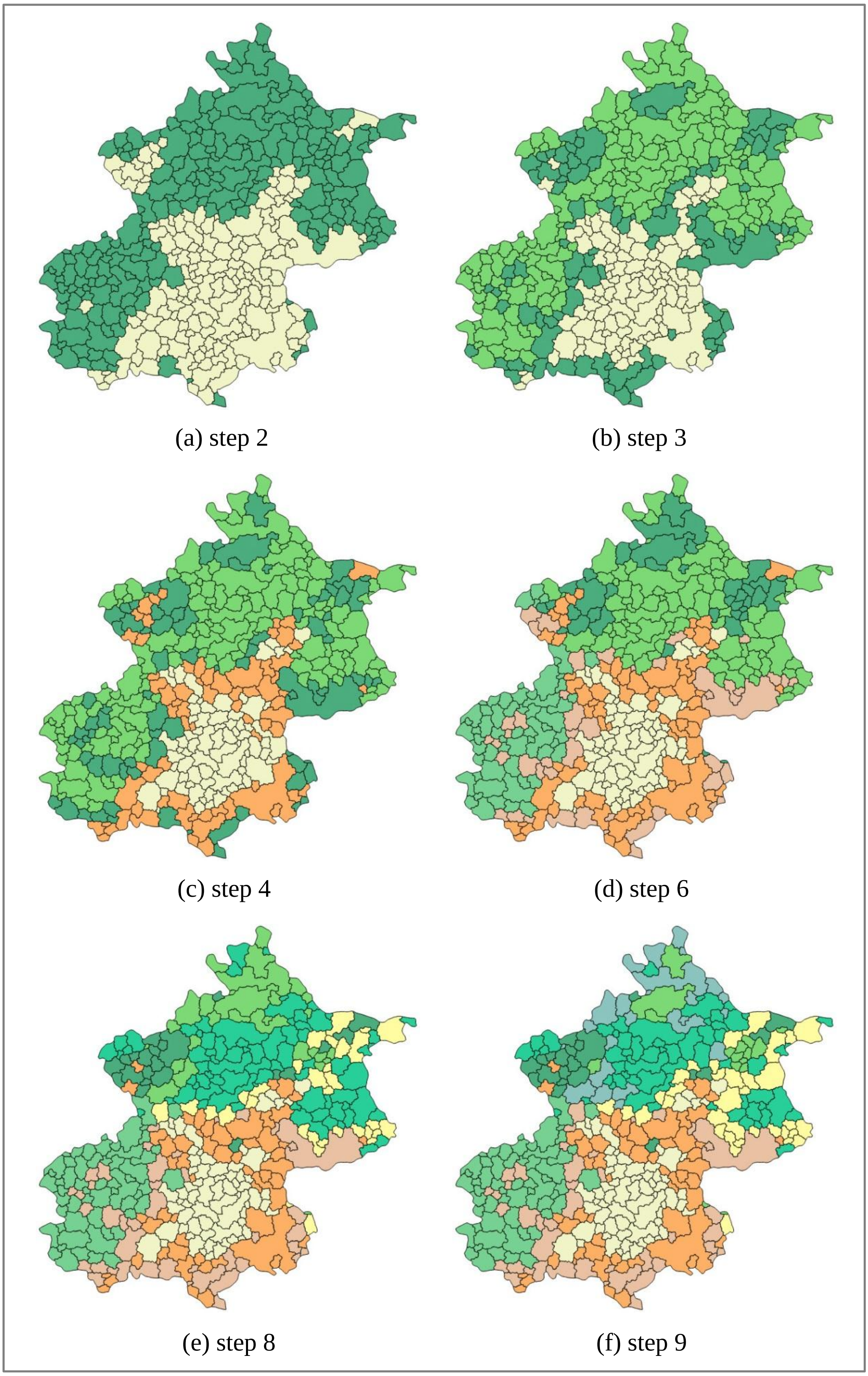


Figure 6.4 Key Steps of the Iterative Clustering Process

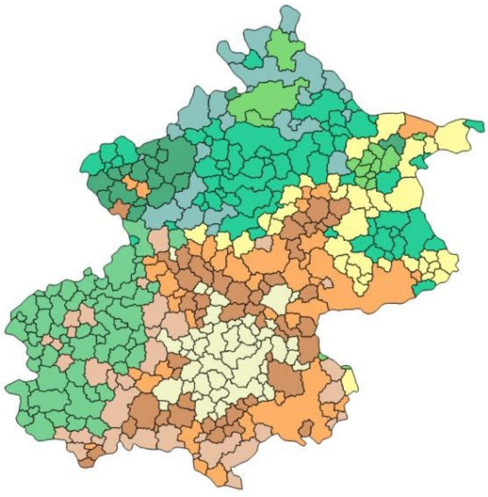

(g) step 10

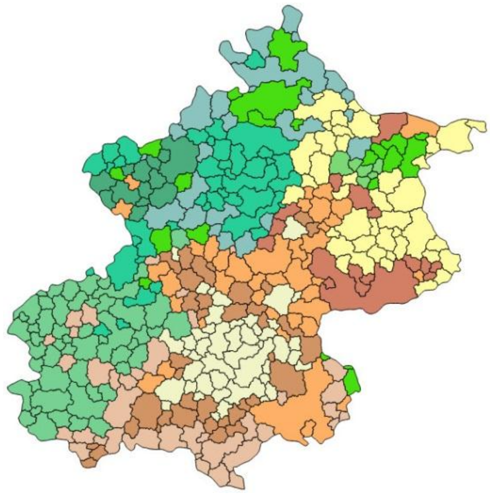

(h) step 12

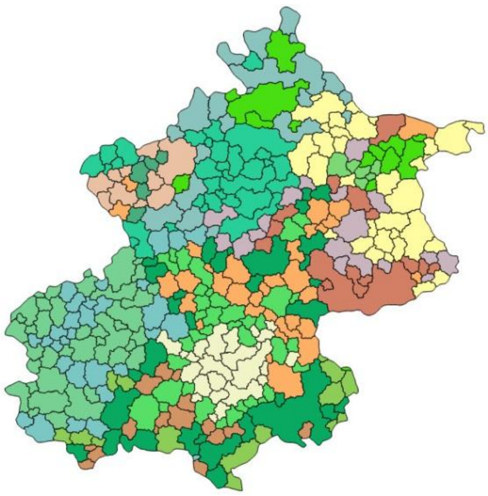

(i) step 17

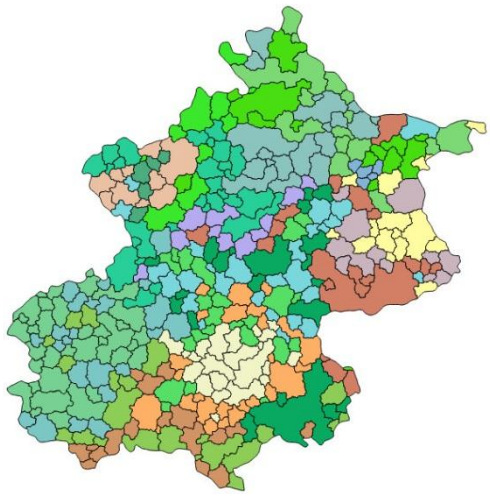

(j) step 21

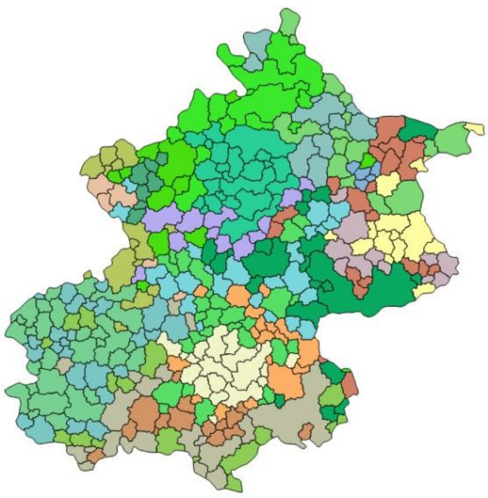

(k) step 23

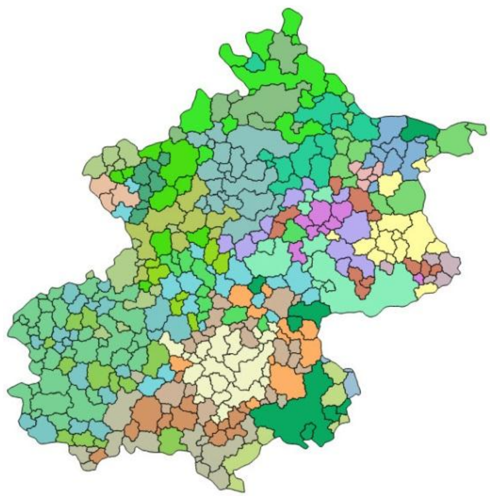

(l) step 32

Figure 6.4 Key Steps of the Iterative Clustering Process (cont’d)

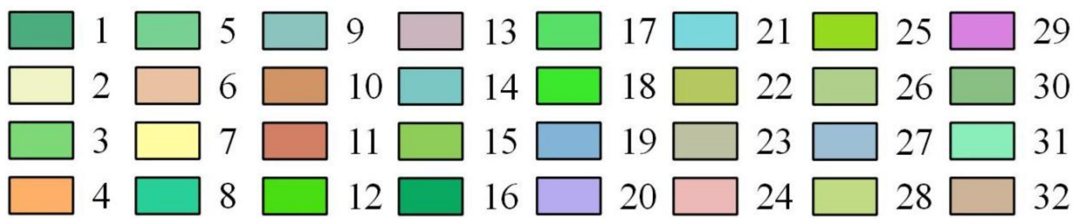


(m) color-reference number mapping

Figure 6.4 Key Steps of the Iterative Clustering Process (cont’d)

### 6.3.2 Merging Analysis Results

The output urban cluster of the clustering process contains 23 regions, so there are 379-23+1=357 times of merge until all regions are merged into one area. All the merging steps are performed. From all the steps, a subset is selected to present here according to the change of the distance between the merged urban and rural areas in the feature space. All the extrema are selected to represent the change of the distance (Figure 6.5). The data produced at the corresponding steps are shown in Table 6.2. The column of step indicates which step the data are produced. The columns starting with mean or standard deviation show the mean or standard deviation of the distances between all merging regions to the mean center of the merged area. The columns ending with urban and rural means the statistics are about the urban and rural areas respectively. The column of distance indicates the distance between the mean centers of urban and rural areas in the feature space. To visualize the merging process, among the 49 extremum steps, there are 25 steps of peak extrema, out of which 18 steps are further selected to show in Figure 6.5. These steps are selected based on a criterion that no another peak step appears within five steps.

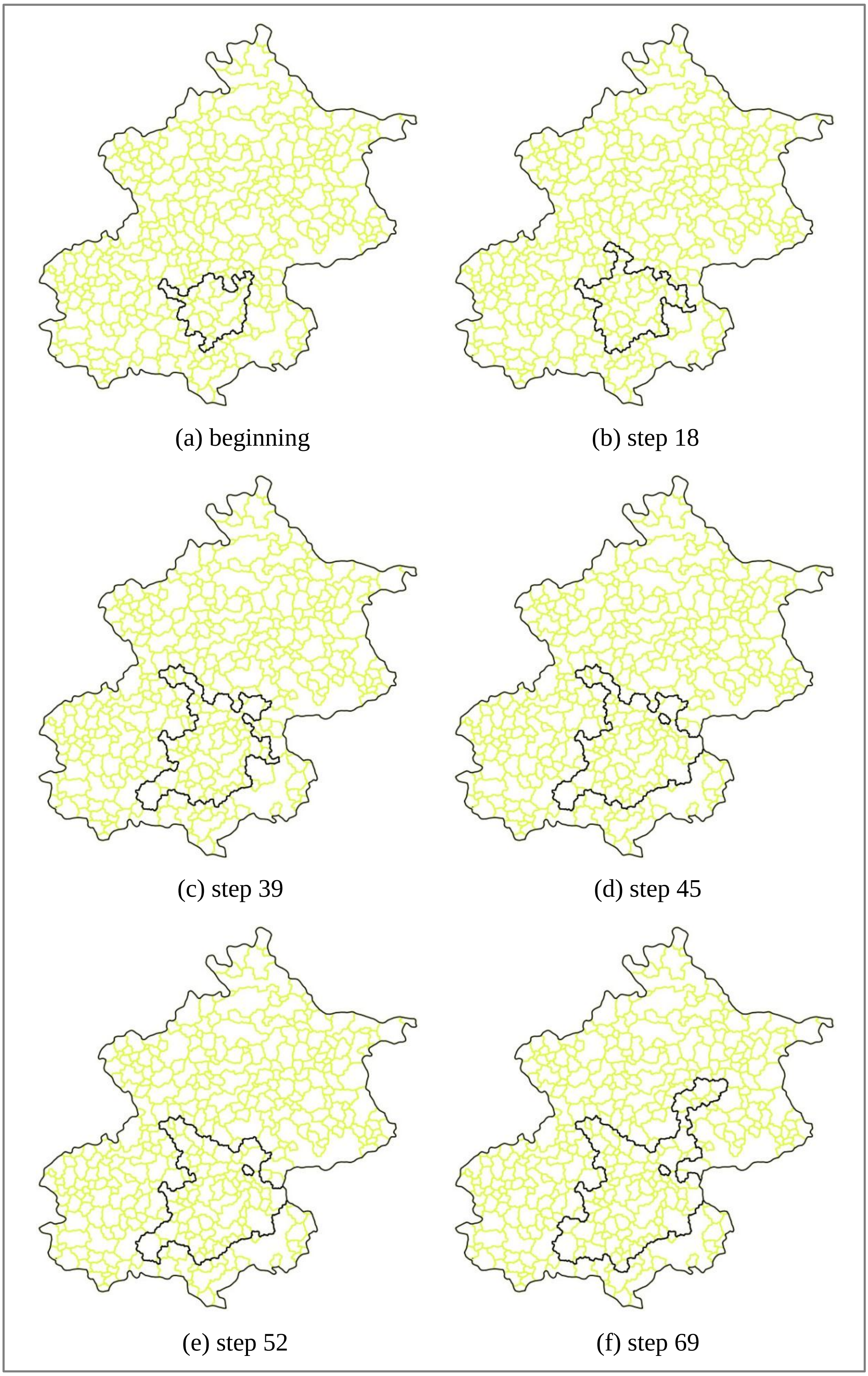


Figure 6.5 Key Steps of the Iterative Merging Process

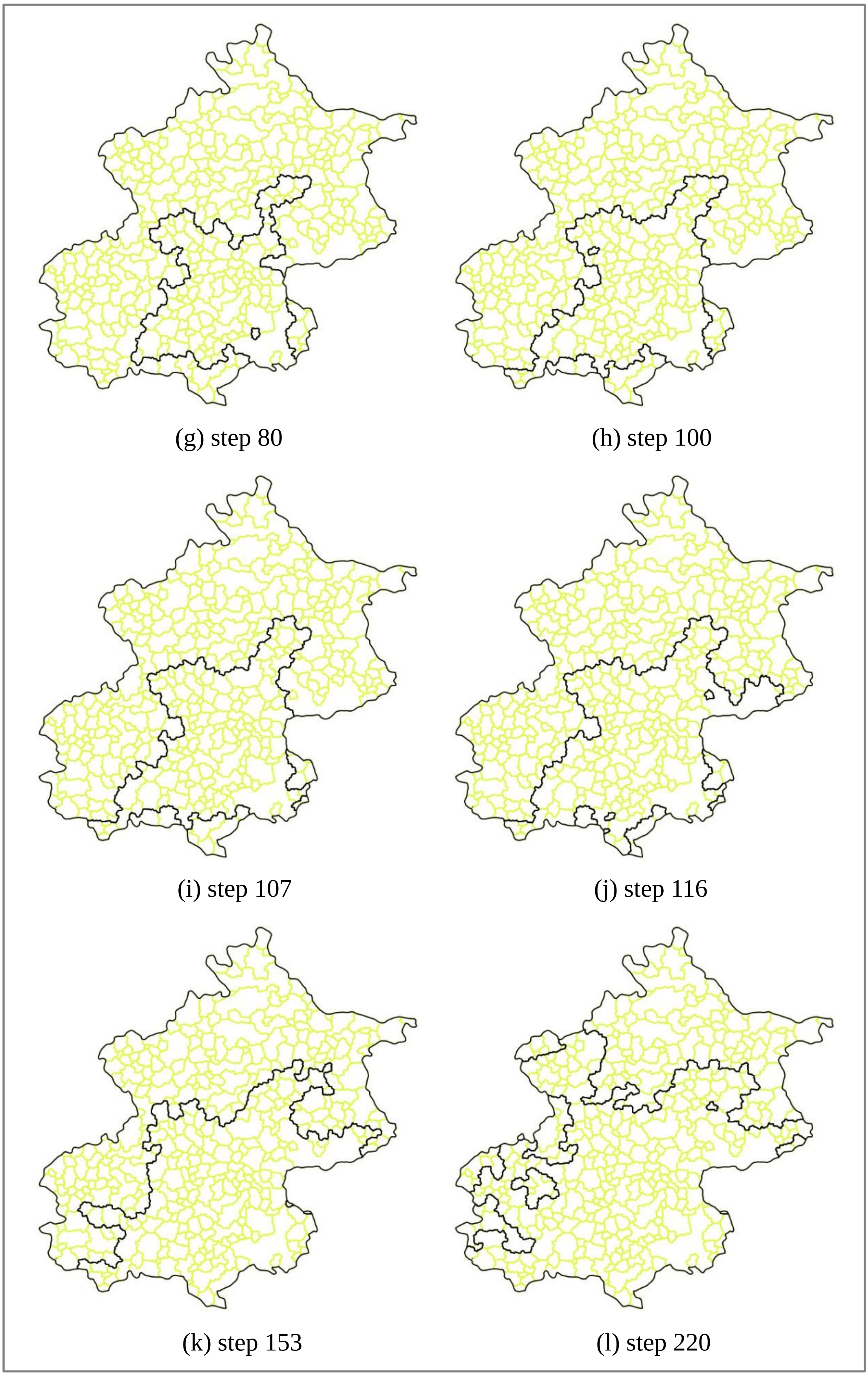


Figure 6.5 Key Steps of the Iterative Merging Process (cont’d)

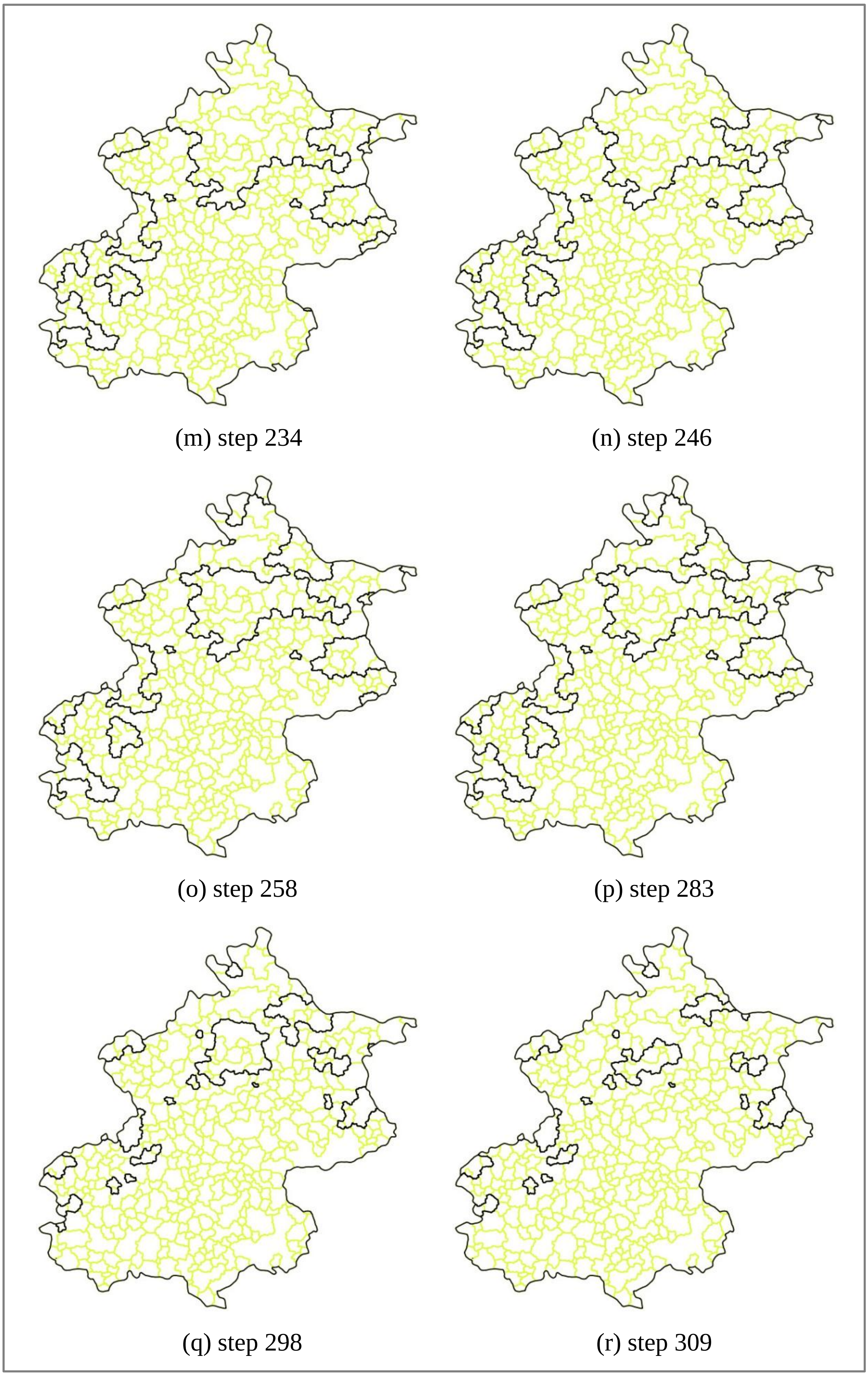


Figure 6.5 Key Steps of the Iterative Merging Process (cont'd)

Table 6.2 The Results of the Key Steps of the Iterative Merging Process

| step | mean urban | std. dev. urban | mean rural | std. dev. rural | distance |
|---|---|---|---|---|---|
| beginning | 0.118117 | 0.071206 | 0.595828 | 0.257933 | 1.071758 |
| 18 | 0.147322 | 0.072001 | 0.565198 | 0.242987 | 1.106673 |
| 19 | 0.148766 | 0.072033 | 0.563775 | 0.242723 | 1.105467 |
| 21 | 0.146596 | 0.070774 | 0.559846 | 0.241747 | 1.112449 |
| 22 | 0.147473 | 0.070809 | 0.558232 | 0.24144 | 1.111985 |
| 36 | 0.153423 | 0.07681 | 0.530935 | 0.228324 | 1.132284 |
| 37 | 0.154742 | 0.07725 | 0.529186 | 0.227628 | 1.132154 |
| 39 | 0.157253 | 0.078599 | 0.525251 | 0.226438 | 1.132856 |
| 43 | 0.164578 | 0.080283 | 0.517464 | 0.226794 | 1.130012 |
| 45 | 0.167434 | 0.081039 | 0.513765 | 0.223874 | 1.130856 |
| 51 | 0.180007 | 0.083852 | 0.503814 | 0.221779 | 1.125689 |
| 52 | 0.181736 | 0.084647 | 0.501947 | 0.219938 | 1.125832 |
| 53 | 0.183766 | 0.085001 | 0.500194 | 0.219597 | 1.125015 |
| 54 | 0.185532 | 0.085784 | 0.49848 | 0.218239 | 1.125059 |
| 55 | 0.188089 | 0.086756 | 0.49697 | 0.218065 | 1.123516 |
| 56 | 0.190494 | 0.087761 | 0.494674 | 0.217739 | 1.123657 |
| 62 | 0.204243 | 0.090282 | 0.484304 | 0.21589 | 1.116654 |
| 69 | 0.203227 | 0.08957 | 0.467341 | 0.202941 | 1.130475 |
| 79 | 0.227968 | 0.092605 | 0.444852 | 0.204461 | 1.114516 |
| 80 | 0.229258 | 0.092986 | 0.442747 | 0.203009 | 1.115078 |
| 96 | 0.270791 | 0.109131 | 0.417278 | 0.209114 | 1.092179 |
| 100 | 0.271703 | 0.108184 | 0.408453 | 0.202584 | 1.094749 |
| 106 | 0.282269 | 0.111878 | 0.399646 | 0.202233 | 1.091288 |
| 107 | 0.283159 | 0.111827 | 0.397313 | 0.200436 | 1.091832 |
| 109 | 0.289172 | 0.113329 | 0.3936 | 0.202801 | 1.085277 |
| 111 | 0.290838 | 0.113226 | 0.389006 | 0.201058 | 1.086778 |
| 115 | 0.30798 | 0.118987 | 0.379945 | 0.210045 | 1.067751 |
| 116 | 0.308601 | 0.118792 | 0.37769 | 0.207979 | 1.068291 |
| 152 | 0.403536 | 0.173371 | 0.351147 | 0.234156 | 0.997775 |
| 153 | 0.404264 | 0.17285 | 0.349354 | 0.233946 | 0.998196 |
| 202 | 0.518046 | 0.212806 | 0.39495 | 0.244215 | 0.814716 |
| 220 | 0.513489 | 0.2121 | 0.295884 | 0.203338 | 0.885313 |
| 225 | 0.522126 | 0.212911 | 0.299103 | 0.20581 | 0.863531 |
| 234 | 0.521155 | 0.211732 | 0.248799 | 0.191214 | 0.903198 |

| | | | | | |
|---|---|---|---|---|---|
| 245 | 0.536455 | 0.215737 | 0.252951 | 0.1969 | 0.881436 |
| 246 | 0.537597 | 0.216149 | 0.248662 | 0.193329 | 0.88148 |
| 247 | 0.539531 | 0.216626 | 0.24776 | 0.195342 | 0.873061 |
| 258 | 0.548273 | 0.21982 | 0.167127 | 0.204283 | 0.911346 |
| 260 | 0.550317 | 0.220486 | 0.162573 | 0.207127 | 0.910349 |
| 261 | 0.550883 | 0.220376 | 0.160337 | 0.207764 | 0.91064 |
| 282 | 0.573129 | 0.229283 | 0.159636 | 0.235327 | 0.87525 |
| 283 | 0.57329 | 0.228962 | 0.157501 | 0.236325 | 0.875607 |
| 297 | 0.586028 | 0.235226 | 0.17206 | 0.258071 | 0.849929 |
| 298 | 0.586892 | 0.235695 | 0.160726 | 0.263517 | 0.851585 |
| 300 | 0.588527 | 0.236539 | 0.164171 | 0.267537 | 0.84823 |
| 301 | 0.588948 | 0.236409 | 0.160557 | 0.269525 | 0.848786 |
| 308 | 0.594898 | 0.241556 | 0.173329 | 0.285834 | 0.829628 |
| 309 | 0.595576 | 0.241643 | 0.154013 | 0.27627 | 0.83418 |
| 343 | 0.617359 | 0.253795 | 0.52965 | 0.114201 | 0.722058 |

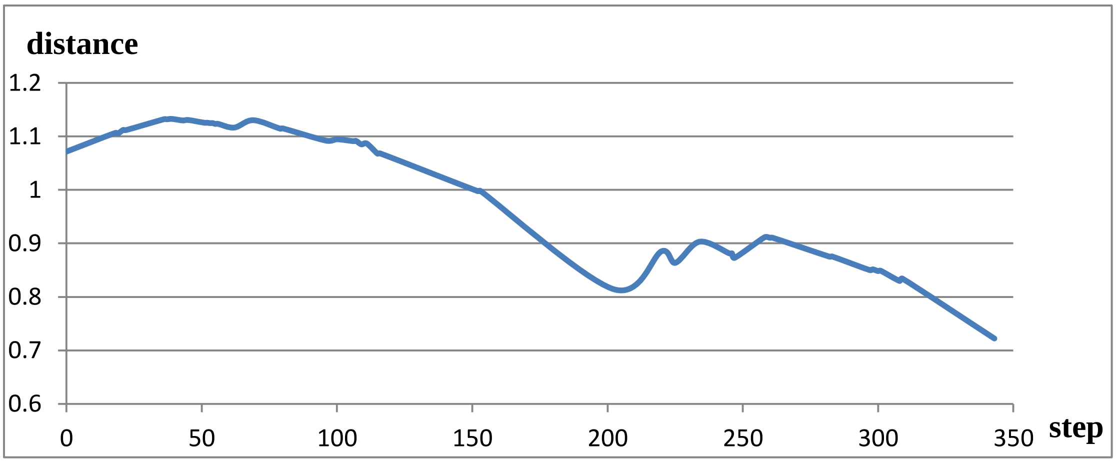


Figure 6.6 Change of Distance between Urban and Rural Areas in Feature Space

From Table 6.2 and Figure 6.6, it can be seen that the maximum of the urban-rural distance appears at the step 39, which is shown in Figure 6.5(c). The resulting urban and rural areas of this step are the most distinguishable according to the eight proportional and textural features. They form an urban-rural division of the study area, which is shown in Figure 6.7. The urban area is shown in yellow, and the surrounding rural area is shown in green. The results show that an urban area is identified through the iterative merging process. The urban area is taken as the final output of the whole urban recognition process.

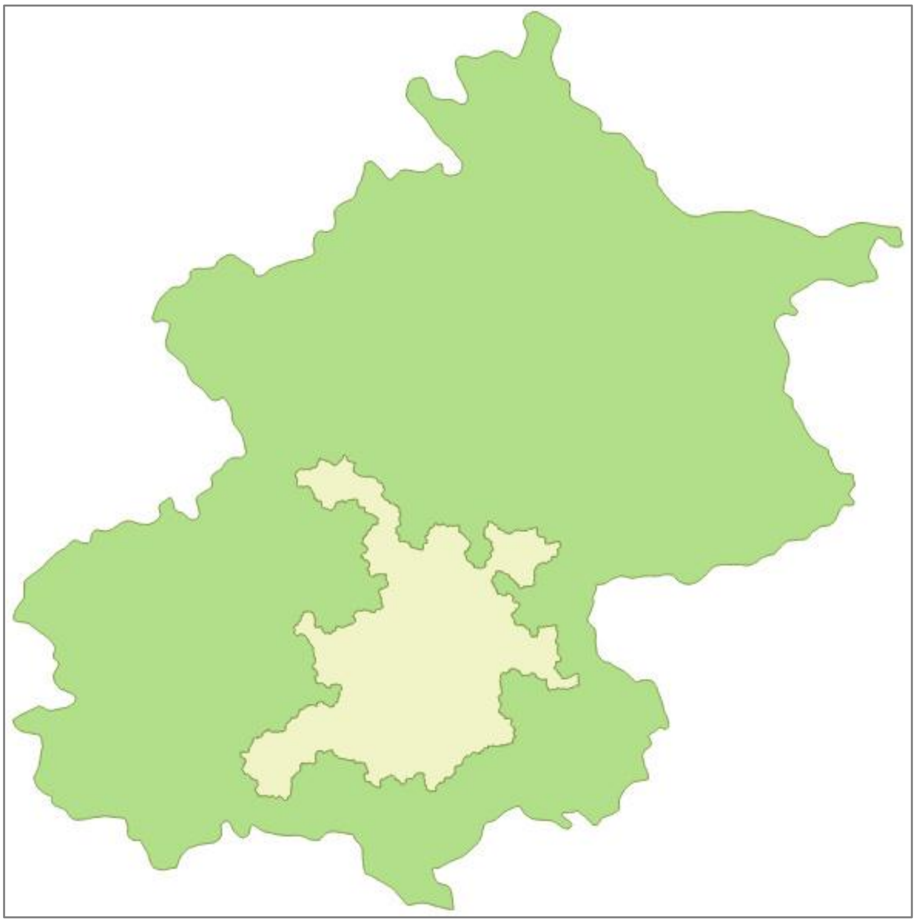

Figure 6.7 The Result of Urban Area Recognition

## 6.4 Evaluation of the Recognized Urban Area

Different from other urban objects with physical boundaries, e.g. roads and buildings, urban areas are of no distinct visible boundaries. The sampling method used to evaluate the accuracy of land cover / land use (LCLU) classification or object extraction is not appropriate to be used to evaluate the recognized urban area of the proposed approach, because no physical boundary in the reality can be used to determine if a sample point is inside the urban area. Therefore, a qualitative approach is adopted, based on some facts about the study area. If the recognition result is consistent with the existing facts about the study area, then the result is accepted. According to the description of the study area in Section 3.3, some facts are summarized from the referenced materials as follows.

1) The urban area is within the municipal districts of Beijing. A region of municipal district level does not mean that the whole region is urbanized. Many places of a municipal district are rural, but the upgrade of administrative level reflects that the region is going to be developed towards an urban area. Hence, the realistic urban extent should be smaller than the entire extent of the municipal districts, and should not include rural countries.

2) The urban area contains the entire Dongcheng and Xicheng districts. In the functional division, they are the capital function core area. In the analytical division, they are the inner center. They are inside the third ring road. In the map of Beijing's urban area in the atlas of Beijing, these two districts are entirely inside the map. Hence, these two districts are definitely urban.

3) The urban area contains some parts of Chaoyang, Fengtai, Shijingshan and Haidian districts. In the functional division, they are the urban function expansion area. In the analytical division, they are the outer center. They lie between the second and sixth ring roads. Small parts of Fengtai and Haidian are beyond the sixth ring road. In the map of Beijing's urban area in the atlas of Beijing, most of Haidian is inside the map, and the other three districts are entirely within the map. Thus these four districts are not fully but partly urbanized.

4) The urban area contains small parts of Mentougou, Fangshan, Tongzhou, Shunyi, Changping and Daxing districts, among which Mentougou contributes the smallest

part. These regions are linked by the sixth ring road. In the map of Beijing's urban area in the atlas of Beijing, these districts are partly inside the map. In the analytical division, they are the inner periphery. In the functional division, except Mentougou districts, the other five districts are the urban development new area, which means they are newly urbanizing regions. The exclusion of Mentougou from the urban development new area reflects that it is less urbanized than the other five regions.

5) The urban area does not include Huairou and Pinggu districts, and Miyun and Yanqing countries. In the functional division, they are the ecological conservation area. In the analytical division, they are the outer periphery. Moreover, no ring road is built across these regions. Furthermore, in the map of Beijing's urban area in the atlas of Beijing, these four regions are entirely outside the map.

6) The location and extent of the urban area are approximately consistent with those of the ring road system. As pointed out by urban scholars, the ring roads constitute the underlying pattern of urban growth in Beijing. Accordingly, the outmost ring road, i.e. the sixth ring road, encloses most of the urban area. Almost all the urban area is enclosed by the fifth ring road, as it is entirely inside the map of Beijing's urban area.

The consistency of the recognized urban area with these facts is checked by overlaying the recognition result on the referenced data (Figure 6.8). By overlaying the administrative boundaries on the recognition result, it is verified that the facts 1-5 are satisfied (Figure 6.8(a)). By overlaying the recognized urban area on the administrative division, it can be easily seen that the urban area is within the municipal districts and does not overlap the rural countries (Figure 6.8(b)). By overlaying the recognized urban area on the functional and analytical divisions, it can be easily seen that the urban area accords well with the underlying patterns of them (Figure 6.8(c,d)).

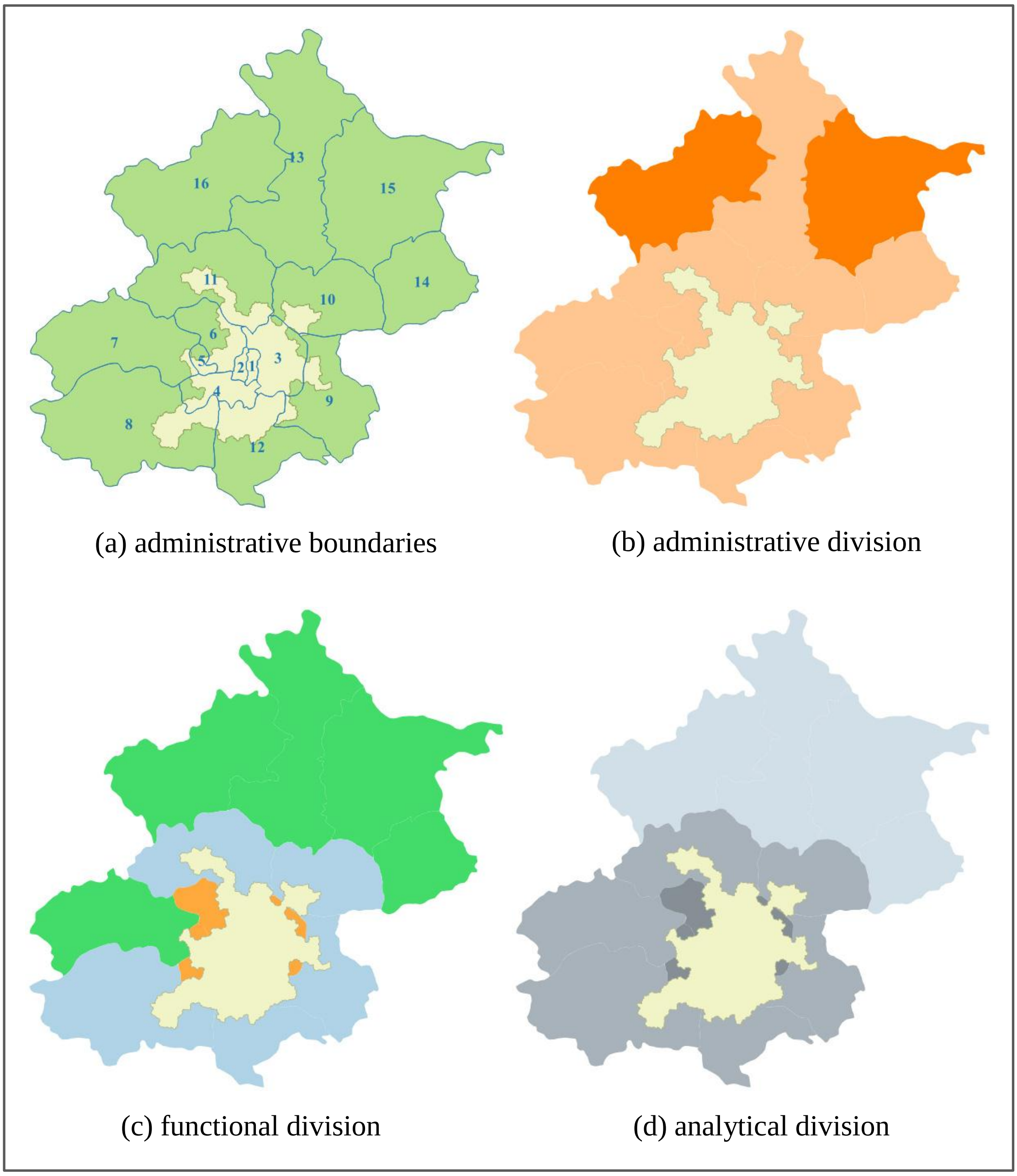


(a) administrative boundaries (b) administrative division

(c) functional division (d) analytical division

Figure 6.8 Overlap of Recognition Result with Referenced Data

The percentages of the overlapping areas of the recognized urban area and the sixteen administrative regions are calculated and shown in Table 6.3. It can be seen that Dongcheng and Xicheng districts are 100% overlapping the urban area, which is consistent with the fact 2. The overlapping percentages of the outer center regions range from 40.9% to 84.7%, satisfying the fact 3. Except Mentougou, which overlaps the urban area by only 1.9%, the overlapping percentages of the other five inner periphery regions range from 11.2% to 31.7%, satisfying the fact 4. The four outer periphery regions contains on urban area, consistent with the fact 5.

Table 6.3 Overlapping Percentage of Urban Area with Administrative Regions

| **Ref. No.** | **Name** | **Percentage** |
|---|---|---|
| 1 | Dongcheng | 100% |
| 2 | Xicheng | 100% |
| 3 | Chaoyang | 84.7% |
| 4 | Fengtai | 83.5% |
| 5 | Shijingshan | 60.5% |
| 6 | Haidian | 40.9% |
| 7 | Mentougou | 1.9% |
| 8 | Fangshan | 11.6% |
| 9 | Tongzhou | 12.3% |
| 10 | Shunyi | 11.2% |
| 11 | Changping | 19.8% |
| 12 | Daxing | 31.7% |
| 13 | Huairou | 0% |
| 14 | Pinggu | 0% |
| 15 | Miyun | 0% |
| 16 | Yanqing | 0% |

By overlaying the ring roads on the recognition result, it can be seen that the location and extent of the urban area are approximately consistent with those of the ring road system (Figure 6.9). The intersection of the region enclosed by each ring road and the urban area is computed. The percentage of the intersection area by the total area of the enclosed region is then calculated and listed in Table 6.4. The regions enclosed by the second to fourth ring roads are entirely urban. 98.2% of the region enclosed by the fifth ring road is urban area. Within the sixth ring road, the urban area takes up 73.1% of the region. The data show that the recognition result satisfies the fact 6.

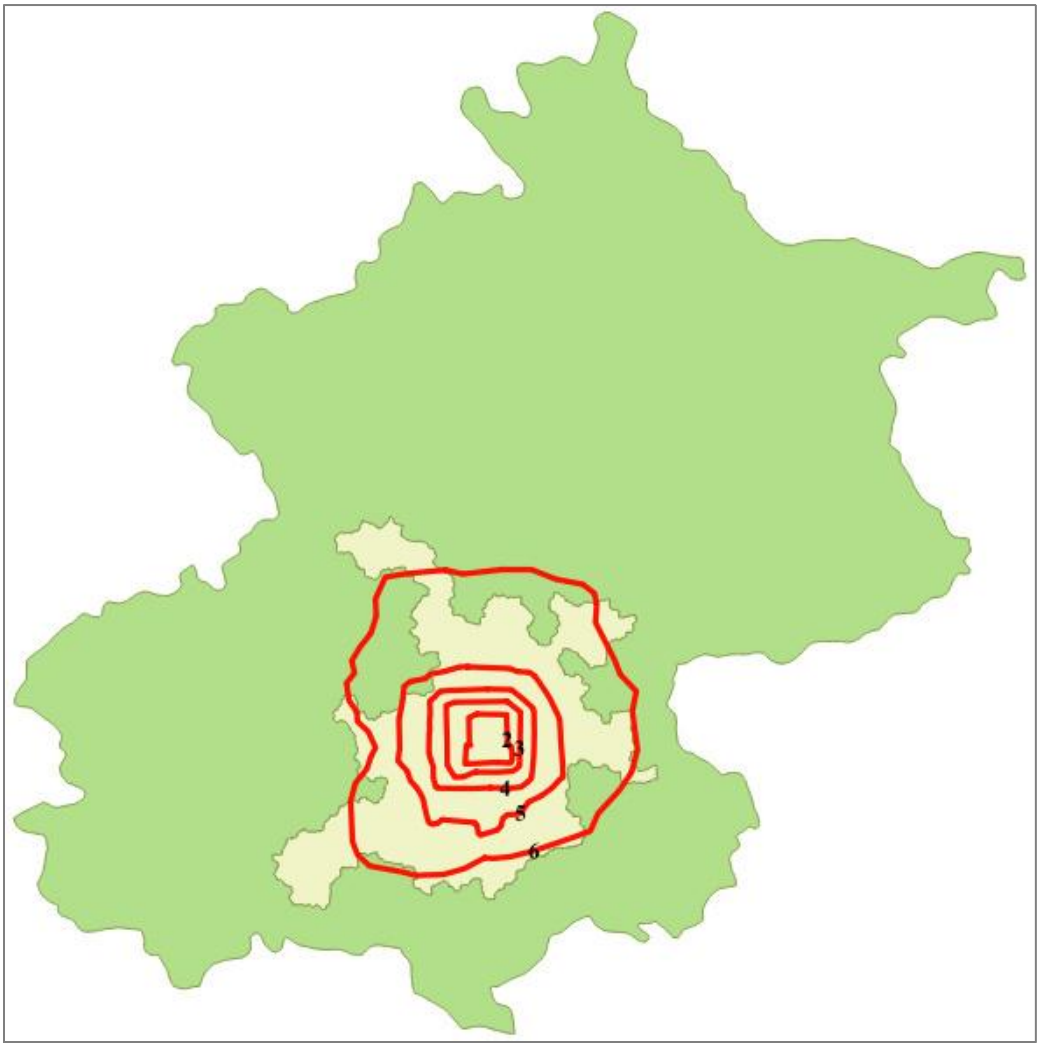


Figure 6.9 Overlap of Recognition Result with Concentric Ring Roads

Table 6.4 Overlapping Percentage of Urban Area with Ring Road Enclosed Regions

| **Ring Road** | **Percentage** |
|---|---|
| 2nd | 100% |
| 3rd | 100% |
| 4th | 100% |
| 5th | 98.2% |
| 6th | 73.1% |

# Chapter 7 Conclusions and Recommendations

This thesis proposes an urban recognition approach using remote sensing data. A summery is given first, followed by a statement of the main conclusions. The limitations of the proposed approach are discussed next. Future work is recommended at the end.

## 7.1 Summary

An urban area is a concentration of human beings and activities. Recognition of an urban area means the identification of the spatial extent of the urban area. In other words, an urban-rural boundary can be drawn to delineate an urban area as a geographical entity. Traditionally, it is done by censuses and surveys. It is recognized that there is a spatial mismatch in census data. The cost of generating and maintaining census and survey data is enormous. The urban and rural areas classification using census and survey data is not efficient. Increasing availability of remotely sensed data and processing techniques facilitates the development of new approaches to studying urban issues. Some methods have been developed to recognize urban areas using remote sensing images and techniques. Due to the raster nature of image data, these methods are classification based approaches. The per-pixel classification process determines whether the area covered by the pixel is urban or not, but no boundary is drawn to delineate an urban area as a geographical entity. This research adopts a new strategy to develop an urban area recognition approach using remote sensing data. It firstly reviews current definitions of urban area, including census definitions used by different countries, and urban scholars' definitions adopted in urban studies. From those definitions, some characteristics inherent in urban areas are extracted, which is discussed in Chapter 2. Urban-rural differences are further identified and discussed in Chapter 3. Then based on the urban-rural differences, relevant information and processes that constitute an urban area recognition algorithm are identified. The proposed algorithm comprises four steps, i.e. zoning, clustering, identification and merging. According to the urban characteristics, places can be characterized by land cover composition and configuration, which can be represented using eight proportional and textural features and extracted from remote sensing images. Chapter 4 evaluates if the eight features are effective to characterize urban and rural areas through a clustering analysis. Chapter 5 discusses the zoning method for the approach. It compares homogeneous division with the administrative division of a city region by observing the change of the average grey-level ranges in all image bands through a continuous region splitting process. Chapter 6 develops an iterative clustering and merging algorithm for the remaining steps of the proposed approach. A clustering analysis is made for observing the change of output clusters along a series of clustering operations. A merging analysis is then made for observing the change of the distance between urban and rural areas in the feature space along a series of merging steps. The result shows that the proposed algorithm recognizes the urban area successfully. The recognized urban area is evaluated by overlapping it with referenced data to check if it satisfies the facts about the study area.

## 7.2 Conclusions

The key conclusions of this thesis are drawn as follows.

1) Four urban characteristics are identified from current definitions of an urban area. They are a) urban areas contain large and dense built-up areas; b) urban areas contain heterogeneous elements; c) urban areas are dominant by non-agricultural activities; and d) urban areas are distinguishable from their surrounding rural areas. To distinguish between urban and rural areas, these urban characteristics can be expressed in the following manner, to present the differences between urban and rural areas. They are a) urban areas are composed of large and dense built-up areas, providing space for non-agricultural human activities, while rural areas are mainly composed of agricultural or natural lands, i.e. vegetated areas; b) the physical elements of urban areas are more heterogeneous, while the ones of rural areas are more homogeneous; and c) these differences are observable.

2) Eight remote sensing image features are related to the urban characteristics, they are, the four proportions of vegetation, impervious surface, soil and water / shade, and the four textural features including angular second moment, inverse difference moment, contrast and entropy. They correspond to two types of information. Four proportional features correspond to land cover composition, and four textural features correspond to land cover configuration. The experiment results show that the combination of the eight features is valid for characterizing different kinds of areas and effective for distinguishing between urban and rural areas.

3) The multi-resolution image segmentation algorithm is suitable for dividing a city region into homogeneous sub-regions that accord with the physical landscape. In the experiment of the algorithm with Landsat TM data, all the seven spectral bands show a decrease in the average grey-level range along a continuous region splitting process performed for all administrative regions of the study area. The average grey-level

ranges in six of the seven bands are further reduced by removing the administrative boundary constraint.

4) An urban area is successfully recognized through an iterative clustering and merging process, performed on the homogeneous regions output from the image segmentation process with the eight proportional and textual features. An experiment shows that the iterative clustering and identification is able to identify an area that can be definitely labelled as urban. This area satisfies a) single-connectedness, b) the highest proportion of impervious surface, c) the lowest proportion of vegetation and d) unchanged in more than three following steps. Another experiment shows that the iterative merging process is able to identify the urban and rural areas of a city region with the maximum distance between them in the feature space.

5) The resulting urban area is evaluated by a fact consistency checking. Different from other urban objects with physical boundaries, urban areas are of no distinct visible boundaries. The sampling method used to evaluate the accuracy of land cover / land use (LCLU) classification or object extraction is not appropriate for evaluating the resulting urban area, because no physical boundary in the reality can be used to determine whether a sample point is inside the urban area or not. Hence, a qualitative approach is adopted, based on some facts about the study area. By overlapping the resulting urban area with some referenced data, it is verified that all the facts about the study area are satisfied by the recognition result. Therefore, the result is accepted.

## 7.3 Limitations and Future Work

One of the limitations of the proposed approach is that it is not fully automated yet. The whole recognition process is created by chaining a number of sub-processes. Most of these sub-processes are achieved in a fully automated manner, except the extraction of the four proportional features. The technique of linear spectral unmixing is used to extract the proportions of the four V-I-S land cover types. The unmixing process involves an endmember selection step, which requires expert knowledge and human-computer interaction. Hence, the whole process cannot be achieved without human intervention. Future study of a fully automated method for extracting these features is of interest. A recommendation is studying if spectral indices, as reviewed in Section 2.2.2, can be used to substitute the proportions for representing land cover composition. The spectral indices corresponding to the four land cover types could be NDVI, SAVI or MSAVI for vegetation, NDBI for impervious surface, NDBaI for soil, NDWI or MNDWI for water / shade. The choice of spectral indices depends on the availability of the required spectral bands. The second limitation is that it is only based on the information of land cover, derived from remote sensing data. However, as seen in the urban definitions discussed in Section 2.1, besides the built environment, the social and economic aspects are often considered in defining an urban area. Hence, a future effort can be made to incorporate social and economic data into the proposed method to see if it can better recognize an urban area.

Moreover, another trend of the definitional argument about urban and rural areas revolves the concept of urban-rural continuum. Weeks et al. (2005) and Weeks (2008) argued that urban and rural are not really representing a dichotomy, but are ends of a continuum. A place on urban fringe that cannot be determined as absolutely urban or rural can be considered as “urban to some extent”. The discussion of urban-rural continuum dates back to 1950s, as Bertrand’s (1958) observation that “proponents of the continuum theory feel that rural-urban differences occur in a relative degree in a range extending between two polar extremes of rural and urban”. Nowadays, the concept of urban-rural continuum is widely discussed and adopted by international organizations, such as the United Nations and the World Bank (Siechiping et al., 2015; Ulrike et al., 2015; UN-Habitat, 2015). It is considered that an urban-rural continuum is more useful in social science research than an urban-rural dichotomy (Hugo et al., 2001; Weeks et al., 2005). This research, correspondingly, can be extended to construct an urban-rural continuum, according to the change of urban-rural distance described in Section 6.3.2. Between the two ends of the urban-rural continuum, corresponding to peri-urban or sub-urban areas, places belong to an urban area with a certain probability or confidence level, instead of being classified as absolutely urban or rural. A distinct boundary, or a boundary as a fuzzy zone, can be derived from the continuum when it is necessary. This may lead to more possible approaches to studying the issues of urban-rural boundaries and urbanization process.

Furthermore, the proposed approach recognizes the main urban area of a city. In the real world, there usually exist satellite cities, i.e. disconnected urban areas, which means the urban area of a city is not necessarily single connected. It is interested to study if the proposed approach can be extended to identify satellite cities as well. In the iterative merging process, each merge results in a change of urban-rural distance in the feature space. Satellite cities may be found during the change. Another extension of this study can be applying the proposed algorithm to remote sensing data of a city in different times. Recognition of urban areas using data in some years may lead to a method for modelling and monitoring urban growth.

# References


Adams, J.B., Kapos, V., Smith, M.O., Almeida Filho, R., Gillespie, A.R. & Roberts, D.A., 1990. A new Landsat view of land use in Amazonia. *International Archives of Photogrammetry and Remote Sensing*, 28, 177-185.

Adams, J.B., Smith, M.O. & Gillespie, A.R., 1989. Simple models for complex natural surfaces: A strategy for the hyperspectral era of remote sensing. *Proceedings of the 12th Canadian Symposium on Remote Sensing*, 1, 16-21.

Adams, J.B., Smith, M.O. & Johnson, P.E., 1986. Spectral mixture modelling: A new analysis of rock and soil types at the viking lander 1 site. *Journal of Geophysical Research*, 91 (B8), 8098-8112.

Aghababaee, H., Niazmardi, S. & Amini, J., 2013. Urban area extraction in SAR data. *International Archives of the Photogrammetry, Remote Sensing and Spatial Information Sciences*, XL-1/W3, 1-5.

Ali Rizvi, I. & Krishna Mohan, B., 2010. Object-oriented method for automatic extraction of road from high resolution satellite images. *Iranian Journal of Earth Sciences*, 2, 55-62.

Angiuli, E. & Trianni, G., 2014. Urban mapping in Landsat images based on normalized difference spectral vector. *IEEE Geoscience and Remote Sensing Letters*, 11(3), 661-665.

A.T. Kearney, 2014. *2014 global cities index and emerging cities outlook: Global cities, present and future*.

Baatz, M. & Schape, A., 2000. Multiresolution segmentation: An optimization approach for high quality multi-scale image segmentation. *In* Strobl, V.J., Blaschke, T. & Griesebner, G. ed. *Angewandte geographische* *informationsverarbeitung xii.*

Ban, Y., Jacob, A. & Gamba, P., 2015. Spaceborne SAR data for global urban mapping at 30m resolution using a robust urban extractor. *ISPRS Journal of Photogrammetry and Remote Sensing,* 103, 28-37.

Baraldi, A. & Parmiggiani, F., 1990. Urban area classification by multispectral SPOT images. *IEEE Transactions on Geoscience and Remote Sensing,* 28(4), 674-680.

Barnsley, M.J., 1999. Digital remote sensing data and their characteristics. *In* Langley, P., Goodchild, M., Maguire, D.J. & Rhind, D.W. ed. *Geographical Information Systems: Principles, techniques, applications, and management.* N.Y., 451-466.

Beall, J. & Fox, S., 2009. *Cities and development* London: Routledge.

Beijing Goverment, 2012. The main functional area planning of beijing.

Benz, U.C., Hofmann, P., Willhauck, G., Lingenfelder, I. & Heynen, M., 2004. Multi-resolution, object-oriented fuzzy analysis of remote sensing data for GIS-ready information. *ISPRS Journal of Photogrammetry and Remote Sensing,* 58 (3-4), 239-258.

Berger, A.S., 1978. *The city: Urban communities and their problems* Boston: Brown.

Bertrand, A. L., 1958. The nature of rural-urban differentials. *In* BERTRAND, A. L. ed. *Rural Sociology: An Analysis of Contemporary Rural Life.* McGraw-Hill.

Bessettes, V. & Desachy, J., 1998. Extraction and classification of urban areas on SPOT images. *Geoscience and Remote Sensing Symposium Proceedings*, 2583-2586.

Bianchin, A. & Foramiti, S., 2001. Implementing a procedure to extract urban areas based on Multispectral Classification and Mathematical Morphology. *2nd Italian GRASS users meeting*.

Boardman, J.W., 1993. Automating spectral unmixing aviris data using convex geometry concepts. *Summaries of the Fourth Annual Airborne Geoscience Workshop,* 2, 11-14.

Boardman, J.W. & Kruse, F.A., 1994. Automated spectral analysis: A geological example using AVIRIS data. *Proceedings of ERIM Tenth Thematic Conference on Geologic Remote Sensing*, 407-418.

Boardman, J.W., Kruse, F.A. & Green, R.O., 1995. Mapping target signatures via partial unmixing of AVIRIS data. *Summaries of the Fifth Annual JPL Airborne Earth Science Workshop,* 1.

Brennan, R. & Webster, T.L., 2006. Object-oriented land cover classification of LiDAR-derived surfaces. *Canadian Journal of Remote Sensing,* 32 (2), 162-172.

Bro, R. & Sidiropoulos, N.D., 1998. Least squares algorithms under unimodality and non-negativity constraints. *Journal of Chemometrics*, 12, 223-247.

Brockerhoff, M.P., 2000. An urbanizing world. *Population Bulletin,* 55 (3), 3-44.

Cao, X., Chen, J., Imura, H. & Higashi, O., 2009. A SVM-based method to extract urban areas from DMSP-OLS and SPOT VGT data. *Remote Sensing of Environment,* 113, 2205-2209.

Chen, J., 1996. *Satellite image processing for urban land cover composition analysis and runoff estimation*. Ph.D thesis, University of Utah.

Chen, Y., Su, W., Li, J. & Sun, Z., 2009. Hierarchical object oriented classification using very high resolution imagery and lidar data over urban areas. *Advances in Space Research,* 43, 1101-1110.

Chen, Y., Xu, J., He, X. & Wang, J., 2015. Analysis on the optimal system parameters of space-borne SAR for urban areas extraction. *Optik*, 126, 1236-1239.

Childe, V.G., 1950. The urban revolution. *The Town Planning Review,* 21 (1), 3-17.

Congalton, R., 1991. A review of assessing the accuracy of classications of remotely sensed data. *Remote Sensing of Environment*, 37, 35-46.

Corbane, C., Baghdadi, N., Descombes, X., Junior, E. W., Villeneuve, N. & Petit, M., 2009. Comparative study on the performance of multiparameter SAR data for operational urban areas extraction using textural features. *IEEE Geoscience and Remote Sensing Letters*, 6(4), 728-732.

De Kok, R., Wever, T. & Fockelmann, R., 2003. Analysis of urban structure and development applying procedures for automatic mapping of large area data. *The International Archives of the Photogrammetry, Remote Sensing and Spatial Information Sciences*, Regensburg.

Dekker, R. J., 2003. Texture analysis and classification of ERS SAR images for map updating of urban areas in the Netherlands. *IEEE Transactions on Geoscience and Remote Sensing,* 41(9), 1950-1958.

Deng, C. & Wu, C., 2013. The use of single-date modis imagery for estimating large-scale urban impervious surface fraction with spectral mixture analysis and machine learning techniques. *ISPRS Journal of Photogrammetry and Remote Sensing,* 86, 100-110.

Dong, Y., Chen, H., Yu, D., Pan, Y. & Zhang, J., 2011. Building extraction from high resolution sar imagery in urban areas. *Geo-spatial Information Science,* 14 (3), 164-168.

Duan, Y., Shao, X., Shi, Y., Miyazaki, H., Iwao, K. & Shibasaki, R., 2015. Unsupervised global urban area mapping via automatic labeling from ASTER and PALSAR satellite images. *Remote Sensing,* 7, 2171-2192.

Eppler, U., Fritsche, U. R. & Laaks, S., 2015. Urban-rural linkages and global sustainable land use. *GLOBALANDS Issue Paper*.

Fenstermaker, L., 1991. A proposed approach for national to global scale error assessments. *Proceedings of GIS/LIS '91, ASPRS, ACSM, AAG, AM/FM International and URISA,* 1, 293-300.

Foppa, N., Wunderle, S. & Hauser, A., 2002. Spectral unmixing of NOAA-AVHRR data for snow cover estimation. *EARSeL-LISSIG-Workshop Observing our Cryosphere from Space*, Bern.

Gao, B., 1996. NDWI: A normalized difference water index for remote sensing of vegetation liquid water from space. *Remote Sensing of Environment,* 58 (3), 257-266.

Gamba, P., Aldrighi, M. & Stasolla, M., 2011. Robust extraction of urban area extents in HR and VHR SAR images. *IEEE Journal of Selected Topic in Applied Earth Observations and Remote Sensing,* 4(1), 27-34.

Gamba, P., Dell'acqua, F., Lisini, G. & Trianni, G., 2007. Improved VHR urban area mapping exploiting object boundaries. *IEEE Transactions on Geoscience and Remote Sensing,* 45(8), 2676-2682.

Gamba, P. & Lisini, G., 2013. Fast and efficient urban extent extraction using ASAR wide swath mode data. *IEEE Journal of Selected Topic in Applied Earth Observations and Remote Sensing,* 6(5), 2184-2195.

Gitas, I.Z., Mitri, G.H. & Ventura, G., 2004. Object-based image classification for burned area mapping of Creus Cape, Spain, using NOAA-AVHRR imagery. *Remote Sensing of Environment*, 92, 409-413.

Gluch, R., Quattrochi, D.A. & Luvall, J.C., 2006. A multi-scale approach to urban thermal analysis. *Thermal Remote Sensing of Urban Areas,* 104 (2), 123-132.

Gomez-Chova, L., Fernandez-Prieto, D., Calpe, J., Soria, E., Vila, J. & Camps-Valls, G., 2006. Urban monitoring using multi-temporal SAR and multi-spectral data. *Pattern Recognition Letters,* 27, 234-243.

Gong, P. & Zhang, A., 1999. Noise effect on linear spectral unmixing. *Geographic*

*Information Sciences: A Journal of the Association of Chinese Professionals in Geographic Information Systems*, 5 (1), 52-57.

Gotlieb, C.C. & Kreyszig, H.E., 1990. Texture descriptors based on co-occurrence matrices. *Computer Vision, Graphics and Image Processing,* 51 (1), 70-86.

Grey, W. & Luckman, A., 2003. Mapping urban extent using satellite radar interferometry. *Photogrammetric Engineering & Remote Sensing*, 69(9), 957-961.

Han, Y., Kim, H., Choi, J. & Kim, Y., 2012. A shape-size index extraction for classification of high resolution multispectral satellite images. *International Journal of Remote Sensing,* 33 (6), 1682-1700.

Haralick, R.M., 1979. Statistical and structural approaches to texture. *Proceedings of the IEEE,* 67 (5), 786-804.

Haralick, R.M., Shanmugam, K. & Dinstein, I.H., 1973. Textural features for image classification. *IEEE TRansactions on Systems, Man and Cybernetics,* 3 (6), 610-621.

Harding, A. & Blokland, T., 2014. *Urban theory: A critical introduction to power, cities and urbanism in the 21st century* London: SAGE.

Haskell, K.H. & Hanson, R.J., 1981. An algorithm for linear least squares problems with equality and nonnegativity constraints. *Mathematical Programming,* 21 (1), 98-118.

Hay, A., 1979. Sampling designs to test land-use map accuracy. *Photogrammetric Engineering and Remote Sensing,* 45 (4), 529-533.

He, C., Shi, P., Xie, D. & Zhao, Y., 2010. Improving the normalized difference built-up index to map urban built-up areas using a semiautomatic segmentation approach. *Remote Sensing Letters*, 1 (4), 213-221.

He, C., Xia, G. & Sun, H., 2006. An adaptive and iterative method of urban area extraction from SAR images. *IEEE Geoscience and Remote Sensing Letters,* 3(4), 504-507.

Henderson, M., Yeh, E. T., Gong, P., Elvidge, C. & Baugh, K., 2003. Validation of urban boundaries derived from global night-time satellite imagery. *International Journal of Remote Sensing,* 24(3), 595-609.

Herbert, D.T. & Thomas, C.J., 1990. *Cities in space: City as place* Savage, Maryland: Barnes & Noble.

Hofmann, P., 2001a. Detecting informal settlements from IKONOS image data using methods of object oriented image analysis: An example from Cape Town (South Africa). *In* Jurgens, C. ed. *Remote sensing of urban areas.*

Hofmann, P., 2001b. Detecting urban features from IKONOS data using an object-oriented approach. *First Annual Meeting of the Remote Sensing and Photogrammetry Society*, Nottingham.

Hu, S., Tong, L., Frazier, A. E. & Liu, Y., 2015. Urban boundary extraction and sprawl analysis using Landsat images A case study in Wuhan, China. *Habitat International,* 47, 183-195.

Hu, X. & Weng, Q., 2011. Impervious surface area extraction from IKONOS imagery using an object-based fuzzy method. *Geocarto International,* 26 (1), 3-20.

Huete, A.R., 1988. A soil-adjusted vegetation index (SAVI). *Remote Sensing of Environment*, 25 (3), 295-309.

Hugo, G., Champion, A. & Lattes, A., 2001. New conceptualisation of settlement for demography: Beyond the rural-urban dichotomy. *Conference of International Union for the Scientific Study of Population*.

Hung, M.-C., 2003. *Remote sensing and GIS for urban environmental modeling, monitoring and visualization*. Ph.D thesis, University of Utah.

Imhoff, M. L., Lawrence, W. T., Stutzer, D. C. & Elvidge, C. D., 1997. A technique for using composite DMSP/OLS "City Lights" satellite data to map urban area. *Remote Sensing of Environment*, 61, 361-370.

Jing, W., Yang, Y., Yue, X. & Zhao, X., 2015. Mapping urban areas with integration of DMSP/OLS nighttime light and MODIS data using machine learning techniques. *Remote Sensing*, 7, 12419-12439.

Johnson, J.H., 1972. *Urban geography: An introductory analysis* Oxford; Toronto: Pergamon Press.

Johnston, R.J., 1980. *City and society: An outline for urban geography* Penguin: Harmondsworth.

Kailath, T., 1967. The divergence and bhattacharyya distance measures in signal selection. *IEEE Transactions on Communication Theory*, 15, 52-60.

Kajimoto, M. & Susaki, J., 2013. Urban-area extraction from polarimetric SAR images using polarization orientation angle. *IEEE Geoscience and Remote Sensing Letters*, 10(2), 337-341.

Kaplan, D.H., Wheeler, J.O. & Holloway, S.R., 2004. *Urban geography* Hoboken, NJ: Wiley.

Kasimu, A. & Tateishi, R., 2008. Global urban mapping using population density, MODIS and DSMP data with the reference of Landsat images. *The International Archives of the Photogrammetry, Remote Sensing and Spatial Information Sciences*, Commission ThS-17, 1523-1528.

Kay, S.M., 1993. *Fundamentals of statistical signal processing: Estimation theory* Englewood Cliffs, New Jersey: Prentice Hall.

Kaya, S., Llewellyn, G. & Curran, P.J., 2004. Displaying earthquake damage in urban area using a vegetation-impervious-soil model and remotely sensed data. *The XXth Congress International Society of Photogrammetry and Remote Sensing*, Turkey.

Kayabol, K. & Zerubia, J. A comparison of texture and amplitude based unsupervised SAR image classifications for urban area extraction. IEEE International Geoscience and Remote Sensing Symposium, 2012 Munich. 4054-4057.

Keshava, N. & Mustard, J.F., 2002. Spectral unmixing. *IEEE Signal Processing Magazine*, 2, 44-57.

Knox, P.L. & Mccarthy, L., 2012. *Urbanization: An introduction to urban geography* Boston: Pearson.

Kovacs, A. & Sziranyi, T., 2013. Improved Harris feature point set for orientation-sensitive urban-area detection in aerial images. *IEEE Geoscience and Remote Sensing Letters*, 10(4), 796-800.

Kressler, F.P., Mucher, C.A., Steinnocher, K.T. & Thunnissen, H.A.M., 2000. Evaluation of medium-resolution satellite images for land use monitoring using spectral mixture analysis. *International Archives of Photogrammetry and Remote Sensing*, Vol. XXXIII, Part B7.

Lawson, C.L. & Hanson, R.J., 1974. *Solving least squares problems* Englewood Cliffs, New Jersey: Prentice Hall.

Lorette, A., Descombes, X. & Zerubia, J., 2000. Texture analysis through a Markovian modelling and fuzzy classification application to urban area extraction from satellite images. *International Journal of Computer Vision*, 36(3), 221-236.

Lorinc, J., 2008. *Cities* Toronto, Ont.: Groundwood Books.

Lu, D., Song, K., Zeng, L., Liu, D., Khan, S., Zhang, B., Wang, Z. & Jin, C., 2008. Estimating impervious surface for the urban area expansion: Examples from Changchun, Northeast China. *The International Archives of the Photogrammetry, Remote Sensing and Spatial Information Sciences*, Vol. XXXVII, Part B8.

Lu, D. & Weng, Q., 2004. Spectral mixture analysis of the urban landscape in

Indianapolis with Landsat ETM+ imagery. *Potogrammetric Engineering & Remote Sensing*, 9, 1053-1062.

Lu, D. & Weng, Q., 2009. Extraction of urban impervious surfaces from an IKONOS image. *International Journal of Remote Sensing,* 30 (5), 1297-1311.

Macqueen, J., 1967. Some methods for classification and analysis of multivariate observations. *Proceedings of 5th Berkeley Symposium on Mathematical Statistics and Probability,* 1, 281-297.

Madhavan, B.B., Kubo, S., Kurisaki, N. & Sivakumar, T.V.L.N., 2001. Appraising the anatomy and spatial growth of the Bangkok metropolitan area using a vegetation-impervious-soil model through remote sensing. *International Journal of Remote Sensing,* 22 (5), 789-806.

Marangoz, A.M., Oruc, M. & Buyuksalih, G., 2004. Object-oriented image analysis and semantic network for extracting the roads and buildings from IKONOS pan-sharpened images. *ISRPS 2004 Annual Conference*, Turkey.

Mathieu-Marni, S., Moisan, S. & Vincent, R., 1996. A knowledge based system for the computation of land cover mixing and the classification of multi-spectral satellite imagery. *International Journal of Remote Sensing,* 17 (8), 1483-1492.

Maunier, R., 1910. The definition of the city. *American Journal of Sociology,* 15 (4), 536-548.

Mcfeeters, S.K., 1996. The use of the normalized difference water index (NDWI) in the delineation of open water features. *International Journal of Remote Sensing,* 17 (7), 1425-1432.

Mhangara, P. & Odindi, J., 2012. Potential of texture-based classification in urban landscapes using multispectral aerial photos. *South African Journal of Science,* 109 (3/4), 1-8.

Mhangara, P., Odindi, J., Kleyn, L. & Remas, H., 2011. *Road extraction using object* *oriented classification* [Online]. [Accessed 10 July 2015]. Available from: http://www.researchgate.net/publication/267856733_Road_extraction_using_object_oriented_classification

Miliaresis, G. & Kokkas, N., 2007. Segmentation and object-based classification for the extraction of the building class from LiDAR DEMs. *Computers and Geosciences*, 33 (8), 1076-1087.

Miller, R.B. & Small, C., 2003. Cities from space: Potential applications of remote sensing in urban environmental research and policy. *Environmental Science and Policy,* 6, 129-137.

Ministry of Commerce of the People's Republic of China, 2007. *Beijing: Survey* [Online]. [Accessed 10 July 2015]. Available from : http://english.mofcom.gov.cn/aarticle/zt_business/lanmub/200703/20070304508799.html

Moriyama, T., Uratsuka, S., Umehara, T., Satake, M., Nadai, A., Maeno, H., Nakamura, K. & Yamaguchi, Y., 2004. A study on extraction of urban areas from polarimetric synthetic aperture radar image. *IEEE International Geoscience and Remote Sensing Symposium.*

Mumford, L., 1937. What is a city? *Architectural Record,* 1937, 92-96.

National Bureau of Statistics of the People's Republic of China, 2001. *Data of the fifth national census of China: Beijing* [Online]. [Accessed 10 July 2015]. Available from: http://www.stats.gov.cn/tjsj/tjgb/rkpcgb/dfrkpcgb/200203/t20020331_30363.html

National Bureau of Statistics of the People's Republic of China, 2006. *Provisions of urban-rural classification* [Online]. [Accessed 10 July 2015]. Available from: http://www.stats.gov.cn/statsinfo/auto2073/201310/t20131031_450613.html

National Bureau of Statistics of the People's Republic of China, 2012. *Data of the sixth national census of China: Beijing* [Online]. [Accessed 10 July 2015]. Available from: http://www.stats.gov.cn/tjsj/tjgb/rkpcgb/dfrkpcgb/201202/t20120228_30381.html

Netzband, M. & Jürgens, C., 2008. Urban and suburban areas as a research topic for remote sensing. *In* Rashed, T. & Jürgens, C. ed. *Remote sensing of urban and suburban areas* Springer, 1-9.

Oxford University Press, 1989. The Oxford English Dictionary. *In* Simpson, J.A. & Weiner, E.S.C. eds.

Paddison, R. ed. 2001. *Handbook of urban studies,* London: SAGE.

Pearson, K., 1901. On lines and planes of closest fit to systems of points in space. *Philosophical Magazine*, 2, 559-572.

Phinn, S., Stanford, M., Scarth, P., Murray, A.T. & Shyy, P.T., 2002. Monitoring the composition of urban environments based on the vegetation-impervious surface-soil (VIS) model by subpixel analysis techniques. *International Journal of Remote Sensing,* 23 (20), 4131-4153.

Portugal, L.F., Júdice, J.J. & Vicente, L.N., 1994. A comparison of block pivoting and interior-point algorithms for linear least quares problems with nonnegative variables. *Mathematics of Computation*, 63 (208), 625-643.

Potere, D., Schneider, A., Angel, S. & Civco, D. L., 2009. Mapping urban areas on a global scale: which of the eight maps now available is more accurate? *International Journal of Remote Sensing,* 30(24), 6531-6558.

Pradhan, B., Hagemann, U., Tehrany, M.S. & Prechtel, N., 2014. An easy to use ArcMap based texture analysis program for extraction of flooded areas from TerraSAR-X satellite image. *Computers and Geosciences,* 63, 34-43.

Qi, J., Chehbouni, A., Huete, A.R., Kerr, Y.H. & Sorooshian, S., 1994. A modified soil adjusted vegetation index. *Remote Sensing of Environment*, 48, 119-126.

Qiao, Y., Liu, H., Bai, M., Wang, X. & Zhou, X., 2009. The decision tree algorithm of urban extraction from multi-source image data. *ISPRS Wuhan 2009 Workshop*, Wuhan.

Qiu, A., 2012. Understanding the urbanisation rate in China. *Cities Development Initiative for Asia March 2012 Newsletter*.

Quarmby, N.A., Townshend, J.R.G., Settle, J.J., White, K.H., Milnes, M., Hindle, T.L. & Silleos, N., 1992. Linear mixture modelling applied to AVHRR data for crop area estimation. *International Journal of Remote Sensing*, 13 (3), 415-425.

Raymaekersa, D., Bauwensa, I., Van Orshovena, J., Gulincka, H., Engelc, B. & Dosselaered, N., 2005. Spectral unmixing of low resolution images for monitoring soil sealing. *The International Archives of the Photogrammetry, Remote Sensing and Spatial Information Sciences,* 36 (8/W27), 1-6.

Richards, J.A. & Jia, X., 2005. *Remote sensing digital image analysis: An introduction* Berlin: Springer.

Ridd, M.K., 1995. Exploring a V-I-S (vegetation-impervious surface-soil) model for urban ecosystem analysis through remote sensing: Comparative anatomy for cities. *International Journal of Remote Sensing,* 16 (12), 2165-2185.

Roessner, S., Segl, K., Heiden, U. & Kaufmann, H., 2001. Automated differentiation of urban surface based on airborne hyperspectral imagery. *IEEE Transactions on Geoscience and Remote Sensing,* 39 (7), 1523-1532.

Rogers, A.S. & Kearney, M.S., 2004. Reducing signature variability in unmixing coastal marsh thematic mapper scenes using spectral indices. *International Journal of Remote Sensing,* 25 (12), 2317-2335.

Rouse, J.W., Haas, R.H., Schell, J.A. & Deering, D.W., 1973. Monitoring vegetation systems in the great plains with erts. *Third Earth Resources Technology Satellite-1 Symposium Volume I: Technical Presentations*, 309.

Salentinig, A. & Gamba, P., 2015. Combining SAR-based and multispectral-based extractions to map urban areas at multiple spatial resolutions. *IEEE Geoscience and Remote Sensing Magazine*, 100-112.

Salomonson, V.V. & Appel, I., 2004. Estimating fractional snow cover from MODIS using the normalized difference snow index. *Remote Sensing of Environment,* 89, 351-360.

Schneider, A., Friedl, M. A., Mclver, D. K. & Woodcock, C. E., 2003. Mapping urban areas by fusing multiple sources of coarse resolution remotely sensed data. *Photogrammetric Engineering & Remote Sensing,* 69(12), 1377-1386.

Schneider, A., Friedl, M. A. & Potere, D., 2009. A new map of global urban extent from MODIS satellite data. *Environmental Research Letters,* 4, 1-11.

Schneider, A., Friedl, M. A. & Potere, D., 2010. Mapping global urban areas using MODIS 500-m data: New methods and datasets based on 'urban ecoregions'. *Remote Sensing of Environment,* 114, 1733-1746.

Shanmukha Rao, D., Prasad, A.V.V. & Nair, T., 2015. Application of texture characteristics for urban feature extraction from optical satellite images. *International Journal of Image, Graphics and Signal Processing,* 1, 16-24.

Shi, H., Chen, H., Bi, F., Pang, F. & Yang, X., 2015. A real-time urban area detection algorithm based on feature location optimization and integration. *Chinese Journal of Electronics,* 43(7), 1369-1374.

Siechiping, R., Kago, J., Zhang, X., Augustinus, C. & Tuts, R., 2015. Urban-rural linkages and the role of land tenure. *2015 World Bank Conference on Land and Poverty*.

SinoMaps Press, 2008. *Atlas of beijing*.

Sirmacek, B. & Unsalan, C., 2009. Urban-area and building detection using SIFT keypoints and graph theory. *IEEE Transactions on Geoscience and Remote Sensing*, 1-12.

Sirmacek, B. & Unsalan, C., 2010. Urban area detection using local feature points and spatial voting. *IEEE Geoscience and Remote Sensing Letters*, 7(1), 146-150.

Sjoberg, G., 1965. The origin and evolution of cities. *Scientific American*, 213 (3), 54-63.

Small, C., 2001. Estimation of urban vegetation abundance by spectral mixture analysis. *International Journal of Remote Sensing*, 22, 1305-1334.

Small, C., Pozzi, F. & Elvidge, C. D., 2005. Spatial analysis of global urban extent from DMSP-OLS night lights. *Remote Sensing of Environment*, 96, 277-291.

Stathakis, D. & Faraslis, I., 2014. Monitoring urban sprawl using simulated PROBA-V data. *International Journal of Remote Sensing*, 35(7), 2731-2743.

Susaki, J. & Kishimoto, M., 2015. Urban area extraction using airborne X-band fully polarimetric Pi-SAR2 imagery. *The International Archives of the Photogrammetry, Remote Sensing and Spatial Information Sciences*, XL-3/W2, 219-226.

Swain, P.H. & Davis, S.M., 1978. *Remote sensing: The quantitative approach* New York: Mcgraw-Hill College.

Tang, Q., Wang, L., Li, B. & Yu, J., 2012. Towards a comprehensive evaluation of V-I-S sub-pixel fractions and land surface temperature for urban land-use classification in the USA. *International Journal of Remote Sensing*, 33 (19), 5006-6019.

Tang, T. & Dai, L., 2014. Accuracy test of point-based and object-based urban building feature classification and extraction applying airborne LiDAR data.

*Geocarto International*, 29 (7), 710-730.

Taubenbock, H., Esch, T., Wurm, M., Roth, A. & Dech, S., 2010. Object-based feature extraction using high spatial resolution satellite data of urban areas. *Journal of Spatial Science,* 55 (1), 117-132.

Tempfli, K., Kerle, N., Huurneman, G.C. & Janssen, L.L.F. eds. 2009. *Principles of remote sensing*, Enschede: ITC.

Tian, G., Wu, J. & Yang, Z., 2010. Spatial pattern of urban functions in the Beijing metropolitan region. *Habitat International*, 34, 249-255.

Trias-Sanz, R., Lomenie, N. & Barbeau, J., 2004. Using textural and geometric information for an automatic bridge detection system. *Advanced Concepts for Intelligent Vision Systems*, 325-332.

UN-Habitat, 2015. Enhance urban-rural linkages to harness the transformative power of urbanization for sustainable development. *United Nations Urban-Rural Linkage Flyer.*

United Nations Department of Economic and Social Affairs, 2012. *World urbanization prospects the 2011 revision.* New York.

United Nations Department of Economic and Social Affairs, 2013. United nations demographic yearbook 2013.

United States Census Bureau, 2014. TIGER/Line shapefiles technical documentation.

United States Census Bureau, 2015. *2010 census urban area FAQs* [Online]. [Accessed 10 July 2015]. Available from: https://www.census.gov/geo/reference/ua/uafaq.html

Wacker, A.G., 1971. *The minimum distance approach to classification*. Ph.D thesis, Purdue University.

Wan, B., Guo, Q., Fang, F., Su, Y. & Wang, R., 2015. Mapping US urban extents from MODIS data using one-class classification method. *Remote Sensing*, 7, 10143-10163.

Ward, D., Phinn, S.R. & Murray, A.T., 2000. Monitoring growth in rapidly urbanizing areas using remotely sensed data. *Professional Geographer,* 52 (3), 371-386.

Weeks, J.R., 2008. Defining urban areas. *In* Rashed, T. & Jürgens, C. ed. *Remote sensing of urban and suburban areas* Springer, 33-45.

Weeks, J.R., Larson, D.P. & Fugate, D.L., 2005. Patterns of urban land use as assessed by satellite imagery: An application to Cairo, Egypt. *In* Entwisle, B. & Stern, P.C. ed. *Population, land use, and environment.* Washington DC: National Academies Press (US).

Wei, Y., Liu, Z. & Song, Y., 2008. Spectral mixture analysis of impervious surface in Changchun, China based on normalized image. *Proceedings of International Workshop on Geoscience and Remote Sensing*, 1, 815-818.

Wheatley, P., 1969. *City as symbol* London: Lewis.

Wirth, L., 1938. Urbanism as a way of life. *The American Journal of Sociology,* 44 (1), 1-24.

Woolley, L., 1963. The urbanism of society. *In* Hawkes, J. & Woolley, L. ed. *History of mankind: A global view of cultrual and scientific development.* Paris: UNESCO.

Wu, C. & Murray, A.T., 2003. Estimating impervious surface distribution by spectral mixture analysis. *Remote Sensing of Environment,* 84, 493-505.

Xu, H., 2006. Modification of normalised difference water index (NDWI) to enhance open water features in remotely sensed imagery. *International Journal of Remote Sensing,* 27 (14), 3025-3033.

Xu, H., 2008. A new index for delineating built-up land features in satellite imagery. *International Journal of Remote Sensing,* 29 (14), 4269-4276.

Xu, X., Zhou, Y. & Ning, Y., 1997. *Urban geography* Beijing: Higher Education

Press.

Yang, Y., Sun, H. & Cao, Y., 2008. Unsupervised urban area extraction from SAR imagery using GMRF. *Pattern Recognition and Image Analysis,* 18(1), 156-162.

Yu, B., Liu, H., Wu, J., Hu, Y. & Zhang, L., 2010. Automated derivation of urban building density information using airborne LiDAR data and object-based method. *Landscape and Urban Planning,* 98, 210-219.

Yu, S., Berthod, M. & Giraudon, G., 1999. Toward robust analysis of satellite images using map information-application to urban area detection. *IEEE Transactions on Geoscience and Remote Sensing,* 37(4), 1925-1939.

Yuan, F. & Bauer, M.E., 2007. Comparison of impervious surface area and normalized difference vegetation index as indicators of surface urban heat island effects in Landsat imagery. *Remote Sensing of Environment,* 106, 375-386.

Yue, A., Zhang, C., Yang, J., Su, W., Yun, W. & Zhu, D., 2013. Texture extraction for object-oriented classification of high spatial resolution remotely sensed images using a semivariogram. *International Journal of Remote Sensing,* 34 (11), 3736-3759.

Zha, Y., Gao, J. & Ni, S., 2003. Use of normalized difference built-up index in automatically mapping urban areas from tm imagery. *International Journal of Remote Sensing*, 24 (3), 583-594.

Zhang, J., He, C., Zhou, Y., Zhu, S. & Shuai, G., 2014. Prior-knowledge-based spectral mixture analysis for impervious surface mapping. *International Journal of Applied Earth Observation and Geoinformation,* 28, 201-210.

Zhang, X., Cai, C. & Li, P., 2014. Regional urban area extraction using DMSP-OLS data and MODIS data. *35th International Symposium on Remote Sensing of Environment,* 17, 1-6.

Zhao, H. & Chen, X., 2005. Use of normalized difference bareness index in quickly mapping bare areas from TM/ETM+. *Geoscience and Remote Sensing Symposium*, 1666-1668.

Zhao, Y., Du, H., Du, P. & Cai, Y., 2010. Pixel unmixing for urban environment monitoring using multi-temporal satellite images. *Proceedings of the 18th International Conference on Geoinformatics*, 1-6.

Zhong, P. & Wang, R., 2007. A multiple conditional random fields ensemble model for urban area detection in remote sensing optical images. *IEEE Transactions on Geoscience and Remote Sensing*, 45(12), 3978-3988.

Zhou, W., Huang, G., Troy, A. & Cadenasso, M.L., 2009. Object-based land cover classification of shaded areas in high spatial resolution imagery of urban areas: A comparison study. *Remote Sensing of Environment,* 113, 1769-1777.

Zhou, W. & Troy, A., 2008. An object-oriented approach for analysing and characterizing urban landscape at the parcel level. *International Journal of Remote Sensing,* 29 (11), 3119-3135.

Zhou, W. & Troy, A., 2009. Development of an object-based framework for classifying and inventorying human-dominated forest ecosystems. *International Journal of Remote Sensing,* 30 (23), 6343-6360.

Zhou, W., Troy, A. & Grove, M., 2006. Measuring urban parcel lawn greenness by using an object-oriented classification approach. *Geoscience and Remote Sensing Symposium,* Denver, 2693-2696.

Zhou, W., Troy, A. & Grove, M., 2008. Modeling residential lawn fertilization practices: Integrating high resolution remote sensing with socioeconomic data. *Environmental Management,* 41, 742-752.

Zhou, Y., Smith, S. J., Elvidge, C. D., Zhao, K., Thomson, A. & Imhoff, M., 2014. A cluster-based method to map urban area from DMSP/OLS nightlights. *Remote*

*Sensing of Environment*, 147, 173-185.

Zhou, Y., Smith, S. J., Zhao, K., Imhoff, M., Thomson, A., Bond-Lamberty, B., Asrar, G. R., Zhang, X., He, C. & Elvidge, C. D., 2015. A global map of urban extent from nightlights. *Environmental Research Letters*, 10, 2-11.

Zhou, Y. & Wang, Y.Q., 2008. Extraction of impervious surface areas from high spatial resolution imagery by multiple agent segmentation and classification. *Photogrammetric Engineering and Remote Sensing* 74 (7), 857-868.

Zoran, M., Savastru, R., Savastru, D., Miclos, S., Mustata, M.N. & Baschir, L., 2008. Urban landcover mapping using multiple endmember spectral mixture analysis. *Journal of Optoelectronics and Advanced Materials*, 10 (3), 701-706.